DEPARTMENT OF EXPERIMENTAL MEDICINE

PhD COURSE IN EXPERIMENTAL MEDICINE

Curriculum of BIOCHEMISTRY

The ABA/LANCL1-2 system in ROS regulation in cardiomyocytes and in skeletal muscle differentiation and thermogenesis: evaluation of potential LANCL2 agonists

Candidate

Dr. Bujar-Ari CAUSHI

Tutor

Prof. Laura STURLA

Coordinator of the PhD course

Prof. Ernesto FEDELE

Academic Year 2024-2025

XXXVIII Cycle

ABSTRACT

Abscisic acid (ABA) is an evolutionarily conserved hormone that originated in some of the earliest living organisms, with modern ABA-producing cyanobacteria likely representing their descendants. Its emergence occurred prior to the divergence of the plant and animal kingdoms, and its fundamental role as a signaling molecule mediating cellular responses to environmental stress has been maintained throughout evolution. In mammals, beyond its anti-inflammatory and neuroprotective functions, ABA at nanomolar concentrations modulates the metabolic response to glucose availability by promoting glucose uptake in skeletal muscle and adipose tissue through an insulin-independent mechanism. Moreover, ABA enhances mitochondrial energy production and energy dissipation in both brown and white adipocytes via activation of its receptors LANCL1 and LANCL2. Chronic oral administration of ABA at microgram-per-kilogram body weight doses has been reported to improve glycemic control, lipid homeostasis, and morphometric parameters in borderline subjects for prediabetes and metabolic syndrome.

In rat H9c2 cardiomyocytes the cross-kingdom stress hormone ABA and its mammalian receptors LANCL1 and LANCL2 modulate the cellular response of cardiomyocytes to hypoxia by activating the AMPK/PGC-1α axis. This activation enhances increasing NO generation, mitochondrial proton gradient, respiration, and improves cell vitality after hypoxia/reoxygenation. In addition, overexpression of LANCL1/2 in rat H9c2 cardiomyocytes markedly increased, whereas silencing decreased, mitochondrial number, OXPHOS complex I activity, proton gradient, glucose- and palmitate-driven respiration, uncoupling protein transcription, and expression of proteins involved in cytoskeletal, contractile, and electrical functions. These effects, together with LANCL1/2-dependent NO production, are mediated by the transcription factor ERRα, which acts upstream of the AMPK/PGC-1α axis and is transcriptionally regulated by the ABA/LANCL1/2 system.

Based on this evidence, this thesis investigated the role of the ABA/LANCL1-2 system in Reactive Oxygen Species (ROS) metabolism in H9c2 cardiomyocytes overexpressing or silenced for LANCL1/2, with or without concomitant ERRα knockdown. Expression of enzymes involved in ROS production and scavenging was assessed by qRT-PCR and Western blot, while mitochondrial proton gradient and ROS levels were measured using specific fluorescent probes. LANCL1/2 overexpression decreased ROS-generating enzymes, increased ROS-scavenging enzymes, and reduced mitochondrial ROS, whereas opposite effects were observed in LANCL1/2-silenced cells. The knockdown of ERRα abrogated all beneficial effects on ROS turnover in LANCL1/2 overexpressing cells. Overall, these results indicate that the ABA/LANCL1-2 system regulates key aspects of cardiomyocyte physiology and ROS turnover via the ERRα/AMPK/PGC-1α axis, highlighting it as a potential target to enhance mitochondrial function and resistance to oxidative

stress. Investigating molecules that specifically activate this system and its receptors represents a promising research avenue. To this end, biochemical assays in H9c2 cells and preliminary binding studies were conducted to assess the interaction of novel potential agonists with human recombinant LANCL2. Recent findings in rat H9c2 cardiomyocytes have demonstrated that the ABA/LANCL1-2 system plays a role in regulating cellular thermogenesis, as evidenced by higher heat production in LANCL1/2-overexpressing cells compared with double-silenced cells. These results are consistent with previous observations in adipocytes and myoblasts, which revealed an enhanced browning process accompanied by an increased basal metabolic rate, elevated substrate oxidation, and upregulated expression of uncoupling proteins. These proteins dissipate the mitochondrial proton gradient to generate heat instead of ATP, thereby contributing to cellular energy expenditure, mechanisms that are crucial for maintaining normal body weight and counteracting obesity.

In this thesis the potential role of the ABA/LANCL1-2 system in regulating the expression of genes involved in skeletal muscle thermogenesis and differentiation was investigated, aiming to provide further insights into the physiological functions of skeletal muscle, a tissue that constitutes approximately 40% of total human body weight and, together with adipose tissue, represents the majority of mammalian cell mass, significantly contributes to body weight balance.

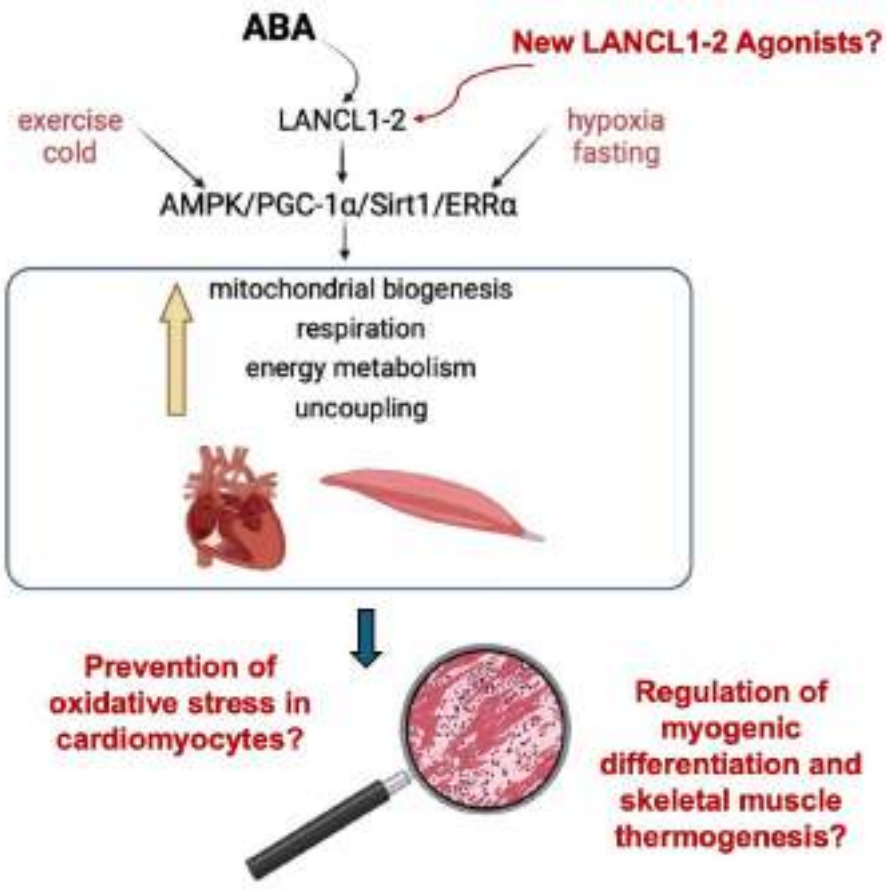

INDEX

1. INTRODUCTION

1.1. Abscisic acid, a plant and animal hormone.

2-cis, 4-trans-Abscisic acid (ABA) is a 15-carbon weak acid (pKa 4.8) terpenoid hormone (**Figure 1**) which plays important roles in the regulation of plant responses to environmental stress [1]. ABA has a chiral center, as indicated in **Figure 1**, and the two enantiomers S-(+)-ABA and R-(–)-ABA both have a hormonal activity [2]. The S-(+)-ABA is the naturally occurring isomer found in plants and is primarily responsible for ABA's biological functions. However, the R-(–)-ABA enantiomer has also been shown to exhibit activity in certain plant [3]. The isoprenoid hormone is also present and active in lower Metazoa (Porifera and Hydroids), where it regulates the sponge response to an increase in water temperature and light-induced tissue regeneration in hydroids [4,5]. ABA is present as an endogenous hormone also in humans [6], where it controls innate immune cell function [7,8], the expansion of hemopoietic progenitors [9], glucose homeostasis [6,10-14], adipocytes bowning [15,16], myoblast and cardiomyocytes metabolism [17-19]. Conservation of ABA across the plant and animal kingdoms points to its very early evolution, in a common precursor to Metaphyta and Metazoa, as a messenger involved in the physiological adaptation of cells and organisms to changing environmental conditions.

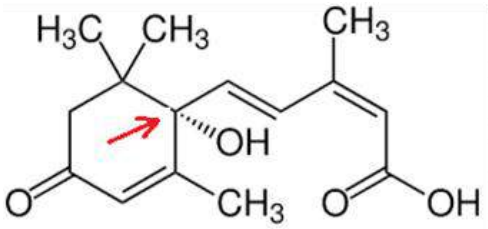

Figure 1. Structure of 2-cis, 4-trans-Abscisic Acid. Abscisic acid (ABA) possesses an asymmetric carbon atom (indicated by the red arrow), giving rise to two enantiomeric forms: S-(+)-ABA and R-(–)-ABA.

ABA is naturally found in a wide range of fruits and vegetables, examples of which are listed in **Table 1.** However, in most of these foods, the concentration of ABA is relatively low and generally insufficient to serve as a significant dietary source. To overcome this limitation, specialized extraction techniques have been developed to produce ABA-enriched fruit extracts. These concentrated forms of ABA are already commercially available and are used as active ingredients in various nutraceutical and dietary supplement formulations.

Fruits	mg/Kg	Vegetables	mg/Kg
Avocado	2	Soybean	0.79
Citrus	1.25	Barley	0.20
Fig	0.72	Tomato	0.20
Bilberry	0.4	Wheat	0.15
Apricot	0.32	Pea	0.13
Banana	0.22	Cucumber	0.09

Table 1. ABA content espressed in mg/Kg in various fruits and vegetables [10,11,14]. ABA levels are influenced by multiple factors, including the degree of ripeness and the genetic variety of the plant.

1.2. Role of ABA in Plants

ABA, discovered in plants over two decades ago [20-22], is a phytohormone widely known for its key role in regulating plant development and responses to environmental stress. ABA was discovered in plants more than 20 years ago and is a phytohormone widely recognized for its central role in regulating plant development and stress responses. Originally discovered in plants, ABA participates in crucial physiological processes including seed maturation and dormancy, bud development, germination, fruit ripening, and growth regulation. Beyond development, ABA serves as a key mediator of plant adaptation to environmental stressors such as drought, salinity, extreme temperatures, and heavy metal exposure. A well-studied example of ABA's role in abiotic stress tolerance is its function during water scarcity. In response to reduced soil water potential, plant roots synthesize ABA, which is then transported to the leaves. There, ABA triggers the closure of stomata by promoting osmotic changes in guard cells, thereby reducing transpiration and preserving leaf water content. This drought-response mechanism, along with ABA's broader signaling pathways, is highly conserved across plant species, from higher plants to non-vascular mosses, reflecting its early evolutionary role in the adaptation to terrestrial life. Due to its pivotal role in stress physiology, ABA has been the subject of extensive research over the past decades, with growing interest in its application to enhance crop resilience under adverse environmental conditions. A comprehensive analysis of ABA's roles in plant development and responses to abiotic stress can be found in recent detailed reviews [23,24].

1.3 Endogenous ABA in animals

The presence ABA in mammalian tissues was first reported in 1986 by Le Page-Degivry et al., who detected significantly higher levels of ABA in the brains of mice fed an ABA-free synthetic diet

compared to those on standard chow [25]. This finding supported the hypothesis that ABA is endogenously produced in animals. However, this early observation remained largely uninvestigated for over a decade. Around fifteen years later, Professor Zocchi's research group at the University of Genova revisited the question of ABA in animals, while exploring upstream regulators of cyclic ADP-ribose (cADPR), a second messenger known for mobilizing intracellular Ca^{2+} stores and playing a role in insulin secretion [26]. This led to the hypothesis that ABA might function as hormone not only in plants but also in animals. To test this idea, the group conducted experiments on sponges and hydroids, evolutionarily ancient and physiologically simple metazoans. These sessile organisms, despite their limited biological complexity, mainly water filtration and respiration, are highly sensitive to environmental stress. It was found that stressors such as temperature and light could induce ABA production in sponges and hydroids, respectively, and that ABA in turn triggered specific adaptive responses. These responses were mediated through a conserved signaling cascade involving cAMP, protein kinase A (PKA), cADPR, and intracellular calcium mobilization [4,5,27].
These studies opened the door to exploring ABA's role in more complex animal systems. In 2012, a key discovery was made: plasma ABA levels were observed to rise following glucose ingestion in healthy human subjects, reaching low nanomolar concentrations. This provided evidence for ABA's role as an endogenous hormone in mammals [6]. Subsequent research identified key components of ABA signaling in animals. The mammalian proteins LANCL2 (identified in 2011) and LANCL1 (in 2021) were identified as ABA receptors, enabling detailed investigations using LANCL2 KO mice and overexpressing vs. silenced cells [28-32]. These advances have greatly enriched the understanding of ABA's mechanisms of action in animal physiology (**Figure 2**). Finally, *in vivo* studies in rodents and humans [10, 33-37] provided the basis for patenting the use of ABA as a nutraceutical to enhance glucose tolerance and metabolic health, culminating in granted patents in the European Union (2020) and the United States (2021).

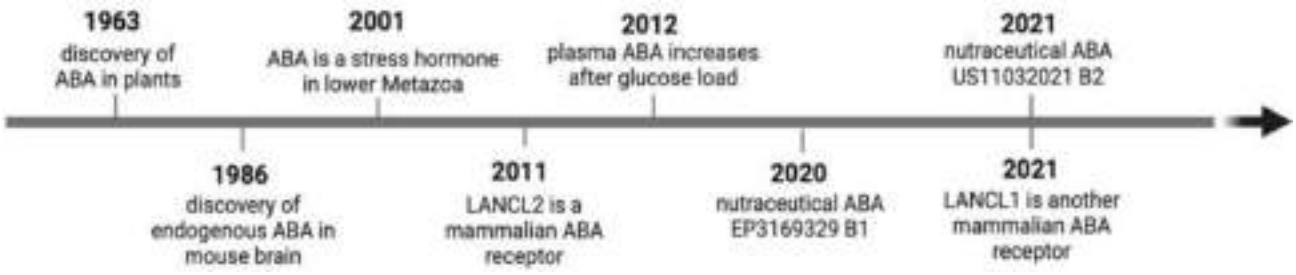

Figure 2. Pivotal steps in the scientific discovery and characterization of ABA as a functional endogenous hormone in animals.

1.4. LANCL1 and LANCL2 function as ABA receptors.

The evolutionary conservation of ABA across both plant and animal kingdoms has prompted investigations into whether its receptors may also be conserved. In plants, the current consensus identifies the PYR/PYL/RCAR protein family as the primary components of the ABA signaling pathway [38–40]. However, one of the earliest candidates proposed as an ABA receptor in Arabidopsis thaliana was GCR2, a membrane-bound G protein-coupled receptor (GPCR) [41,42]. Interestingly, GCR2 shares significant amino acid sequence similarity with the mammalian lanthionine synthetase C-like (LANCL) protein family [42]. The LANCL proteins in mammals are structurally related to bacterial lanthionine synthetase C (LanC), which catalyzes the addition of the thiol of Cys to dehydrated Ser in the biosynthesis of lanthionine-containing peptides known as lanthipeptides. These molecules, such as nisin, possess antimicrobial activity and are widely used as natural food preservatives to inhibit bacterial growth [43]. However, since animals do not produce lantibiotics, it is unlikely that mammalian LANCL proteins fulfill the same enzymatic function as their bacterial counterparts [44]. Further evidence supporting a divergent role comes from studies involving the simultaneous knockdown of LANCL1, LANCL2, and LANCL3 in mammalian cells. These experiments revealed no reduction in brain levels of lanthionine ketimine, a downstream metabolite of lanthionine, suggesting that LANCL proteins are not involved in lanthionine metabolism in mammals [45], leaving their role in mammalian physiology open to investigation.

The LANCL protein family consists of three members with distinct expression patterns and subcellular localizations. LANCL1 is the most abundantly expressed isoform in mammals, with particularly high levels in the brain, and is primarily localized in the cytosol [46]. LANCL2, in contrast, is anchored to the plasma membrane via an N-terminal myristoylation motif [47], enabling its association with membrane signaling pathways. LANCL3 is the least expressed of the three and, like LANCL1, appears to reside in the cytosol. The corresponding genes for LANCL1, LANCL2, and LANCL3 are located on human chromosomes 2, 7, and X, respectively [48-50].

LANCL1 and LANCL2 are widely expressed across most tissues, with notably high levels in the brain, as confirmed by both transcriptomic and proteomic data (see https://www.proteinatlas.org/search/LANCL, accessed on 20 October 2025); in contrast, LANCL3 shows low expression, raising the possibility that it functions as a pseudogene [46,47,51,52].

LANCL2 was the first mammalian protein identified as a receptor for ABA. Several *in vitro* studies have demonstrated that recombinant human LANCL2 binds ABA with high affinity (dissociation constant, Kd ≈ 2.6 nM) [29, 53] and is essential for mediating ABA responses in various mammalian cell types [28]. Unlike classical hormone receptors, LANCL2 displays dual behavior: when myristoylated, it is tethered to the plasma membrane and functionally coupled to G proteins. Upon

de-myristoylation, however, it detaches from the membrane and translocates to the nucleus [47]. Notably, this nuclear migration is triggered by ABA binding [54]. This dual localization and signaling mode suggest that LANCL2 integrates features typical of receptors for peptide (G protein-coupling) and for steroid hormone (nuclear translocation). Such mechanism may reflect either the ancient evolutionary origin of ABA or its unique physicochemical properties. To interact with LANCL2 anchored to the inner plasma membrane, ABA must be transported into the cell by anion exchanger (AE) superfamily proteins [55]. Although protonated ABA is capable of diffusing passively across the lipid bilayer [56], its protonated form represents only a small fraction of the total ABA at the near-neutral pH of plasma and interstitial fluid. Consequently, efficient transport of ABA across cell membranes requires dedicated transporter systems. In contrast, the highly acidic environment of the stomach favors the protonated form of ABA, facilitating its passive diffusion through the gastric epithelium and explaining the hormone's rapid absorption following oral administration [10].

More recently, Spinelli et al. [32] provided evidence that the LANCL1 protein, which shares with LANCL2 a sequence identity of approx. 50%, is also capable of binding ABA, with a calculated dissociation constant (Kd) in the low micromolar range. This value lies in between those of the high- and low-affinity binding sites of LANCL2 for ABA (0.1 and 10 μM, respectively [53]). These findings support the hypothesis that LANCL1, like LANCL2, may serve as a functional receptor for ABA, potentially contributing to its signaling activity under physiological conditions where ABA concentrations vary. Despite this difference in affinity, LANCL1 shares many of the same downstream biological effects, including the stimulation of glucose uptake, the upregulation of muscle glucose transporter expression, and the enhancement of mitochondrial respiration and uncoupling [32]. Interestingly, silencing or genetic ablation of LANCL2 in cells or in mice results in the spontaneous overexpression of LANCL1 [32]. Similarly, silencing of LANCL1 causes a significant increase in the expression of LANCL2 in cells [32]. This observation, together with the redundancy of ABA receptors, points to the physiological relevance of the ABA/LANCL hormone/receptor system in mammals.

1.5. ABA/LANCL1-2 signaling pathways.

The signaling cascade downstream of LANCL2 has been extensively studied in both immune cells including monocytes, macrophages, and T lymphocytes [7,57] and in cell types involved in metabolic regulation, such as adipocytes and skeletal muscle cells [15,35] (**Figure 3**). In innate immune cells, including granulocytes, ABA binding to LANCL2 initiates a well-characterized signaling pathway. This begins with the activation of adenylate cyclase (AC), leading to an increase in intracellular

cAMP levels and subsequent activation of protein kinase A (PKA). PKA then phosphorylates and activates the ADP-ribosyl cyclase CD38, which catalyzes the conversion of NAD^+ to cyclic ADP-ribose (cADPR). cADPR acts as a potent second messenger that induces a rise in intracellular Ca^{2+} levels through two mechanisms: (1) the release of Ca^{2+} from intracellular stores via ryanodine-sensitive channels in the endoplasmic reticulum, and (2) the influx of extracellular Ca^{2+} through ADPR-gated calcium channels located in the plasma membrane.

Additionally, ABA binding with LANCL2 also activates the phospholipase C (PLC) pathway, leading to the production of inositol-1,4,5-trisphosphate (IP_3), which further promotes intracellular Ca^{2+} release. Concurrently, ABA stimulates a protein kinase C (PKC)-dependent adenylate cyclase, amplifying the cAMP signal [7]. This intricate sequence of signaling events strikingly mirrors the ABA signaling pathway initially described in marine sponges [4], suggesting a conserved evolutionary origin. In hematopoietic progenitor cells, ABA's transcriptional effects are mediated by the increase in intracellular cAMP and the activation of the cAMP response element-binding protein (CREB), a key transcription factor regulating gene expression in response to cAMP signaling [9].

In silico modeling by Leber et al. [58] explored the LANCL2-mediated signaling network in macrophages and regulatory T cells, proposing a role for this receptor in modulating immune tolerance and regulatory responses during *H. pylori* infection. In metabolic tissues, particularly adipocytes, abscisic acid (ABA) has been shown to stimulate glucose uptake by promoting the translocation of GLUT4 to the plasma membrane and increasing its expression [6,15]. This process is mediated through the activation of the phosphoinositide 3-kinase (PI3K) pathway, highlighting ABA's role in regulating glucose metabolism independently of insulin signaling [6].

In skeletal muscle cells, the AMP-activated protein kinase (AMPK) pathway plays a key role in mediating ABA's effects at nanomolar concentrations (**Figure 3**). These effect are mediated by both receptors LANCL1 and LANCL2. The overexpression of either LANCL1 or LANCL2 increased the ABA-induced stimulation of glucose uptake and increased the effect of metformin, a stimulator of cell glucose uptake via GLUT4 and AMPK [17]. Conversely, silencing both LANCL1 and LANCL2 had the opposite effect, abrogating the effect of ABA on glucose uptake and significantly reducing the metformin, indicating that ABA and metformin share the same effector kinase AMPK. The overexpression of LANCL1 or LANCL2 stimulate, upon ABA binding, AMPK protein expression and phosphorylation, PGC-1α, Sirt1, and GLUT4 expression, indicating a transcriptional control by LANCL1/2 on these genes. Moreover, the ABA-induced enhancement of glucose transport is abolished when cultured myocytes or murine muscle biopsies are pre-treated with the AMPK inhibitor dorsomorphin, indicating that AMPK is essential for this response [35]. More recently, studies in rat cardiomyocytes and human adipocytes have further elucidated the downstream signaling

mechanisms of ABA. In these cells, both AMPK and the orphan nuclear receptor/transcription factor estrogen-related receptor alpha (ERRα) have been implicated in mediating ABA's action downstream of LANCL2. ABA stimulation in these contexts triggers a complex transcriptional program that promotes mitochondrial biogenesis, enhances oxidative metabolism, and increases mitochondrial uncoupling and oxidative phosphorylation (OXPHOS), largely through coordinated activation of AMPK and ERRα [16,18,19].

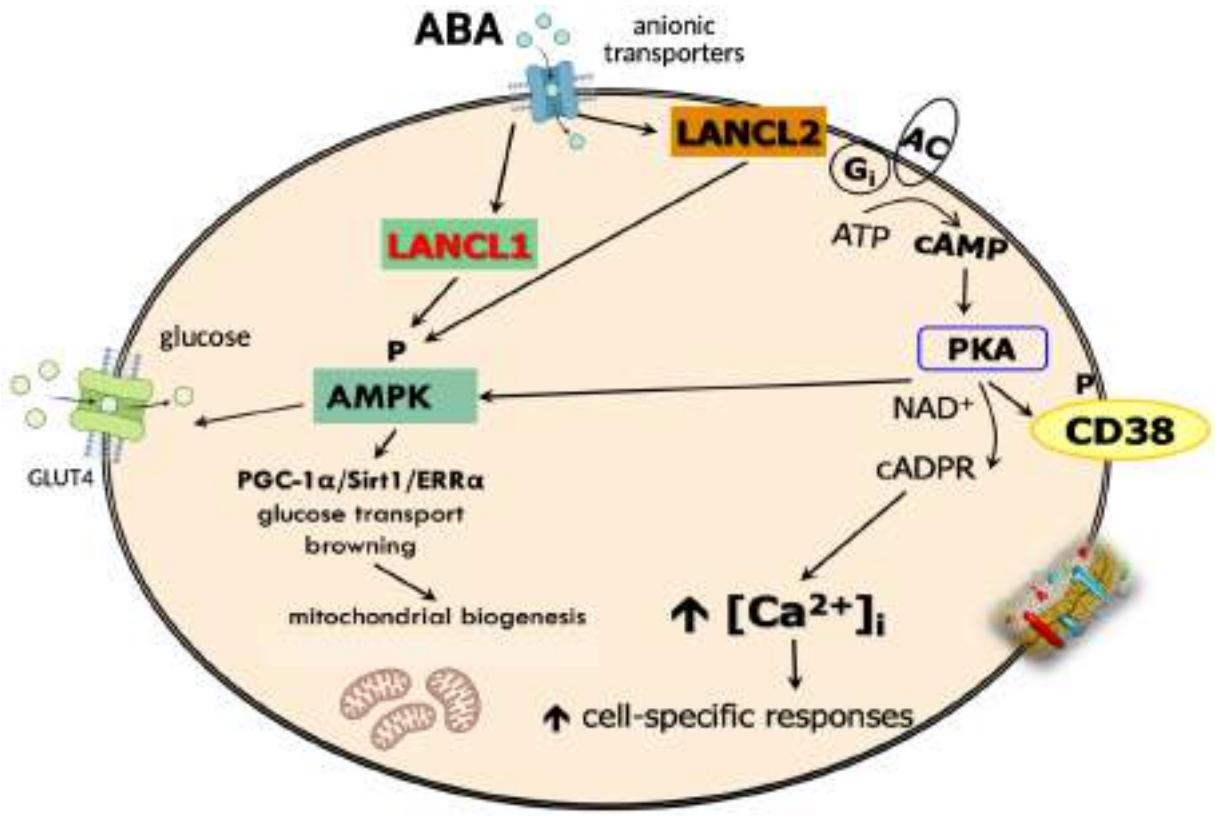

Figure 3. ABA-activated signaling pathways and key metabolic effects. At neutral pH, deprotonated ABA enters the cell via an anionic transporter and binds to cytosolic LANCL1 or membrane-anchored LANCL2. Both receptors activate AMPK and the PGC-1α/Sirt1/ERRα axis, promoting transcriptional programs that enhance glucose uptake, mitochondrial activity, and antioxidant responses. LANCL2 also activates PKA, which phosphorylates CD38, leading to the production of cADPR and ADPR. These messengers trigger a cytosolic Ca^{2+} wave via release from ryanodine-sensitive stores (cADPR) and extracellular influx (ADPR).

1.6. ABA a hormone with multiple regulatory functions.

Over the past two decades, numerous tissue-specific functions of ABA have been identified, revealing its diverse physiological roles across different organ systems. These discoveries have greatly expanded the understanding of ABA as an endogenous signaling molecule beyond its classical role in plants. The following list summarize some of the most prominent and well-characterized functions

of ABA in various mammalian tissues. Most of these functions are only briefly addressed in this introduction, while the present thesis specifically focuses on the roles of ABA in cardiomyocytes and skeletal muscle, as well as on the investigation and characterization of novel LANCL agonists (see Sections 1.6, 1.7, and 1.8).

Control of blood glucose levels: the role of the ABA/LANCL1-2 system has been extensively investigated through *in vitro*, *in vivo*, and clinical studies, all demonstrating a significant function of this hormone in glycemic control. Nanomolar concentrations of ABA modulate the metabolic response to glucose by stimulating glucose uptake in skeletal muscle and adipose tissue via an insulin-independent mechanism [6, 35]. Plasma ABA (ABAp) levels increase after an oral glucose load in healthy individuals but not in those with type 2 diabetes (T2D) or gestational diabetes (GDM) [6, 59]. In GDM, normal ABAp levels are restored after childbirth alongside the resolution of diabetes, indicating ABAp's important role in maintaining normal glucose tolerance and suggesting a new ABA-related mechanism in diabetes [59]. Additionally, ABAp is very low or undetectable in type 1 diabetes (T1D) patients [6], implying that β-cells are the main source of endogenous ABA in humans, and ABA supplementation improve glycemic control in a murine model of type 1 diabetes [60]. Moreover, chronic ABA intake at microgram doses per kilogram of body weight has been shown to improve blood glucose and lipid profiles, while reducing waist circumference and body mass index in individuals at risk of prediabetes and metabolic syndrome [16, 33, 61]. For a detailed and updated overview of the literature on the role of ABA in blood glucose regulation, refer to recent comprehensive reviews [11,12, 14, 34, 62].

Inflammation: ABA has been shown to produce significant anti-inflammatory effects in rodent models of inflammatory bowel disease, atherosclerosis, and viral infection, administration of exogenous [63-68]. Interestingly, ABA is also produced autocrinally by various innate immune cells, including granulocytes, monocyte-macrophages, and microglia, when these cells are exposed to pro-inflammatory stimuli. Moreover, exogenous ABA has been observed to enhance several pro-inflammatory activities in these same cell types [7,69–71]. This dual behavior highlights the complexity of ABA's involvement in inflammation, suggesting that its effects may vary depending on concentration, cell type, and context. Consequently, further research is needed to clarify the distinct roles of ABA in inflammatory processes and to determine the specific conditions under which it exerts anti- or pro-inflammatory actions.

Stem cell regeneration: ABA promotes the expansion of human uncommitted hematopoietic progenitors (HP) in vitro by increasing intracellular calcium via a cADPR-mediated pathway. It also triggers transcriptional changes in $CD34^+$ cells, including NF-κB activation and cytokine gene expression [9]. Additionally, human mesenchymal stem cells (MSC) produce and release ABA in response to specific growth factors [72].

Neuroprotection: ABA has shown promise in preventing age-related neurodegeneration. In Alzheimer's disease (AD) mouse models, early ABA treatment improved cognitive function and reduced neuroinflammation, while later treatment was less effective. In Parkinson's disease (PD) models, ABA helped relieve motor symptoms but did not improve cognitive issues. These findings suggest that ABA may help prevent neurodegenerative diseases by its trophic, anti-inflammatory, and antioxidant properties and reducing insulin resistance [13, 73-78].

Control of adipocyte browning and energy expenditure: Activation of the LANCL1-2/PGC-1α/ERRα pathway in white and brown adipocytes, triggered by LANCL protein overexpression and further enhanced by ABA, leads to multiple metabolic and functional changes that collectively improve the energy production and dissipation capacity of adipose tissue. These changes include increased glucose transport through upregulation of GLUT4, enhanced mitochondrial biogenesis, membrane potential ($\Delta\Psi$), and respiration, as well as elevated expression of receptors for "browning" hormones and uncoupling proteins UCP-1 and UCP-3 [15, 16]. *In vivo*, oral administration of sub-microgram doses of ABA to mice for 30 days induces overexpression of browning-related genes and significantly raises mitochondrial DNA content and oxidative phosphorylation complex I in white and brown adipose tissues, while also stimulating UCP-1 protein expression in brown adipose tissue. A single dose of ABA at 1 μg/kg body weight further promotes glucose uptake by brown adipose tissue in rats [15, 16]. The finding that ABA can reduce inflammation in white adipose tissue in mice on a high-fat diet is particularly significant, suggesting that ABA-containing nutraceuticals may help in mitigating low-grade inflammation in adipose tissue [79,80].

1.7. Role of ABA/LANCL1-2 system in cardiomyocytes functions and metabolism

Recent sudies have highlighted the significant role of ABA and its mammalian receptors, LANCL1 and LANCL2 on cardiomyocytes under both normal oxygen levels and hypoxic stress [18]. Findings show that ABA and its receptors are key regulators of the cardiomyocyte response to low oxygen conditions. In hypoxia, the H9c2 rat cardiomyocyte cell line produces endogenous ABA, which activates the ABA/LANCL1/2 signaling pathway. This activation initiates a cascade involving

AMPK and PGC-1α, leading to transcriptional and post-transcriptional changes that enhance nitric oxide (NO) production. Furthermore, NADPH levels and the NADPH/NADP ratio are significantly higher in cells overexpressing LANCL1/2 compared to those with silenced expression. Since NADPH is vital for NO synthesis and maintaining cellular redox balance, these findings underscore its importance. Notably, H9c2 cells overexpressing LANCL1/2 under hypoxic conditions exhibit a stronger mitochondrial proton gradient (ΔΨ) than cells lacking LANCL1/2, suggesting that the ABA-LANCL1/2 system helps preserve mitochondrial function and supports energy production in cardiomyocytes during hypoxia and subsequent reoxygenation [18]. Mitochondrial function is essential for cardiomyocyte contractility and electrical activity [81, 82]. The ABA/LANCL1-2 system enhances mitochondrial number and membrane potential (ΔΨ) under normal oxygen conditions, boosting cellular respiration and energy production via the AMPK/PGC-1α/ERRα pathway [19]. Furthermore, LANCL1/2-overexpressing H9c2 cells exhibit higher basal and maximal respiration rates than silenced cells, driven largely by an enhanced oxidative metabolism, especially of glucose. In H9c2 cells overexpressing LANCL1/2, glucose transporter and glycolytic enzyme expression increased approximately two fold, leading to a 40% increase in glucose uptake, further tripled by ABA treatment, compared to silenced cells [19]. These cells also showed higher ATP/ADP ratios, increased NAD^+ levels, and elevated fatty acid metabolism, supported by increased expression of fatty acid transport (such as carnitine palmitoyltransferase, CPT1β) and oxidation (such as acyl-coenzyme A dehydrogenase) [19]. In summary, overexpression of LANCL1/2, combined with their activation by ABA treatment, improve cardiomyocyte "fitness" and transforms H9c2 cardiomyoblasts into highly metabolically active "super-cells" (**Figure 4**)

Moreover, the ABA/LANCL1-2 system is closely interconnected with the transcription factor ERRα, which mediates most of the transcriptional effects observed in LANCL1/2-overexpressing cells. This relationship is bidirectional: LANCL1/2 overexpression enhances ERRα transcription and expression, while their silencing markedly reduces it. Conversely, ERRα knockdown lowers endogenous LANCL1/2 mRNA levels in H9c2 cells and significantly diminishes or abolishes the transcriptional and functional effects induced by LANCL1/2 overexpression. ERRα belongs to the estrogen-related receptor (ERR) subfamily, part of the nuclear receptor superfamily, which also includes ERRβ and ERRγ [83]. Nuclear receptors act as ligand-regulated transcription factors that translate external signals, such as hormones, vitamins, or metabolites, into gene expression changes. ERRα, an orphan receptor with no identified natural ligand, is ubiquitously expressed and is the predominant isoform within its family. It plays a pivotal role in regulating mitochondrial function and thermogenesis in cardiomyocytes [84]. From early myocyte maturation through adulthood, ERRα works in concert with PGC-1α, with which it maintains a positive reciprocal regulation [85–87].

Together, the ERRα/PGC-1α axis governs cardiac energy metabolism, mitochondrial respiration and biogenesis, and overall metabolic flexibility, thereby enhancing cardiac performance [88,89] (**Figure 4**).

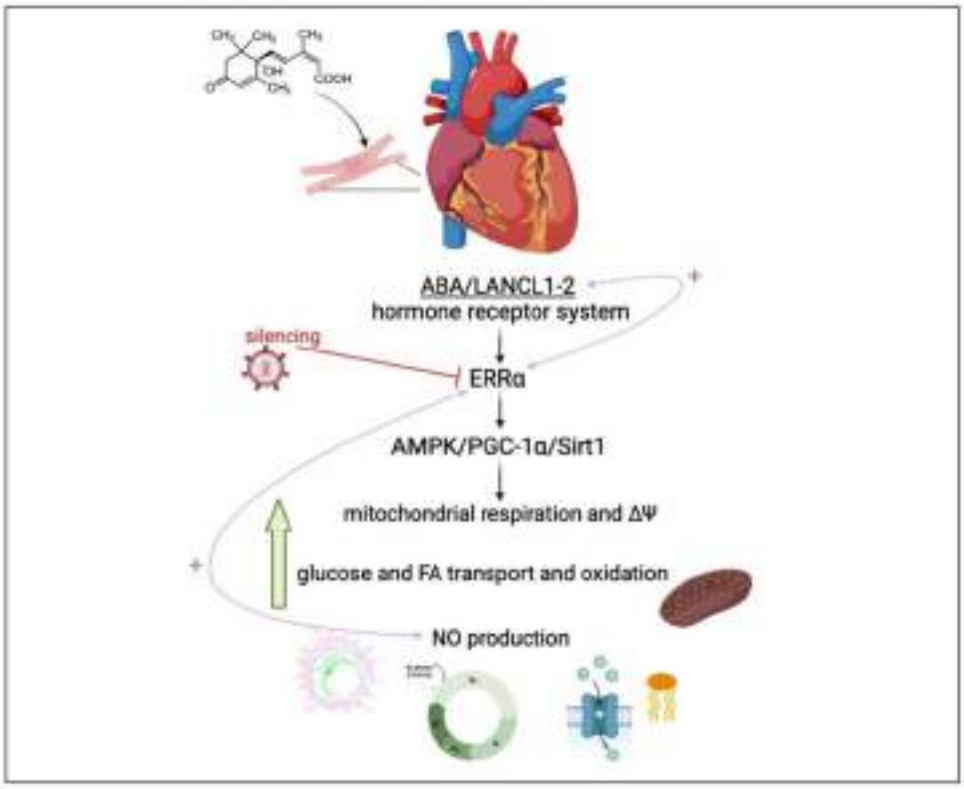

Figure 4. The ABA/LANCL1-2 hormone–receptor system regulates cardiomyocyte function and energy metabolism through nitric oxide (NO) and the transcription factor ERRα. In H9c2 rat cardiomyocytes, LANCL1/2 overexpression activates the AMPK/PGC-1α/Sirt1 axis via ERRα [18,19], establishing a reciprocal regulatory loop in which LANCL1/2 and ERRα enhance each other's transcription. This signaling cascade promotes increased oxidative metabolism, ATP production, and NO synthesis, creating a positive feedback mechanism that sustains a high-energy, metabolically efficient state [18,19].

In light on these previous findings, first this thesis investigates the role of the ABA/LANCL1-2 system in the regulation of reactive oxygen species (ROS) metabolism in H9c2 rat cardiomyocytes overexpressing LANCL1/2, compared with LANCL1/2-silenced H9c2 cells.

ROS such as superoxide anion ($O_2^{\bullet -}$), hydroxyl radical (•OH) are generated within cells through endogenous processes like mitochondrial oxidative phosphorylation and the activity of enzymes including cyclooxygenase-2 (COX2), xanthine oxidase (XO), and NADPH oxidase (NOX) or from external sources such as ionizing radiation and bacterial infection [90,91]. At physiological levels, ROS act as signaling molecules in gene regulation and transduction pathways. However, excessive

ROS production disrupts cellular redox balance, damaging lipids, proteins, and nucleic acids, and leading to oxidative stress. This condition contributes to the pathogenesis of several diseases, including obesity, diabetes, cardiovascular and respiratory disorders, neurodegenerative diseases, rheumatoid arthritis, and cancer [92,93]. To maintain redox homeostasis, cells rely on antioxidant defenses comprising non-enzymatic molecules, such as vitamins E and C, β-carotene, glutathione (GSH), coenzyme Q, and bilirubin, and enzymatic systems, including superoxide dismutase (SOD), glutathione peroxidase (GPX), and catalase [94].

Transcriptional control of metabolic genes is central to ROS regulation, with estrogen-related receptors (ERRs) emerging as key modulators of energy metabolism and oxidative balance [95,96]. In particular, ERRα controls the transcription of key enzymes in the TCA cycle and numerous genes encoding components of oxidative phosphorylation (complexes I–V, coenzyme Q, and cytochrome c) [95]. The PGC-1α/ERRα complex further regulates the expression of genes involved in ROS metabolism, including those encoding NOX4, NOX5, XDH, CAT, GPX, and SOD2 [95,97].

This thesis aimed to elucidate the role of the ABA/LANCL1-2 system in ROS production and detoxification by analyzing the expression of key enzymes involved in these pathways and its possible interaction with ERRα signaling in H9c2 cardiomyocytes [98]. H9c2 cardiomyocytes were chosen for its known protection against hypoxia/reoxygenation-induced oxidative damage upon LANCL1/2 overexpression [18].

1.8. Role of ABA/LANCL1-2 system in skeletal muscle.

The primary role of the ABA/LANCL1-2 system in skeletal muscle is the regulation of glucose uptake. Skeletal muscle, which accounts for about 40% of total body weight in humans and, together with adipose tissue, represents the majority of mammalian cell mass [99-101], responds to ABA with enhanced glucose uptake and metabolism, potentially improving whole-body glucose homeostasis [102-104]. Initial studies on rat L6 myoblasts showed that nanomolar concentrations of ABA stimulate glucose uptake to a level comparable with insulin by promoting GLUT-4 translocation, independently of insulin [6]. Subsequent *ex vivo* experiments confirmed that ABA enhances glucose uptake in murine muscle biopsies through AMPK activation, as inhibition by dorsomorphin blocked the effect [35, 105-107]. *In vivo*, treatment of rats with 1 µg ABA/kg BW significantly increased skeletal muscle glucose uptake, accelerated blood glucose clearance, and doubled whole-body glucose uptake [35]. ABA-treated rats also exhibited a reduced plasma glucose AUC, while insulin secretion was markedly lower, indicating that ABA improves glycemia with minimal β-cell stimulation [10]. Additional evidence of ABA's stimulation of muscle glucose uptake comes from

studies on chronically ABA-treated mice, which displayed increased skeletal muscle glycogen content and improved glucose tolerance. These mice also showed enhanced physical performance when given free access to a running wheel: ABA-treated animals ran approximately 2.5 times longer, covered nearly twice the distance, and reached a maximal speed 3.2 times higher than untreated controls [35]. In a separate study, administration of an ABA-enriched extract at 0.125 µg/kg body weight improved glucose tolerance, insulin sensitivity, and fasting blood glucose in diet-induced obesity (DIO) and db/db mouse models, without elevating insulin levels. The extract further promoted muscle metabolism by upregulating genes involved in glycogen synthesis, glucose and fatty acid metabolism, and mitochondrial function. However, the absence of LANCL2 in muscle tissue abolished these effects, resulting in higher fasting blood glucose [36]. The action of ABA on muscle cells is dependent on AMPK activation, which subsequently enhances GLUT4 and GLUT1 expression, mitochondrial respiration, and the production of uncoupling proteins such as sarcolipin and UCP3 [17,108-110]. The observed increase in uncoupling protein expression aligns with recent findings in rat H9c2 cardiomyocytes, where the ABA/LANCL receptor system was shown to regulate cellular thermogenesis, as evidenced by higher heat production in LANCL1/2-overexpressing cells compared with double-silenced cells [111]. Overall, ABA/LANCL1-2–mediated stimulation of muscle glucose uptake, thermogenesis, and metabolism may play a significant role in supporting normal body weight [112,113]. In this thesis the potential role of the ABA/LANCL1-2 system in regulating the expression of genes involved in skeletal muscle thermogenesis and differentiation was investigated, aiming to provide further insights into the broader physiological functions of this signaling pathway in skeletal muscle.

1.9. Investigation and functional characterization of novel LANCL agonists.

Considering the significant and beneficial effects of the ABA/LANCL1-2 system on the metabolism of diverse cell types, investigating molecules that can specifically activate this system and its receptors constitutes a particularly promising and impactful area of research.

To date, only a limited number of ABA analogues have been biologically evaluated and investigated as potential LANCL2 ligands, along with other structurally distinct chemical entities [114,115]. The first compound studied was the patented molecule BT-11 [116], identified as a LANCL2 agonist capable of reducing inflammation in multiple mouse models of inflammatory bowel disease (IBD) (Omilancor, Phase 2 recently completed) [117]. BT-11 has also shown therapeutic potential for ulcerative colitis, Crohn’s disease [118], and Alzheimer’s disease [119]. Toxicological studies

demonstrated that BT-11 is a safe and well-tolerated oral drug candidate, with no observed adverse effects [120, 121].

More recently, a novel molecule named NIM-1324 has been identified as an oral LANCL2-targeting compound. In human immune cells, NIM-1324 reduces type I interferon and inflammatory cytokine production, exhibiting an improved pharmacokinetic profile suitable for the treatment of systemic autoimmune diseases [122]. To support the rational design of novel LANCL2 agonists, a computational study involving molecular docking and long molecular dynamics (MD) simulations of both ABA and BT-11 was performed at the University of Genova. These analyses identified the key chemical features required for LANCL2 ligand binding, guiding the virtual screening and selection of a new potential LANCL2 agonist, AR-42 [123].

In this thesis, biochemical assays performed on rat H9c2 cardiomyocytes stimulated with BT-11 and AR-42 are reported. The effects of these agonists on the mitochondrial proton gradient and on the transcriptional activation of the AMPK/PGC-1α/Sirt1 axis were also investigated. In addition, preliminary binding studies were performed to evaluate the interaction of AR-42 with human recombinant LANCL2 protein.

2. MATERIALS AND METHODS

2.1. Cell culture

H9c2 rat cardiomyoblasts (CRL-1446) and C2C12 mouse myoblasts (CRL-1772) (**Figure 5**) were obtained from the American Type Culture Collection (ATCC; LGC Standards, Milan, Italy). The cells were maintained under standard culture conditions using Dulbecco's Modified Eagle Medium (DMEM) with high glucose content (Euroclone, Milan, Italy), enriched with 10% heat-inactivated fetal bovine serum (FBS) and supplemented with 1% penicillin-streptomycin (Euroclone, Milan, Italy). Cultures were kept at a constant temperature of 37°C in a humidified incubator with an atmosphere of 5% CO_2. Subculturing was routinely performed once the cells reached approximately 70–80% confluence in order to maintain them in an actively proliferating state. In total, around 15 serial passages were carried out throughout the study, and all experimental procedures were conducted using cells between passages 5 and 15.

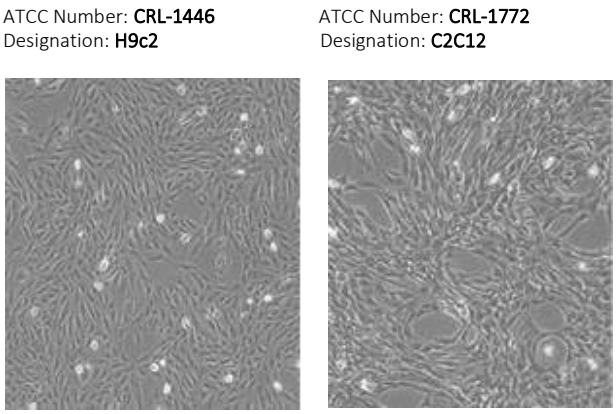

Figure 5. Rat H9c2 cardiomiocytes and murine C2C12 myoblasts.

2.2. Lentiviral and retroviral cell transduction

Lentiviral plasmids pLV[shRNA]-Puro-U6 encoding a control scramble shRNA (plasmid ID: VB010000-0005mme), shRNAs targeting rat LANCL1 and LANCL2 (plasmid IDs: VB181016-1107sen and VB181016-1124zjp, respectively), rat ERRα (plasmid ID: VB221005-1073jxq), mouse LANCL1 and LANCL2 (plasmid IDs: VB250224-1352efz and VB250702-1122vbw, respectively) were purchased from VectorBuilder (Chicago, IL, USA). Overexpression of human LANCL1 and LANCL2 (OVL1+2) in H9c2 rat cardiomyocytes and C2C12 mouse myoblasts was achieved using pBABE vectors constructed as previously described [18]. The empty pBABE vector (Addgene, Watertown, MA, USA) was used as a negative control (PLV). To generate H9c2 and C2C12 cell lines

stably silenced or overexpressing LANCL1 and LANCL2, the following procedures were employed. For gene silencing, lentiviral vector particles were produced in HEK-293T cells (Human Embryonic Kidney 293Tcell line). Briefly, HEK-293T cells were seeded at a density of 3×10^5 cells on 6-cm dish in DMEM supplemented with 10% FBS and 1% penicillin–streptomycin. After 24 hours, cells were co-transfected with the packaging plasmid Δ891, the envelope plasmid VSV-G, and the respective shRNA transfer lentiviral plasmids shRNA-Scramble (SCR)**,** shRNA-LANCL1 and shRNA-LANCL2 (SHL1+L2), shRNA-ERRα (SHERRα) using the PolyJet™ transfection reagent (Tebu-bio, Milan, Italy), according to the manufacturer's instructions (**Figure 6**). After an additional 24 hours, the culture medium of HEK-293T cells was replaced with fresh DMEM supplemented with 10% fetal bovine serum (FBS) and 1% penicillin–streptomycin to promote viral particle production. The supernatants containing lentiviral particles were collected 48 and 72 hours post-transfection, filtered through a 0.45-μm pore-size filter, and used to infect H9c2 or C2C12 cells (1×10^6 cells per 10-cm dish, plated the day before) in the presence of protamine sulfate (final concentration: 5 μg/mL). Following two rounds of infection, cells were selected with puromycin (5 μg/mL for H9c2 and 4 μg/mL for C2C12). Knockdown efficiency was assessed by quantifying LANCL1 and LANCL2 expression at both mRNA and protein levels using real-time PCR and Western blot analysis, respectively. For overexpression of LANCL1 and LANCL2 in H9c2 and C2C12 cells, the same procedure described above was followed, except for the use of the specific overexpression plasmids (as previously indicated) and HEK-Plat-A/Phoenix cells for retroviral packaging. The HEK-Plat-A/Phoenix cell line is a retroviral packaging cell line derived from the HEK-293T cell line. It is specifically designed for rapid, transient production of high-titer retrovirus, using a packaging constructs with an EF1α promoter, which ensures longer stability and high-level expression of retroviral structural proteins (gag, pol, amphotropic env). This results in higher viral yields compared to traditional based retroviral packaging cell lines [124]. These cells were transfected under the same conditions described above using for transfection only the specific plasmids PLV, pBABE-LANCL1 and pBABE-LANCL2 as they already contain the packaging and the envelope plasmids; the retroviral particles produced were subsequently used to infect target cells (**Figure 6**). Overexpression efficiency was verified by Western blot analysis. After transduction, H9c2 cells were incubated with or without 100 nM ABA for 4 hours, while C2C12 overexpressing or silenced cells were differentiated as described in the following paragraph.

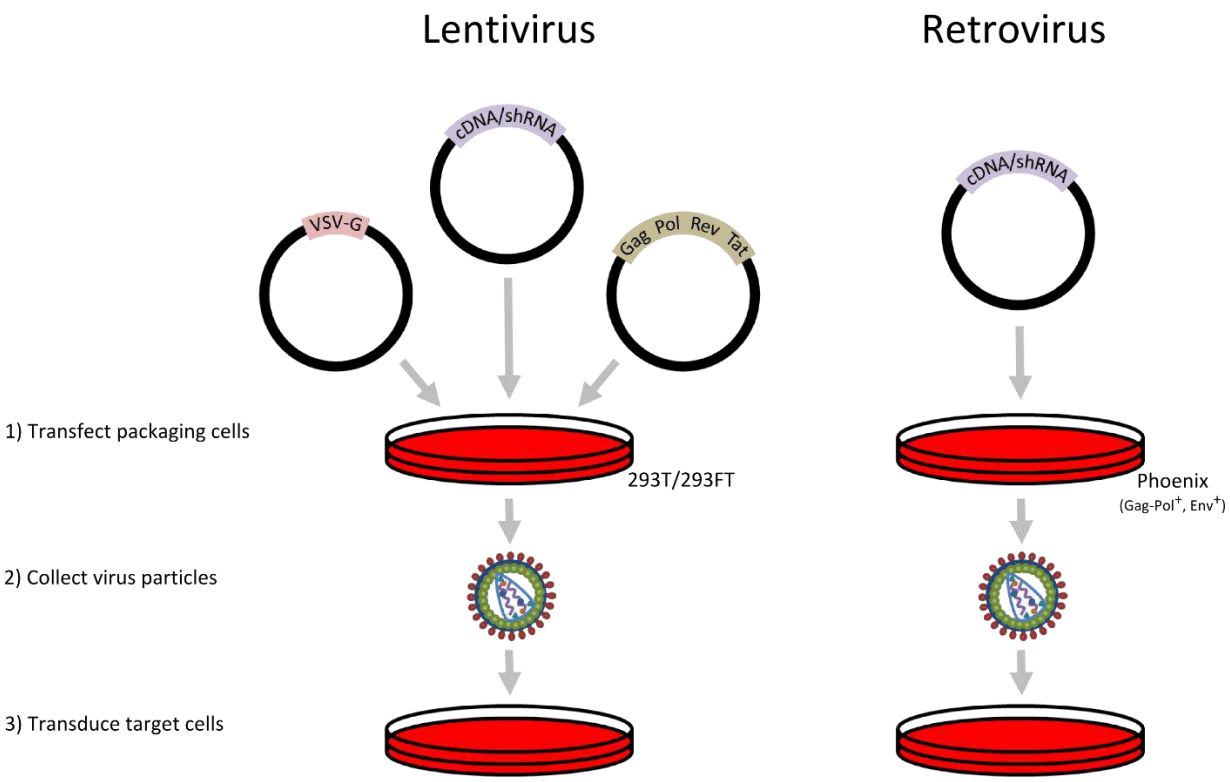

Figure 6. Lentiviru s and retrovirus production in packaging cells.

2.3. C2C12 differentiation protocol

C2C12 myoblast differentiation was carried out following the protocol described by Jang et al. (2022). Prior to cell seeding, all culture plates were pre-coated with a rat collagen solution to create a thin collagen layer on the surface of tissue culture dishes (STEMCELL Technologies, Vancouver, Canada). Briefly, a diluted collagen solution (1:45) was prepared in sterile PBS and added to 6-well or 60 mm culture plates. The plates were then incubated at 37°C for 1 hour to allow coating. After incubation, the collagen solution was removed, and the plates were rinsed once with sterile PBS, air-dried under sterile conditions, and subsequently used for cell plating.

C2C12 myoblasts were seeded at an initial density of 15,000 cells/cm² and maintained for two days to allow proliferation until reaching approximately 90–100% confluence. Cells were cultured in three different growth media conditions: basal DMEM, DMEM supplemented with 10% FBS, or DMEM supplemented with 2% B27 (Life Technologies, Milan, Italy). After the initial proliferation period, the culture media were replaced according to the differentiation scheme described above **(Figure 7)** [125]. Specifically, the cultures maintained in DMEM supplemented with 10% FBS were subsequently replaced with DMEM supplemented with 2% HS (Horse Serum, Euroclone, Milan, Italy), while those grown in DMEM supplemented with 2% B27 were replaced with DMEM

containing 1% B27, respectively. The culture medium was refreshed every two days, and cells were further incubated for 5 additional days to promote myotube formation. Cells grown in basal DMEM were continuously maintained in the same medium for the duration of the experiment and were used as a negative control for differentiation.

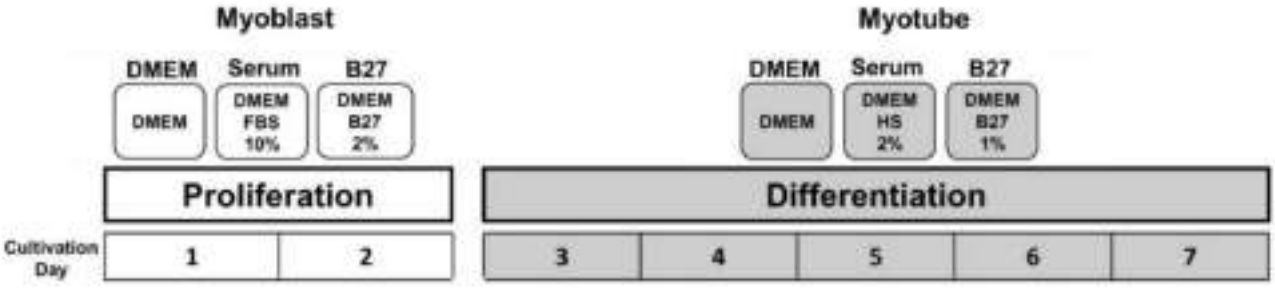

Figure 7. Schematic representation of the experimental protocol for C2C12 myoblasts differentiation, adapted from Jang et al. [125].

2.4. qRT-PCR analysis

Total RNA was extracted from rat H9c2 cariomyocytes and C2C12 differentiated cells using RNeasy Micro Kit (Qiagen, Milan, Italy) according to the manufacturer's instructions. The cDNA was synthesized by using High Capacity cDNA Synthesis Kit (ThermoFisher Scientific, Monza, Italy) starting from 2 μg of total RNA and was used as a template for qPCR analysis: reactions were performed in an QuantStudio1 Real-Time PCR System (ThermoFisher Scientific, Monza, Italy). The rat-and mouse- specific primers were designed using the tool Pick Primers on National Center for Biotechnologies Information (NCBI) database and their sequences are listed in **Table 2** (primer sequences used to amplify rat target genes), **Table 3** (primer sequences used to amplify mouse target genes). Each sample was assayed in triplicate in a 25 μl amplification reaction, containing 4 ng of cDNA, primers mixture (0.4 μM each of sense and antisense primers) and 12.5 μl of 2X PowerUp™ SYBR™ Green Master Mix (ThermoFisher Scientific, Monza, Italy). The amplification program included 40 cycles of two steps, each comprising heating to 95°C and to 62°C, respectively. Fluorescence products were detected at the last step of each cycle. To verify the purity of the products, a melting curve was produced after each run. Values for mouse and rat genes were normalized on Hypoxanthine-guanine Phosphoribosyltransferase-1 (Hprt1) and TATA-Box Binding Protein (Tbp) mRNA expression. Statistical analysis of the qPCR was performed using the QuantStudioTM Design & Analysis Software version 1.5.2 based on the $2^{-\Delta\Delta Ct}$ method [126]. The dissociation curve for each amplification was analyzed to confirm the absence of nonspecific PCR products.

Table 2

Rat genes	Accession N°	Forward Primer 5'-3'	Reverse Primer 5'-3'
Lancl1	NM_053723	TCTTGCTCCTCATCCTGCTCATC	CACTGTACTCGCCGAAGGTCTC
Lancl2	NM_001014187	GGTGCCACGGTGCTCCAG	CCTCGCTGCCAAATCACATCAC
Sod2	NM_017051	TAAGGGTGGTGGAGAACCCA	ACCTTGGACTCCCACAGACA
Nox4	NM_053524	CTGTACAACCAAGGGCCAGA	GCTCTGCTCAAACACAATCCT
Gpx4	NM_017165	CCGTCTGAGCCGCTTATTGA	AATCATCGCGGGATGCACA
Cox2	S67722	GTGAAAACTGTACTACGCCGAG	TACTGTGTTTGGGGTGGGCT
Xor	NM_017154	TCCCTGCGTTTGGTAGCATC	CCAGGAAAAGAGGTGGCTCC
Ppargc1a	NM_031347	GCACACATCGCAATTCTCCC	CTCTGCGGTATTCGTCCCTC
Prkaa1	NM_019142	AGAAGCAGAAGCACGACGG	GAAGGTGCCGACGCCC-
Sirt1	NM_001372090	CAGTGTCATGGTTCCTTTGC	CACCGAGGAACTACCTGAT
eNos	NM_021838	AGGCCTTGGTATTGGTGGTG	TAGGGGCCCGACATTTCC AT
Tbp	NM_001439799	TCAAACCCAGAATTGTTCTCCT	TCTGCTCTAACTTTAGCACCTGT
Hprt1	NM_012583	TTGGTCAAGCAGTACAGCCC	TGGCCTGTATCCAACACTTCG

Table 3

Mouse genes	Accession N°	Forward Primer 5'-3'	Reverse Primer 5'-3'
Lancl1	NM_001190985	GAGGGCCTTTCCGAATCCTT	GGAGTCAGCCTCCCAGTAGA
Lancl2	NM_133737	GCCTCCCTTTCCACCCTAACG	GTCCGCTGTCTTCAGTCCTTCC
MyHC-I	NM_080728	CAGCAGTTGGATGAGCGACT	GCTCATCCTCAATCCTGGCAT
MyHC-IIb	NM_010855	TCACAGTGCCCAGCATTGAT	CATCTGCACTGAATCCCAGG
Myh7	NM_001425737	TTACTTGCTACCCTCAGCTCTTC	CAGCCCCAAATGCAGCCATC
Myog	NM_031189	CCCTACAGACGCCCACAATC	TTTCGTCTGGGAAGGCAACA
Ckm	NM_007710	GGCTCATCCGAAGTCGAACA	TCGATGGACTGGCCCTTTTC
Mt-ND1	NC_005089	CCACGCTTCCGTTACGATCA	CCCTGACAGTCCAAAGGGTT
Sln	NM_025540	CAGGAGCTGTTTATCAACTTCA	TTGGTAGGACCTCACGAGGAG
Ucp3	NM_009464	CCCTCTGCACTGTATGCTGAA	CATCACGTTCCAAGCTCCCA
Tbp	NM_013684	GAAGCTGCGGTACAATTCCAG	CCCCTTGTACCCTTCACCAAT
Hprt1	NM_013556	CCCTGGTTAAGCATACAGCCCC	GTCTGGCCTGTATCCAACACTTC

2.5. Western blot analysis

After transduction, H9c2 cells (1×10^6/well) were plated in 6-well plates and allowed to adhere for 24 h. After serum deprivation and low-glucose DMEM incubation for 18 h, cardiomyocytes were then incubated for 1 h at 37 ◦C with or without 100 nM ABA or other compounds as BT11 and AR42. Thereafter, cells were lysed in ice-cold lysis buffer (20 mM Tris-HCl pH 7.4, 150 mM NaCl, 1 mM EDTA, 1% NP40 and Protease Inhibitor Cocktail) and briefly sonicated, and the protein concentration was determined according to a standard Bradford assay. C2C12 cell lysates were obtained following the same procedure after completion of the differentiation protocol. Proteins (30 μg) were loaded on 10% polyacrylamide gel and separated by SDS-PAGE and proteins were transferred to nitrocellulose membranes (Bio-Rad, Milan, Italy) according to standard procedures. The membranes were blocked for 1 h with 20 mM Tris-HCl pH 7.4, 150 mM NaCl and 1% Tween 20 (TBST) containing 5% non-fat dry milk and incubated for 1 h at room temperature with primary antibodies (**Table 4**). Following incubation with the appropriate secondary antibodies (**Table 4**) and ECL detection (GE Healthcare, Milan, Italy), band intensity was quantified with the ChemiDoc imaging system (Bio-Rad, Milan, Italy). The expression levels of the proteins of interest was normalized against vinculin and actin (the latter only for xanthine oxidase), which were used as housekeeping proteins.

Table 4

Primary Antibody	**Host**	**Concentrations**	**Manufacturer**
Anti-LANCL1	Rabbit	1:250	Novus Biologicals
Anti-LANCL2	Mouse	1:1000	Reference [127]
Anti-XO	Mouse	1:100	Santa Cruz Biotechnology Inc., California
Anti-COX2	Goat	1:200	Santa Cruz Biotechnology Inc., California
Anti-SOD2	Rabbit	1:5000	Abcam
Anti-GPX4	Mouse	1:100	Santa Cruz Biotechnology Inc., California
Anti-ERRα	Mouse	1:200	Santa Cruz Biotechnology Inc., California
Anti-vinculin	Rabbit	1:1000	Cell Signaling Technology, Danvers, MA
Anti-Actin	Mouse	1:1000	Santa Cruz Biotechnology Inc., California
Secondary Antibody	**Concentrations**		**Manufacturer**
Anti-Mouse	1:2000		Santa Cruz Biotechnology Inc., California
Anti-Rabbit	1:1000		Santa Cruz Biotechnology Inc., California
Anti-Goat	1:1000		Santa Cruz Biotechnology Inc., California

2.6. Cell Viability Assay

H9c2 cell viability was assessed using the resazurin assay, as previously described [128]. The resazurin assay, also known as the Alamar Blue assay, is a simple, rapid, and sensitive method used to measure cell viability and metabolic activity. Briefly, H9c2 exponentially growing cells were seeded in 96-well microplates at a density of 1×10^4 cells/well and incubated overnight in complete DMEM medium. After 24 h, cells were treated for 3 hours with hydrogen peroxide (H_2O_2) at two different concentrations of H_2O_2 (200 µM and 600 µM) in 100 µl of serum-free DMEM medium. In a separate experiment, H9c2 cells were incubated for 24 hours with BT-11 or AR-42 at concentrations of 1, 5, 10, 50**,** and 100 µM (100 µL per well). After treatment, 20 ul of resazurin solution (0.15 mg/ml in PBS) was added to each of the well and the plates were incubated at 37 °C for an additional 4 hours. Resazurin is a blue, non-fluorescent, cell-permeable dye that living cells reduce to the pink and highly fluorescent compound resorufin. The amount of resorufin produced is proportional to the number of viable cells and can be measured by fluorescence **(Figure 8).** Fluorescence was measured at 570 nm (excitation) and 590 nm (emission) using a Clariostar Plus plate reader (BMG Lab Technologies, Ortenberg, Germany). Cell viability was expressed as a percentage of untreated control cells (100%).

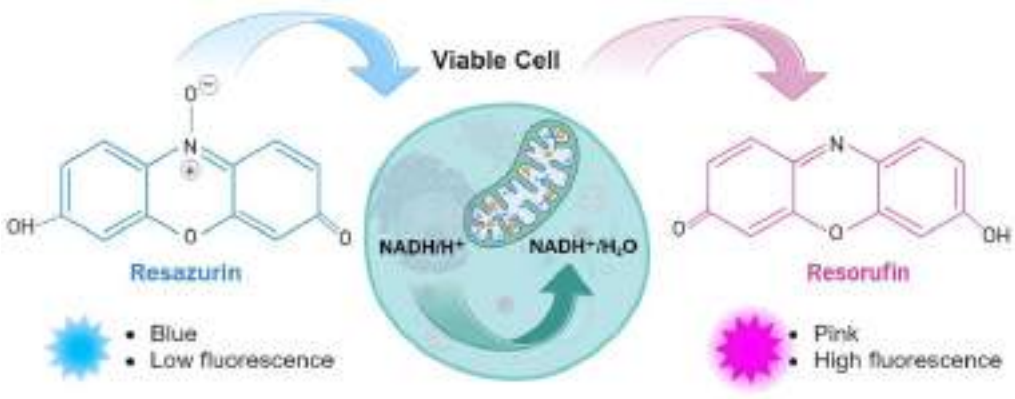

Figure 8. Schematic representation of the underlying mechanism of the resazurin cell viability assay, showing how metabolically active, viable cells reduce the blue, non-fluorescent resazurin to pink, highly fluorescent resorufin.

2.7. Lipid Peroxides Measurement

Lipid peroxidation in live cells was determined using the fluorescence probe C11-BODIPY 581/591 (ThermoFisher Scientific, Milan, Italy) according to the manufacturer's instructions. This assay is based on the property of C11-BODIPY 581/591, a lipophilic fatty acid analog, to integrate into

cellular membranes. Upon oxidation by reactive oxygen species, the probe undergoes a spectral shift: its fluorescence emission changes from 590 nm (red) in the reduced form to 510 nm (green) in the oxidized form due to oxidation of the phenylbutadiene segment of the fluorophore [129]. This shift results in a decreased 590/510 nm fluorescence ratio compared with untreated cells. Briefly, cells were plated and treted with H_2O_2 (200 µM and 600 µM, respectively) as described in paragraph 2.6. After H_2O_2 treament, C11-BODIPY 581/591 reagent was added to each well with a final concentration of 1 µM and incubated for 30 min. After incubation, the medium was removed and the cells were washed three times with PBS and fluorescence emission at 590 and 510 nm was determined using Clariostar plus plate reader.

2.8. ROS detection assays

Intracellular and mitochondrial ROS levels were assessed using two different fluorescent probes: 2',7'-dichlorodihydrofluorescein diacetate (H_2DCFDA) and MitoSOX™ Red [130,131]. H_2DCFDA is a cell-permeable compound that, once inside the cell, is deacetylated by intracellular esterases to a non-fluorescent form. Upon oxidation by ROS, it is converted into the highly fluorescent 2',7'-dichlorofluorescein (DCF), thus serving as a general indicator of overall cellular ROS production. In contrast, MitoSOX™ Red selectively localizes to the mitochondria, where it specifically detects superoxide anions generated within the mitochondrial matrix. For H_2DCFDA-based ROS detection**,** H9c2 cells were seeded in 96-well plates at a density of 1×10^4 cells per well and cultured overnight in high-glucose DMEM supplemented with 10% FBS and 1% penicillin–streptomycin. The following day, cells were washed once with HBSS and incubated for 45 minutes at 37 °C with 10 µM H_2DCFDA in HBSS, either in the absence or presence of 100 nM ABA. After incubation, the supernatant was removed, cells were washed once with HBSS, and 100 µL of fresh HBSS was added to each well. Fluorescence intensity was measured using a Clariostar Plus plate reader at 488 nm excitation and 530 nm emission. For each condition, the mean fluorescence value was calculated from five sequential readings per well**,** with at least eight replicate wells analyzed per experimental group.

For mitochondrial ROS detection**,** MitoSOX™ Red reagent (5 mM; Thermo Fisher Scientific, Monza, Italy) was first dissolved in DMSO according to the manufacturer's instructions and subsequently diluted in HBSS to prepare a 5 µM working solution. Following this, cells were incubated with 500 µL of the working solution for 20 minutes at 37 °C in a humidified CO_2 incubator to allow for probe uptake and mitochondrial localization. After incubation, cells were gently washed with HBSS to remove excess dye and immediately imaged using a Leica TCS SP2 confocal microscope equipped with a 60× oil-immersion objective (NA 1.4). Excitation was performed at 510

nm, and emission was collected at 580 nm to specifically detect the oxidized MitoSOX signal. Quantitative image analysis was carried out using FIJI/ImageJ software (version 2.14.0/1.54f) [132]. After background subtraction, fluorescence intensity was measured within specific selected regions (ROIs). For each condition, multiple fields and at least three independent experiments were analyzed.

2.9. JC-1 analysis

Mitochondrial membrane potential (ΔΨm) was assessed in H9c2 cells using the cationic fluorescent dye JC-1 (ThermoFisher Scientific, Monza, Italy), which exhibits potential-dependent accumulation within mitochondria. At low mithocondrial membrane potentials, JC-1 remains in its monomeric form emitting a green fluorescence (emission at 527 nm), whereas, at high membrane potentials, the dye forms aggregates characterized by a red fluorescence (emission at 590 nm). Thus, mitochondrial depolarization is indicated by a decrease in the red/green fluorescence intensity ratio [133]. Briefly, H9c2 cells were seeded at 3×10^4 onto µ-slide wells, treated or not with 10 µM ABA, BT-11, and AR-42 for 2 h, stained with JC-1 (2.5 µg/mL) for 20 min at 37 ◦C in a 5% CO2 incubator and then imaged live. Quantitative analysis of the red/green fluorescence ratio, reflecting the mitochondrial proton gradient, was performed after background subtraction using ImageJ software. For each condition, multiple fields and cells (ROIs) were analyzed across at least three independent experiments, and the mean fluorescence ratio was used as an indicator of mitochondrial membrane potential.

2.10. Expression and purification of recombinant human LANCL2 protein

Recombinant human LANCL2 protein was produced in *Escherichia coli* BL21 cells transformed with the pGEX-6P1 expression vector containing the LANCL2 coding sequence, constructed as previously described [29]. Bacterial cultures were grown in Luria–Bertani (LB) medium (Merck, Milan, Italy) supplemented with 200 µg/mL ampicillin at 37 °C with shaking until reaching an optical density (A_{600}) of 0.4. Protein expression was then induced by adding isopropyl β-D-1-thiogalactopyranoside (IPTG) to a final concentration of 0.2 mM, followed by incubation for 16 hours at 20 °C to promote soluble expression of the GST-tagged LANCL2 fusion protein (LANCL2–GST). Cells were harvested by centrifugation and lysed by sonication in 125 mM Tris-HCl pH 8.0 and 150 mM NaCl. After lysis, Triton X-100 was added to a final concentration of 1% (v/v), and lysates were incubated for 30 minutes at 4 °C under gentle agitation to ensure complete solubilization of membrane-associated proteins. The lysates were then clarified by centrifugation at 10,000 × g for 15 minutes at

4 °C. The resulting supernatant containing the LANCL2–GST fusion protein was purified by affinity chromatography on glutathione (GSH)–Sepharose 4B resin (Euroclone, Milan, Italy), according to the manufacturer's instructions. LANCL2-GST was eluted from GSH-Sepharose-4B by incubating the resin for 15 min at 25 °C with 10 mM GSH in 50 mM Tris–HCl, pH 8.0. Release of native LANCL2 was achieved with the PreScission Protease (Euroclone, Milan, Italy), by incubating the GSH-Sepharose-bound fusion protein for 16 h at 4 °C in Tris–HCl pH 7.5, 150 mM NaCl, and 1 mM DTT (dithiothreitol). GSH was removed from LANCL2 recombinant protein through an Amicon Ultra centrifugal filters with a 30 kDa molecular weight cutoff (Millipore, Milan, Italy) and both proteins were simultaneously concentrated. Protein concentration was quantified by the Bradford assay (Bio-Rad, Milan, Italy), while protein purity and homogeneity were assessed by SDS–PAGE. Gels were visualized using QC Colloidal Coomassie Staining Solution (Bio-Rad, Milan, Italy).

2.11. Surface plasmon resonance (SPR)

The binding of AR42 to recombinant hGST-LANCL2 was measured by surface plasmon resonance (SPR) on a Biacore T200 instrument at 25°C using a CM7 sensor chip (GE Healthcare, Milan, Italy). These experiments were performed in collaboration with University of Pavia as already described before [53]. First, the pre-concentration ability of the chip in a range of pH values (10 mM Na acetate, pH 4, 4.5, 5 and 5.5) was evaluated at a standard concentration (30 μg/ml). The covalent coupling of hGST-LANCL2 was then performed using 10 mM Na acetate pH 4 through standard amine coupling. A surface without the immobilized protein was used as a reference channel. All experiments were performed with a running buffer consisting of PBS with the addition of 0.05% Tween 20 (PBS-P) using a flow rate of 30 μl/min. Evaluation of AR42 binding to hGST-LANCL2 was performed by injecting AR42 dissolved in DMSO at low micromolar range from 0.01 to 1 μM at a flow rate of 30 ml/min, with a contact time of 30 s and a dissociation time of 120 s. The obtained sensorgrams were used for equilibrium state affinity analysis using the Biacore Evaluation Software version 3.1.

2.12. Thermal Shift Analysis (TSA)

Preliminary Thermal Shift Assay (TSA) experiments were carried out as described before [134] to evaluate the binding of AR-42 to recombinant human LANCL2 (h-LANCL2). The QuantStudio™ 1 instrument (Thermo Fisher Scientific, Milan, Italy), equipped with the Protein Thermal Shift™ Software v1.4, was used for TSA analysis together with the Protein Thermal Shift™ Starter Kit, following the manufacturer's instructions (Life Technologies, Milan, Italy). Briefly, LANCL2

protein was incubated at a concentration of 5 µM in the absence or presence of increasing concentrations of AR-42 (ranging from 5 µM to 250 µM) in Tris–HCl pH 7.5, 150 mM NaCl, and 1 mM DTT with the Protein Thermal Shift™ dye (Life Technologies, Milan, Italy), which binds to hydrophobic regions exposed during protein denaturation, resulting in increased fluorescence. Two negative controls were included: one containing only the buffer with the same dye concentration, and another with AR-42 at different concentrations and dye in the absence of protein. The thermal protocol consisted of two phases: an initial incubation at 65°C for 2 minutes, followed by a continuous temperature increase at 0.05°C per second up to 99°C, with a final 2-minute hold. The obtained melt curves were analyzed by Protein Thermal Shift™ Software v1.4.

2.13. Statistical Analysis

All data were analyzed with the GraphPad Prism software version 7 (GraphPad Software, San Diego, CA, USA). All parameters were tested by two-tailed Student's t-test. p-values less than 0.05 were considered significant. Data are presented as mean ± standard deviation (SD).

3. RESULTS

Part 1: The ABA/LANCL1-2 hormone/receptors system controls ROS oroduction in cardiomyocytes through ERRα

3.1. Production of LANCL1-2 overexpressing and silenced H9c2 cells

To investigate the role of ABA and its receptors in the regulation of oxidative stress and ROS metabolism in cardiomyocytes, H9c2 cells were engineered to generate stable lines with simultaneous overexpression or silencing of LANCL1 and LANCL2. Overexpression (OVL1+2) and knockdown (SHL1+2) of LANCL1/2 were achieved through retroviral and lentiviral transduction, respectively, and confirmed by Western blot analysis. As shown in **Figure 9**, protein expression levels increased approximately 6 fold for LANCL1 and 30 fold for LANCL2 compared with control cells transduced with the empty vector (PLV).

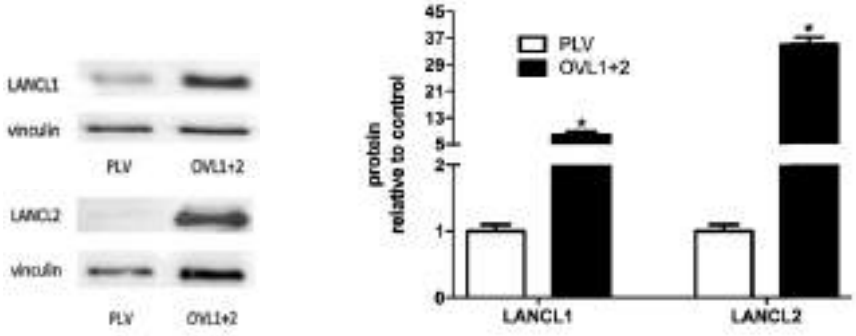

Figure 9: Western blots (left) and densitometric analysis (right) of LANCL1 and LANCL2 expression in OVL1+2 and control (PLV) H9c2 cells. Data are normalized to vinculin. *p < 0.001 compared with PLV cells.

Conversely, in the silenced cell lines, both mRNA and protein levels of the two receptors were markedly reduced by about 76% for LANCL1 and 95% for LANCL2, as determined by Western blotting (**Figure 10,** left and central panels) and qRT-PCR **(Figure 10,** right panel).

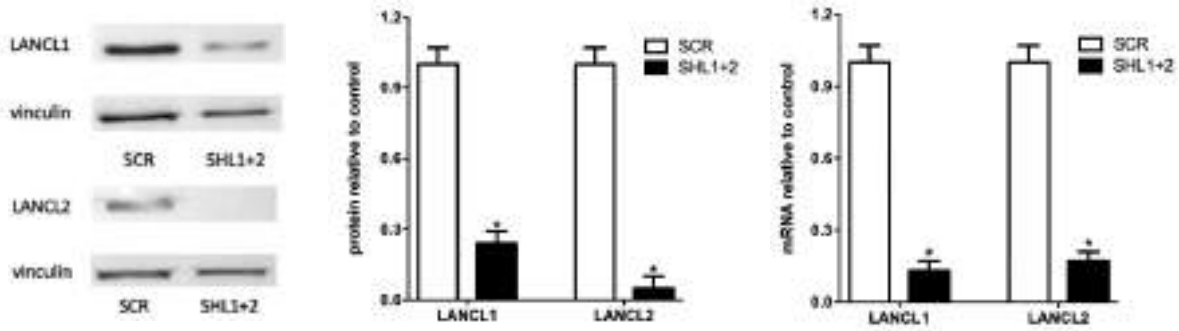

Figure 10: Western blots (left) and densitometric quantification analysis normalized to vinculin (central) of LANCL1 and LANCL2 in double-silenced (SHL1+2) and scrambled control (SCR) H9c2 cells (left). LANCL1/2 mRNA levels in silenced cells relative to control (right). *p < 0.001 vs. control SCR for silencing), unpaired Student's t-test.

3.2. Protection of H9c2 cardiomyocytes from H_2O_2-induced oxidative stress by LANCL1/2 overexpression

To investigate the role of LANCL1 and LANCL2 in protecting cardiomyocytes from oxidative damage, H9c2 cells overexpressing or silenced for both receptors, along with control PLV cells, were exposed to H_2O_2, a widely used inducer of oxidative stress [135]. Following treatment, cell viability was assessed to evaluate the protective effects of the LANCL1/2 system. Exposure to 600 µM H_2O_2 markedly decreased viability in control and LANCL1/2-silenced cells, with a 11% survival rate, whereas overexpressing cells retained 35% viability (**Figure 11).** At lower H_2O_2 concentrations, silenced cells were more susceptible to oxidative stress, showing a survival rate of 66%, compared with 81% in control cells and 92% in LANCL1/2-overexpressing cells (**Figure 11)**. These findings demonstrate that overexpression of LANCL1 and LANCL2 markedly protects H9c2 cells from H_2O_2-induced cytotoxicity, whereas silencing of these proteins increases susceptibility.

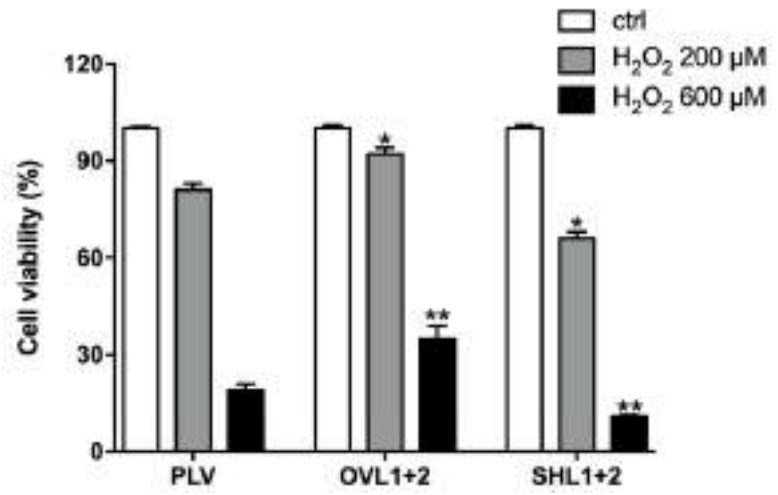

Figure 11. Cell viability was determined using the resazurin assay in H9c2 cells overexpressing LANCL1 and LANCL2 (OVL1+2), double-silenced (SHL1+2), and control (PLV) cells following a 3-hour incubation with 200 or 600 µM H_2O_2, or in the absence of treatment. Results are expressed as the percentage of viable cells relative to untreated controls. Histograms represent the mean ± SD of three independent experiments. * $p < 0.01$, ** $p < 0.001$ versus the corresponding control, determined by unpaired Student's t-test.

3.3. Lipid peroxidation is reduced in H9c2 cells overexpressing LANCL1/2 compared to double-silenced cells and control cells

To evaluate H_2O_2-induced lipid peroxidation, H9c2 cells overexpressing LANCL1/2, double-silenced cells, and control cells were incubated with C11-BODIPY 581/591, a fluorescent probe sensitive to lipid hydroperoxides. Lipid peroxidation was quantified by calculating the fluorescence emission ratio at 590 nm and 510 nm as upon oxidation by reactive oxygen species, the probe undergoes a

spectral shift with fluorescence emission changing from 590 nm (red) to 510 nm (green). In untreated control cells, the 590/510 ratio was high, reflecting low basal peroxidation, whereas H_2O_2 treatment caused a significant decrease in this ratio. In LANCL1/2-overexpressing cells, lipid peroxide formation after H_2O_2 exposure was roughly half that observed in control and silenced cells. Specifically, after 200 μM H_2O_2, the 590/510 ratios were 8.7 (OVL1+2), 6.9 (control), and 4.6 (SHL1+2), and after 600 μM H_2O_2, the ratios were 3.2 (OVL1+2), 2.2 (control), and 1.1 (SHL1+2) (**Figure 12**). Interestingly, LANCL1/2-silenced cells also exhibited a higher basal level of lipid hydroperoxides under untreated conditions compared with overexpressing and control cells.

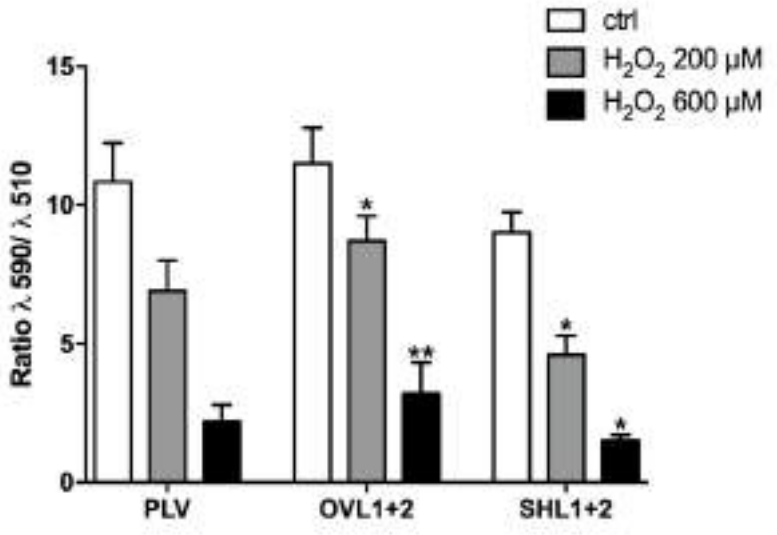

Figure 12. Intracellular lipid hydroperoxide levels were measured using the fluorescent probe C11-BODIPY 581/591. Lipid peroxidation is expressed as the fluorescence emission ratio at 590/510 nm. Histograms show the mean ± SD from three independent experiments. * $p < 0.01$, ** $p < 0.001$ relative to the respective control cells by unpaired t-test.

3.4. LANCLs receptors modulate the expression of radicals-generating enzymes COX2, XO, and NOX4: overexpression reduces while silencing enhances their levels.

The assessment of cell viability and lipid peroxidation following H_2O_2-induced oxidative stress demonstrated that LANCL1 and LANCL2 play a key role in modulating oxidative damage, prompting further investigation into their effects on enzymes involved in ROS generation and scavenging. To elucidate the role of LANCL proteins in inflammation and ROS production in H9c2 cells, the expression of the radical-generating enzymes COX2, XO, and NOX4 was analyzed in cells overexpressing or silenced for both LANCL1 and LANCL2, either in the presence or absence of ABA, using qRT-PCR and Western blotting.

In H9c2 cells overexpressing LANCL1 and LANCL2 (OVL1+2), mRNA levels of COX2, XO, and NOX4 were markedly decreased by 70–80% compared with control cells transduced with the empty

vector (PLV). In contrast, double-silenced cells (SHL1+2) exhibited an approximately 6 fold increase in mRNA expression of these enzymes relative to scrambled control cells (SCR) (**Figure 13,** upper panel). Consistent changes were observed at the protein level for COX2 and XO, as revealed by Western blotting (**Figure 13**, lower panels). These findings indicate that LANCL1/2 expression inversely regulates both the transcription and protein levels of COX2, XO, and NOX4, suggesting that reduced LANCL1/2 expression promotes a pro-inflammatory, radical-generating phenotype in cardiomyocytes.

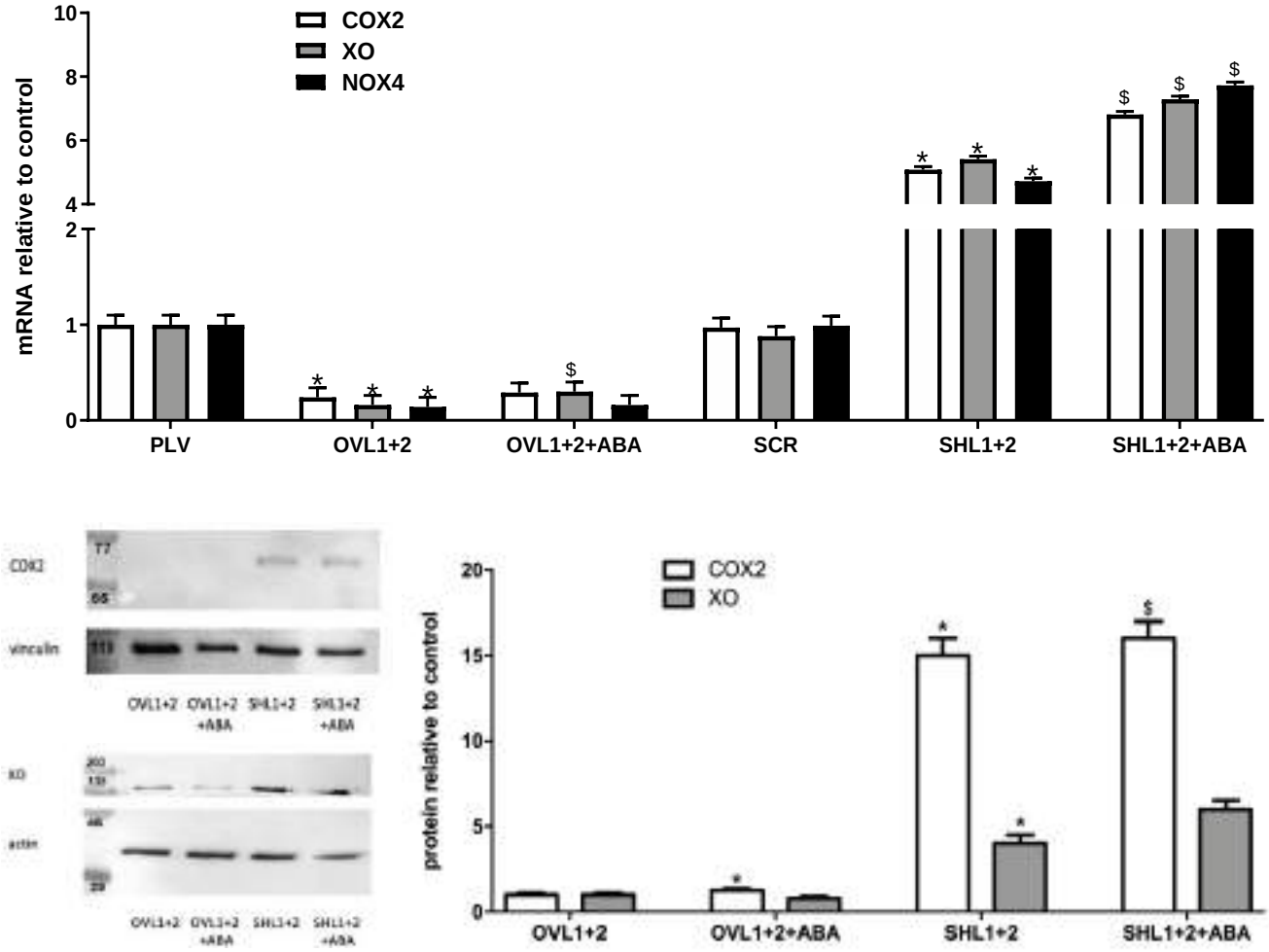

Figure 13. Radical-generating enzyme expression in LANCL1/2-overexpressing and silenced H9c2 cells. qRT-PCR analysis of COX2, XO, and NOX4 mRNA in cells overexpressing (OVL1+2) or silenced (SHL1+2) for LANCL1/2, treated or not with 100 nM ABA for 4 h (upper panel). Values are expressed relative to ABA-untreated control cells (PLV). *p < 0.001 versus untreated controls (PLV or SCR), $p < 0.02 versus ABA-untreated OVL1+2 or SHL1+2 (unpaired t-test). Western blot analysis of COX2 and XO proteins (lower panel, left) and densitometric quantification (lower panel, right; mean ± SD, ≥3 experiments). Protein levels are normalized against vinculin for COX2 and actin for XO and expressed relative to ABA-untreated OVL1+2 cells. *p < 0.001 versus untreated OVL1+2, $p < 0.02 versus ABA-untreated SHL1+2 (unpaired t-test).

3.5. Overexpression of LANCL1/2 enhances, whereas their combined silencing reduces, the transcription and expression of the radical scavenging enzymes SOD2 and GPX4

To further explore the potential involvement of the ABA/LANCL1-2 signaling pathway in the regulation of ROS metabolism, the expression of two major enzymatic antioxidants, superoxide dismutase 2 (SOD2) and glutathione peroxidase 4 (GPX4) was measured. These enzymes play a critical role in cellular defense by either directly scavenging ROS or indirectly preventing their accumulation, thereby protecting cells from oxidative damage and maintaining redox homeostasis. Interestingly, H9c2 cells overexpressing LANCL1 and LANCL2 (OVL1+2) exhibited a substantial upregulation of both SOD2 and GPX4 mRNA, with transcript levels approximately 4-fold and 5-fold higher, respectively, compared with control cells transduced with the empty vector (PLV) (**Figure 14**). Furthermore, treatment of these cells with 100 nM ABA led to an additional significant increase in the transcription of both antioxidant genes, highlighting a potential synergistic effect of LANCL1/2 overexpression and ABA stimulation in enhancing the cellular antioxidant capacity. These findings suggest that the ABA/LANCL1-2 axis may play a central role in regulating antioxidant defenses and protecting cardiomyocytes from oxidative stress.

The expression of the same antioxidant genes analyzed in LANCL1/2-overexpressing H9c2 cells was also examined in cells where both LANCL1 and LANCL2 were silenced. Interestingly, the results showed a completely opposite trend: mRNA levels of SOD2 and GPX4 were significantly reduced in the double-silenced cells compared with controls, and ABA treatment failed to induce any increase in their transcription (**Figure 14).**

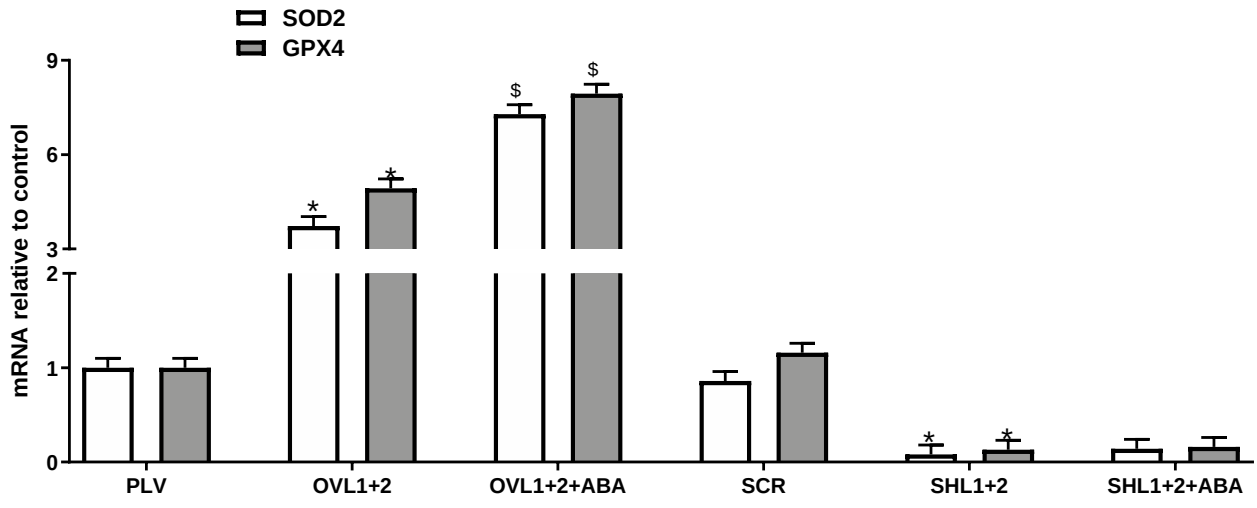

Figure 14. qRT-PCR analysis of SOD2 and GPX4 mRNA in cells overexpressing (OVL1+2) or silenced (SHL1+2) for LANCL1/2, treated or not with 100 nM ABA for 4 h. Values are expressed relative to ABA-untreated control (PLV) cells. *$p < 0.001$ versus untreated controls (PLV or SCR), \$$p < 0.02$ versus ABA-untreated OVL1+2 or SHL1+2 (unpaired t-test).

Western blot analysis confirmed that SOD2 and GPX4 expression was approximately 80-fold higher in LANCL1/2-overexpressing cells relative to double-silenced H9c2 cells (**Figure 15**), highlighting the strong regulatory influence of LANCL1/2 on these key antioxidant enzymes. These findings suggest that the ABA/LANCL1-2 system is not only critical for regulating ROS production but also plays a central role in coordinating the cellular antioxidant defense machinery. Supporting this, previous studies reported that the NADPH/$NADP^+$ ratio is significantly higher in LANCL1/2-overexpressing cells (2.1) compared with double-silenced cells (1.6) [18]. NADPH is essential for the activity of glutathione reductase (GR), which maintains GSH in its reduced form, a critical factor for the antioxidant function of glutathione peroxidase (GPX). The elevated expression of GPX4 in overexpressing cells aligns with these findings, indicating that the entire GSH-dependent detoxification system, including SOD, GPX, and GR, is fully activated. These results collectively highlight a coordinated mechanism by which LANCL1/2 overexpression enhances cellular resistance to oxidative stress through both ROS regulation and reinforcement of enzymatic antioxidant defenses.

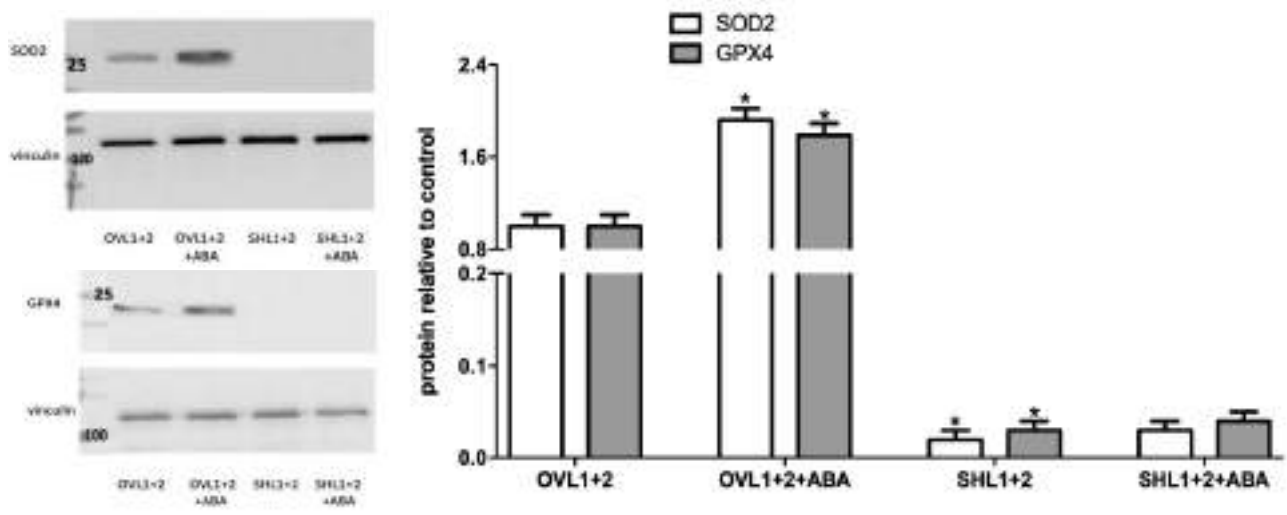

Figure 15. Western blot of SOD2 and GPX4 (left panels) and densitometric quantification (right panel; mean ± SD, ≥3 experiments), normalized to vinculin and expressed relative to ABA-untreated OVL1+2 cells. *$p < 0.001$ versus untreated OVL1+2 (unpaired t-test).

3.6. ROS levels in H9c2 cells are decreased by LANCL1/2 overexpression and enhanced by LANCL1/2 silencing.

To further validate the effects of LANCL1/2 on ROS metabolism, the intracellular and mitochondrial ROS levels was determined using two complementary fluorogenic approaches. H2DCFDA, a general ROS-sensitive probe, is converted by cellular esterases into a non-fluorescent compound that

becomes fluorescent 2′,7′-dichlorofluorescein (DCF) upon oxidation by ROS, providing a readout of total cellular ROS (**Figure 16**).

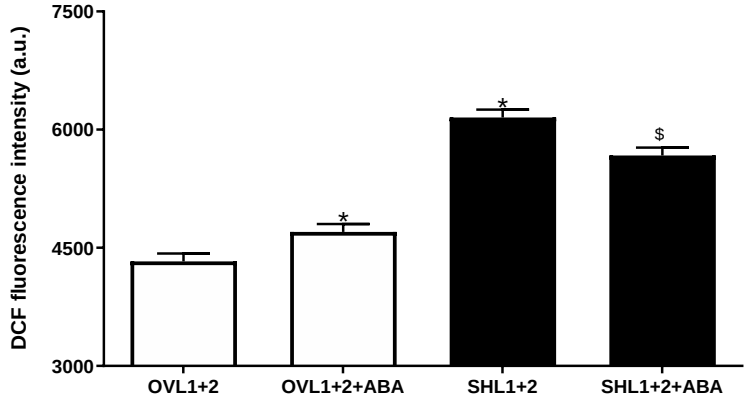

Figure 16. Intracellular ROS levels in H9c2 cells determined by DCF fluorimetric assay. Values are presented as fluorescence intensity (arbitrary units). *p < 0.01 relative to untreated OVL1+2 cells $<0.02 relative to ABA-untreated SHL1+2 cells by unpaired t-test.

In parallel, MitoSOX™, a mitochondrial-targeted probe, generates bright red fluorescence when oxidized by mitochondrial superoxide, enabling specific assessment of mitochondrial ROS (**Figure 17**).

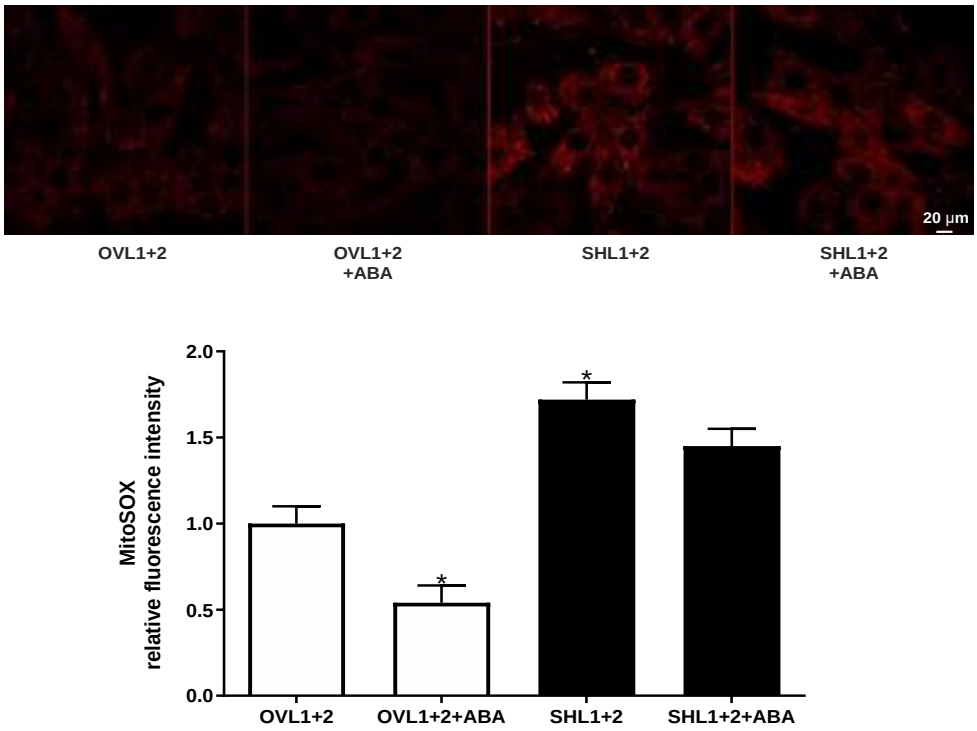

Figure 17. Mitochondrial superoxide levels were assessed by confocal microscopy in MitoSOX-loaded H9c2 cells overexpressing (OVL1+2) or silenced (SHL1+2) for LANCL1 and LANCL2, treated or not with 100 nM ABA for 4 h. Upper panels show representative confocal images, while lower panels display histograms of mean cellular fluorescence from three independent experiments, normalized to ABA-untreated OVL1+2 cells. *p < 0.01 relative to untreated OVL1+2 cells (unpaired t-test).

In both experimental conditions, LANCL1/2-silenced H9c2 cells exhibited an increased basal production of ROS compared with the overexpressing cells. This observation is consistent with the elevated expression of enzymes involved in ROS generation, such as NOX4 and XO, together with the reduced expression of antioxidant enzymes, including SOD2 and GPX, detected in the double-silenced cells. Treatment with ABA decreased mitochondrial ROS production detected byMitosox in the overexpressing cells, whereas no significant effect was observed in the double-silenced ones (**Figure 17**).

Furthermore, these findings align with the enhanced susceptibility of LANCL1/2-silenced cells to H_2O_2-induced oxidative stress, as evidenced by their markedly higher accumulation of lipid peroxides. This suggests that the reduced antioxidant capacity in the absence of LANCL1/2 not only increases ROS levels but also promotes oxidative damage to cellular lipids, further compromising cell viability under stress conditions. Importantly, ABA treatment effectively reduced mitochondrial ROS in LANCL1/2-overexpressing cells, but produced no significant effect in double-silenced cells, emphasizing that LANCL1/2 are essential mediators of ABA-dependent antioxidant responses. These findings reinforce the concept that LANCL1/2 not only modulate the expression of enzymes controlling ROS but also critically influence the actual redox state of cardiomyocytes, determining both basal and inducible oxidative stress responses.

3.7. The ABA/LANCL1-2 system controls ROS metabolism via the transcription factor ERRα

The results described above suggest that the ABA/LANCL1-2 signaling system modulates ROS homeostasis in H9c2 cells by enhancing the expression of radical-scavenging enzymes and coenzymes while concurrently downregulating ROS-generating enzymes. Among the transcriptional regulators potentially involved in this network, the estrogen-related receptors (ERRs) represent a key family of orphan nuclear receptors that play crucial roles in maintaining mitochondrial oxidative metabolism and cellular antioxidant defense [95,96]. In particular, ERRα has emerged as a central regulator of cellular energy metabolism and redox balance contributing to maintaining physiological ROS levels and preventing excessive oxidative damage [95].

To further clarify the molecular mechanisms underlying the protective effects of LANCL1/2 overexpression against oxidative stress, we investigated the involvement of ERRα. To this end, ERRα expression was silenced in LANCL1/2-overexpressing H9c2 cardiomyocytes by lentiviral transduction using a vector encoding specific shRNA sequences. The efficiency of gene silencing was validated both at the protein and mRNA levels. As shown in **Figure 18**, Western blot (left and central panels) and qRT-PCR (right panel) analyses confirmed a strong suppression of ERRα

expression, approximately 80% reduction compared with control cells infected with scrambled shRNA sequences (OVL1+2-SCR).

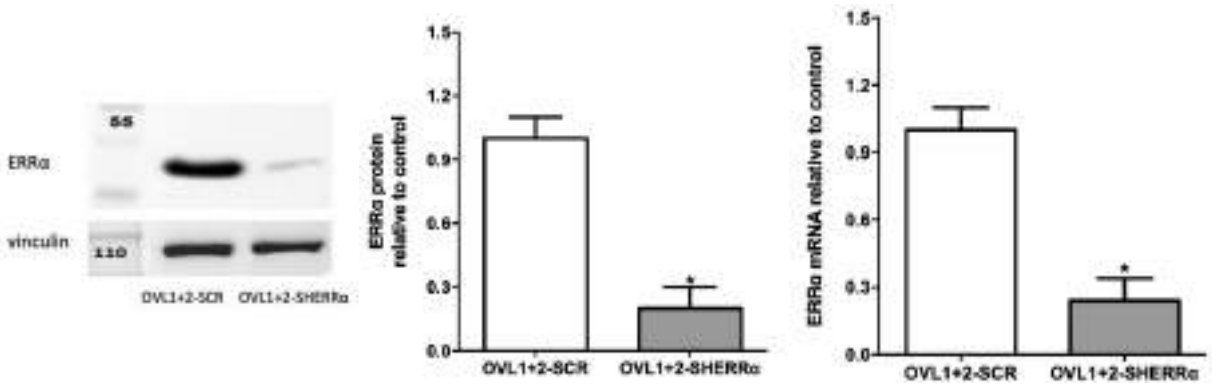

Figure 18. Representative Western blot analysis of ERRα expression in LANCL1/2-overexpressing H9c2 cells silenced for ERRα (OVL1+2-SHERRα) or transduced with scrambled control sequences (OVL1+2-SCR) (left panel). Densitometric quantification of ERRα protein levels is shown in the central panel; values are normalized to vinculin as a housekeeping protein (central panel). ERRα mRNA expression levels in OVL1+2-SHERRα cells relative to OVL1+2-SCR controls (right panel). Data are expressed as mean ± SD from three independent experiments. *p < 0.001 vs. OVL1+2-SCR (unpaired t-test).

Having established an efficient knockdown, we next aimed to assess how ERRα depletion influences ROS metabolism in LANCL1/2-overexpressing cells (OVL1+2-SHERRα). We first examined the transcriptional profile of radical-generating enzymes (COX2, NOX4, and XO) and radical-scavenging enzymes (SOD2 and GPX4) by qRT-PCR. ERRα silencing markedly upregulated the expression of COX2, NOX4, and XO compared with scrambled controls, indicating an increased pro-oxidant transcriptional activity (**Figure 19**).

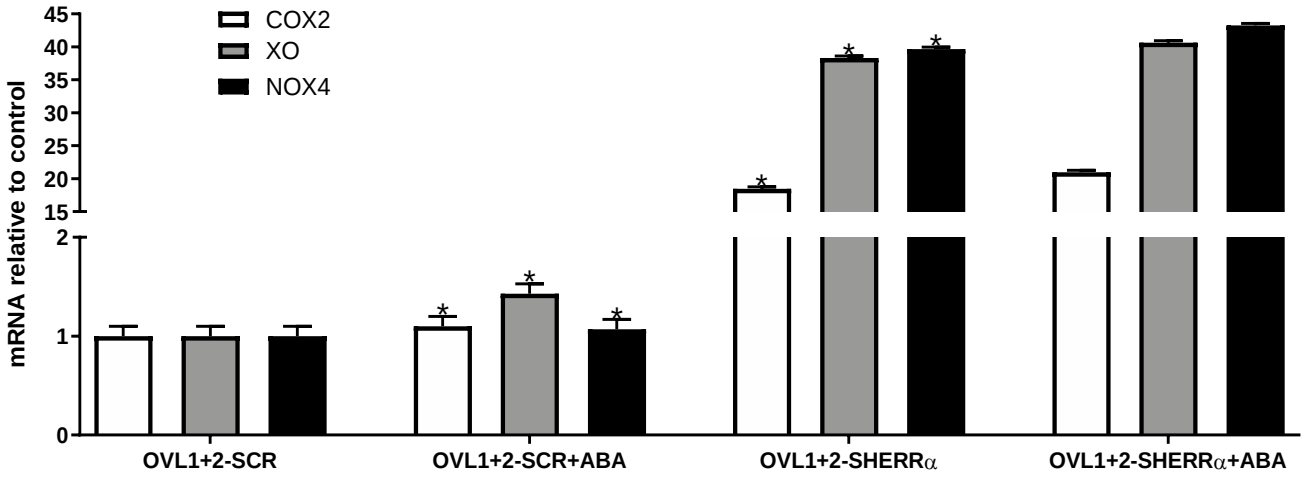

Figure 19. qRT-PCR analysis of radicals-generating enzymes (COX2, XO and NOX4) in OVL1+2 cells silenced for ERRα (OVL1+2-SHERRα) and incubated in the absence or in the presence of 100 nM ABA for 4 h. *p < 0.001 vs. OVL1+2-SCR (unpaired t-test).

Conversely, SOD2 and GPX4 mRNA levels were significantly downregulated in ERRα-silenced cells (**Figure 20).** These changes were particularly pronounced, with logarithmic-scale differences in gene expression, underscoring the strong regulatory impact of ERRα on both oxidative and antioxidant pathways.

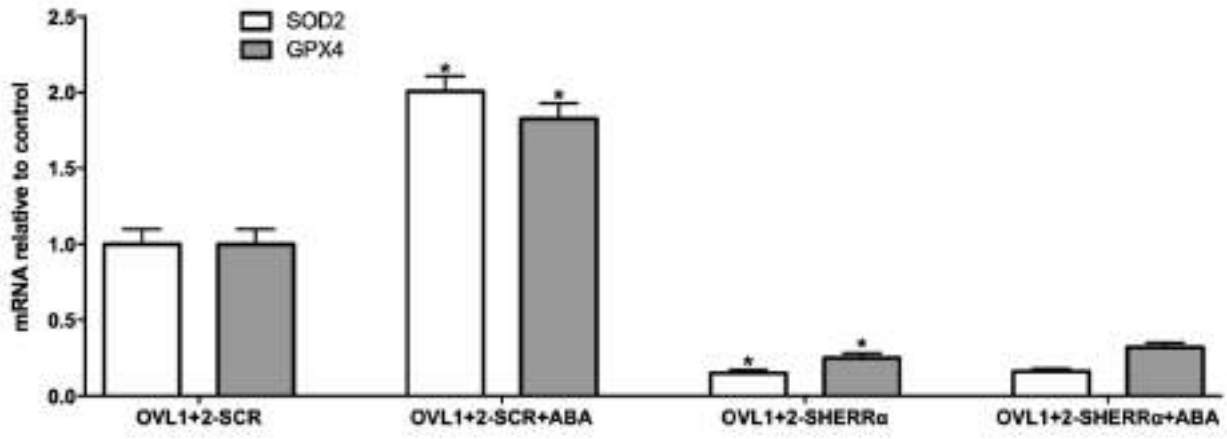

Figure 20. qRT-PCR analysis of radicals-scavanging enzymes (SOD2 and GPX4) in OVL1+2 cells silenced for ERRα (OVL1+2-SHERRα) and incubated in the absence or in the presence of 100 nM ABA for 4 h. *p < 0.001 vs. OVL1+2-SCR (unpaired t-test).

Western blot analysis confirmid a significant increase in radicals-generating COX2 and XO in ERRα-silenced LANCL1/2-overexpressing H9c2 cells compared with control cells transfected with the scrambled sequences for ERRα (**Figure 21**).

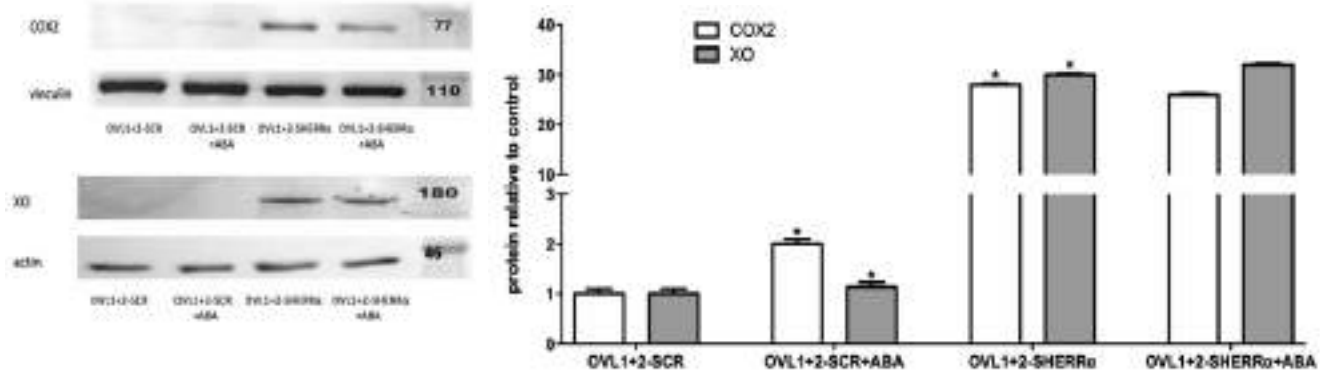

Figure 21. Representative Western blot (left panel) and densitometric quantitation (right panel) of of radicals-generating enzymes (COX2 and XO) in OVL1+2 cells silenced for ERRα (OVL1+2-SHERRα) and incubated in the absence or in the presence of 100 nM ABA for 4 h compared to ABA-untreated OVL1+2-SCR cells. Values are normalized against vinculin for COX2 and actin for XO, as a housekeeping proteins. *p <0.001 relative to ABA-untreated OVL1+2-SCR cells by unpaired t-test. (C).

In parallel, silencing of ERRα in LANCL1/2-overexpressing cells resulted in a marked decrease in the expression levels of SOD2 and GPX4 compared with the OVL1+2-SCR control cells (**Figure 22**).

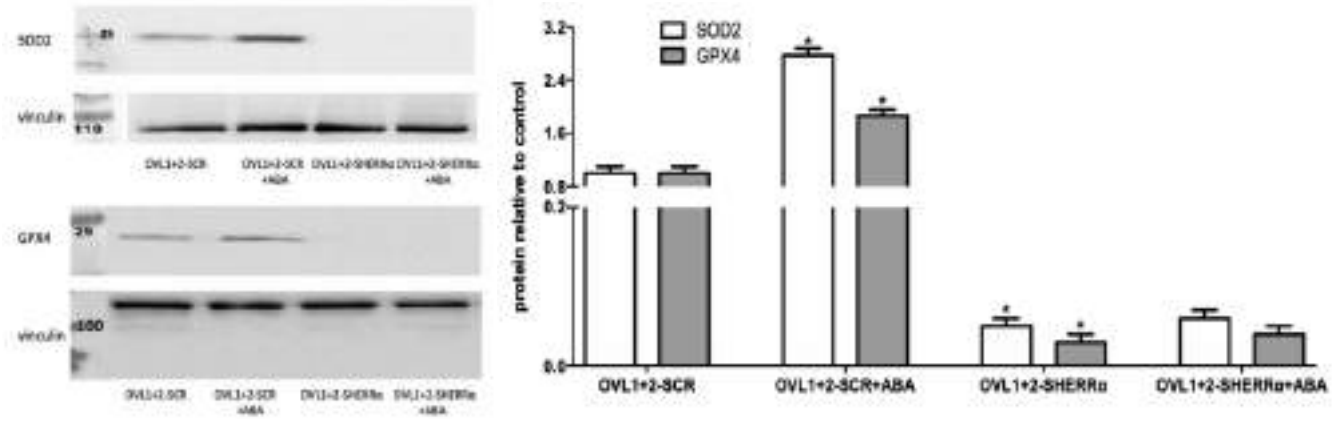

Figure 22. Representative Western blot (left panel) and densitometric quantitation (right panel) of of radicals-scavenging enzymes (SOD2 and GPX4) in OVL1+2 cells silenced for ERRα (OVL1+2-SHERRα) and incubated in the absence or in the presence of 100 nM ABA for 4 h compared to ABA-untreated OVL1+2-SCR cells. Values are normalized against vinculin, as a housekeeping protein. *p <0.001 relative to ABA-untreated OVL1+2-SCR cells by unpaired t-test. (C).

Collectively, these findings demonstrate that ERRα functions as a crucial downstream effector of the LANCL1/2 signaling network, mediating its antioxidant and cytoprotective effects. The loss of ERRα disrupts this regulatory equilibrium, driving the cellular redox state toward a pro-oxidant phenotype characterized by enhanced radical generation and diminished ROS detoxification capacity.

3.8. ERRα silencing enhances ROS generation in LANCL1/2-overexpressing H9c2 cells

To assess whether ERRα contributes to the modulation of ROS levels in LANCL1/2-overexpressing cells, intracellular ROS content was analyzed in ERRα-silenced LANCL1/2-overexpressing H9c2 cells (OVL1+2-SHERRα) and compared with control LANCL1/2-overexpressing cells transfected with scrambled sequences (OVL1+2-SCR). ROS generation was quantified using the mitochondrial superoxide indicator MitoSOX™ previously employed to compare LANCL1/2-overexpressing and double-silenced cells. As shown in **Figure 23**, ERRα silencing led to a marked increase (approximately 2.5-fold over control levels) in ROS accumulation in LANCL1/2-overexpressing cells. These findings indicate that ERRα is a key mediator of the reduced ROS content observed in LANCL1/2-overexpressing relative to double-silenced H9c2 cells (**Figure 23**). The observed 2.5-fold increase following ERRα knockdown effectively counteracts the reduction in ROS normally

associated with LANCL1/2 overexpression. Notably, treatment with ABA significantly decreased intracellular ROS levels (by about 50%) in LANCL1/2-overexpressing cells, despite its known ability to stimulate mitochondrial respiration [18]. In contrast, ERRα silencing abolished the ABA-induced reduction in mitochondrial ROS, confirming the essential role of ERRα in maintaining redox balance downstream of the ABA/LANCL1-2 pathway.

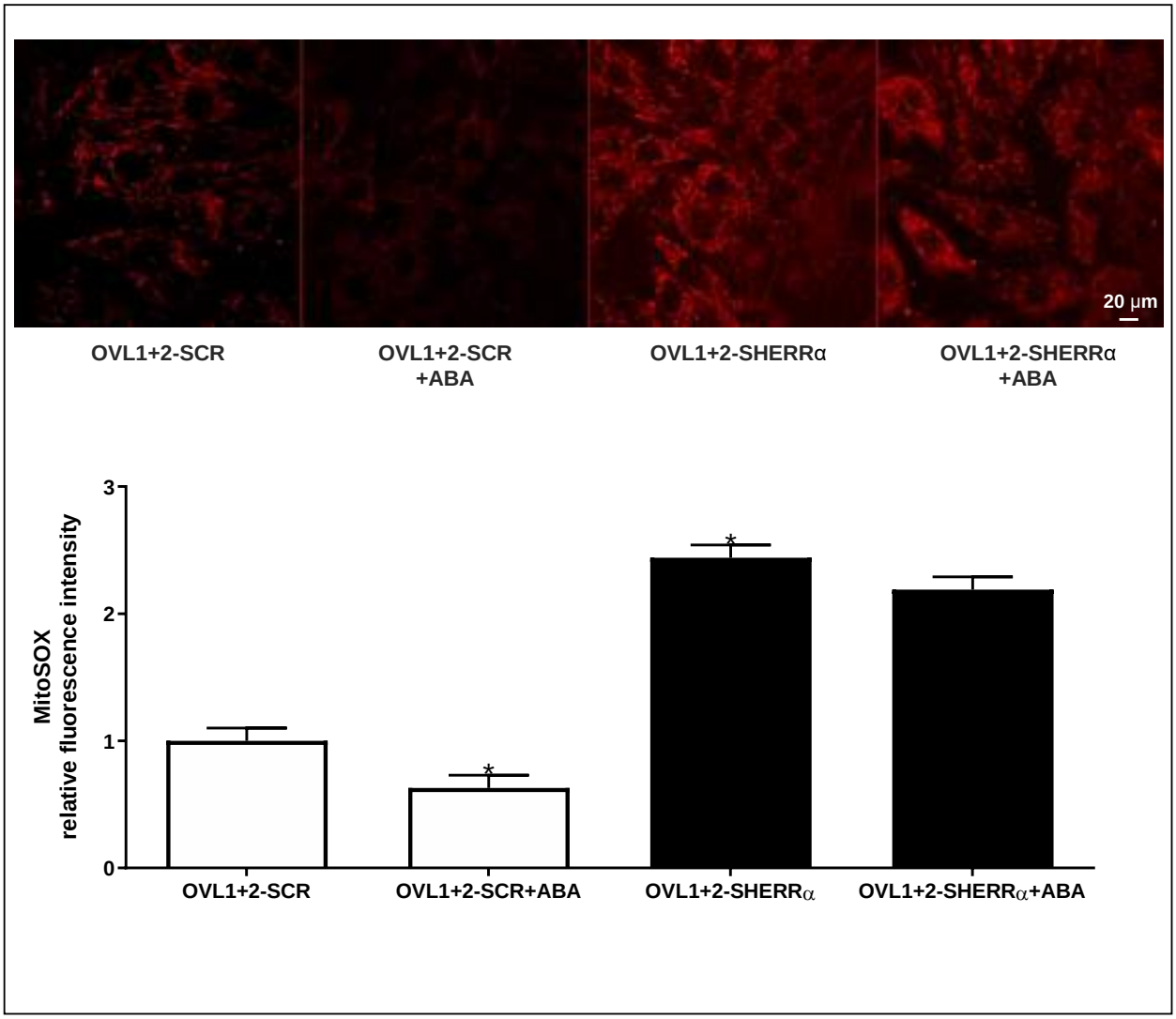

Figure 23. ERRα silencing enhances ROS production in LANCL1/2-overexpressing H9c2 cells. Mitochondrial superoxide anions production were detected on MitoSOX-loaded cells by confocal microscopy in H9c2 cells overexpressing LANCL1 and LANCL2 proteins and silenced (OVL1+2-SHERRα) or not (OVL1+2) for ERRα and incubated in the absence or in the presence of 100 nM ABA for 4 h.; The upper panel shows representative confocal microscopy images illustrating MitoSOX fluorescence under each experimental condition the lower panel presents the histogram summarized quantitative data of the mean ± SD of three independent experiments. *$p < 0.01$ relative to untreated OVL1+2-SCR cells by unpaired t-test.

Part 2: Functional characterization of the novel LANCL2 Agonists BT11 and AR-42

3.9. Evaluation of H9c2 cell viability following treatment with the LANCL2 agonists BT-11 and AR-42.

Cell viability was evaluated using a resazurin-based assay in order to assess the potential cytotoxicity of the tested compounds on H9c2 cardiomyocytes. Cells were incubated 24 h in parallel with increasing concentrations of BT-11 or AR-42 (1, 5, 10, 50, and 100 µM final concentrations). The fluorescence signal corresponding to resorufin formation was then measured as an indicator of metabolic activity and, consequently, of cell viability. No significant decrease in cell viability was observed in cultures treated with either BT-11 or AR-42 compared with untreated controls, even at the highest concentrations tested (**Figure 24).** These data demonstrate that both compounds are well tolerated by H9c2 cells under the conditions used and suggest that they do not exert cytotoxic effects within the tested concentration range. Previous studies have demonstrated that ABA does not exhibit cytotoxic effects and can be administered in vivo without adverse consequences, even at elevated concentrations [136].

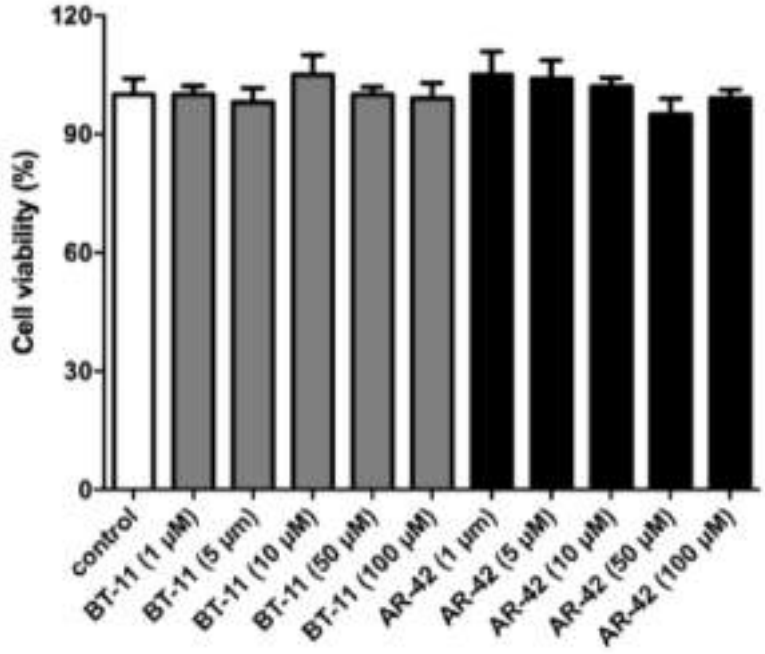

Figure 24: Cell viability as determined by resazurin assay. H9c2 cells were treated for 24 h with increasing concentrations of BT-11 or AR-42 (1–100 µM). Cell viability, assessed by resazurin assay (0.002% final concentration, fluorescence at 590 nm). Results shown are the mean ± SD from three experiments.

3.10. LANCL2 agonists increase mitochondrial function in LANCL2-Overexpressing H9c2 cells

Biochemical assays were performed to compare the effects of BT-11 and the newly identified LANCL2 agonist AR-42 with those of ABA, using LANCL2-overexpressing (OVL2) and LANCL2-silenced (SHL2) H9c2 cardiomyocytes. already generated before by retroviral and lentiviral infection [18]. In these cells the efficiency of LANCL2 modulation was previously confirmed by Western blot analysis [18], showing an ~45-fold upregulation in OVL2 cells and ~90% downregulation in SHL2 cells versus controls. Cells were incubated with the compounds ABA, BT-11, and AR-42 at a concentration of 10 μM for 4 hours. To evaluate mitochondrial activity in both OVL2 and SHL2 cells, we employed the ΔΨ-sensitive fluorescent dye JC-1, a cationic carbocyanine dye that selectively accumulates within mitochondria, where its fluorescence emission shifts from green to red in response to increases in the mitochondrial membrane potential (ΔΨ) [18, 133]. When the mitochondrial membrane potential is low, JC-1 remains in its monomeric form in the cytoplasm, emitting green fluorescence. In SHL2 cardiomyocytes, mitochondrial fluorescence was predominantly green, with only minimal red signal, reflecting a low membrane potential. By contrast, OVL2 cells exhibited largely red mitochondrial fluorescence, and the calculated red/green fluorescence ratio was nearly one order of magnitude higher than that observed in SHL2 cells (**Figure 25**), consistent with previously reported findings [18].

We then investigated how ABA, BT-11, and AR-42 influenced the mitochondrial ΔΨ in these cell models. In OVL2 cells, treatment with any of the three compounds resulted in a pronounced increase in red fluorescence, with the corresponding red/green ratio rising approximately 2.5-fold compared to untreated OVL2 cells (**Figure 25).** In contrast, SHL2 cells displayed only a modest enhancement of red fluorescence following treatment, indicating that the capacity of mitochondria to respond to these compounds is significantly impaired in the absence of LANCL2. Overall, these results demonstrate that LANCL2 overexpression markedly enhances mitochondrial function and amplifies the response to ABA, BT-11, and AR-42, whereas LANCL2 silencing diminishes mitochondrial responsiveness.

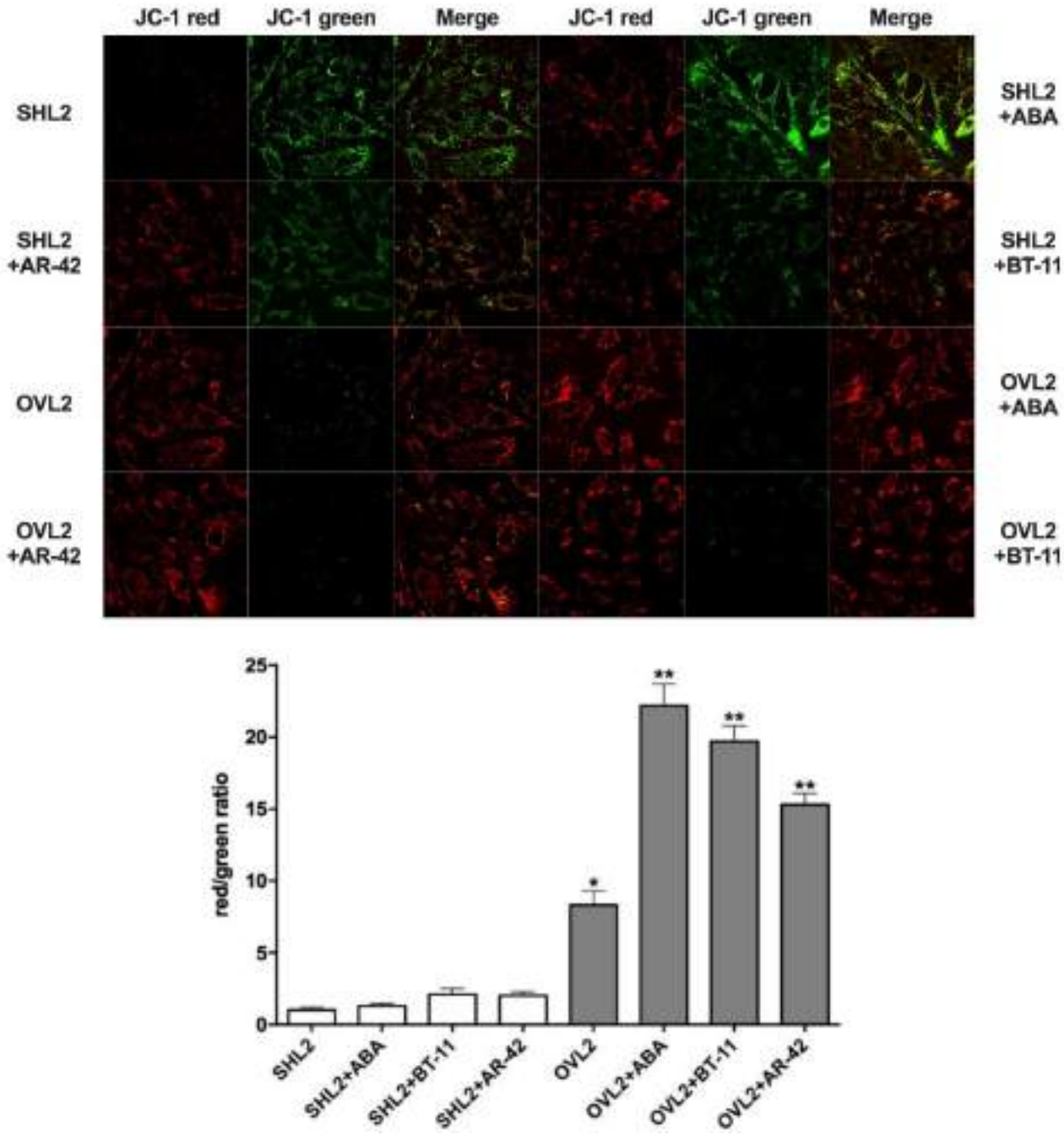

Figure 25. ABA, BT11, and AR42 boosted the mitochondrial proton gradient in H9c2 cells overexpressing LANCL1/2 compared to LANCL2-silenced cells. H9c2 cardiomyocytes with LANCL2 overexpression (OVL2) or silencing (SHL2) were stained with the ΔΨ-sensitive dye JC-1, which shifts emission from green (527 nm) to red (590 nm) as ΔΨ increases (excitation 488 nm). Upper panel: representative confocal images show JC-1 as monomers (green) and J-aggregates (red). The effects of ABA and BT11 on ΔΨ were compared between LANCL2-overexpressing and silenced cells. Lower panel: red/green fluorescence ratios from upper panel were calculated as mean ± SD across at least three microscopic fields (scale bar: 20μm). * $p < 0.05$ and ** $p < 0.01$ relative to the respective SHL2 cells by unpaired *t*-test.

3.11. LANCL2 agonists increase gene transcription level of AMPK/PGC-1α/Sirt1 axis, eNOS and ROS-scavenging enzymes

A detailed analysis of gene transcription in OVL2 and SHL2 H9c2 cardiomyocytes was performed to evaluate the impact of LANCL2 modulation on key regulators of mitochondrial function and cellular oxidative stress and the effects of ABA, BT11 and AR42 on these cells. Specifically, we measured the mRNA levels of AMPK, PGC-1α, Sirt1, eNOS, SOD2 and GPX4. These analyses were conducted in both LANCL2-overexpressing (OVL2) and LANCL2-silenced (SHL2) H9c2 cells, under basal conditions as well as following treatment with ABA, BT-11, or AR-42. The results revealed that LANCL2 overexpression significantly enhanced the transcription of AMPK, PGC-1α, Sirt1, and eNOS, consistent with our previous observations [18]. We also observed a marked upregulation of the antioxidant enzymes SOD2 and GPX4 in OVL2 cells compared with SHL2 cells, confirming that LANCL2 plays a key role in maintaining the oxidative balance in cardiomyocytes. Furthermore, treatment with ABA, BT-11, or AR-42 resulted in a further amplification of the mRNA levels of all these genes in OVL2 cells, highlighting the synergistic effect of LANCL2 overexpression and pharmacological stimulation on mitochondrial function and cellular antioxidant capacity (**Figure 26).** These findings underscore the multifaceted role of LANCL2 in regulating cardiomyocyte bioenergetics and redox homeostasis.

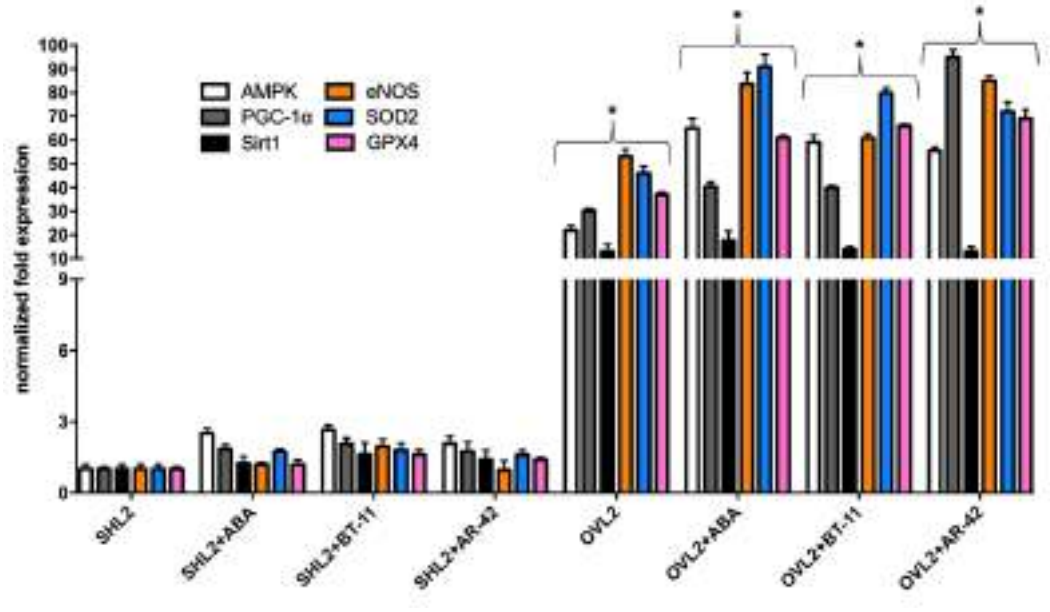

Figure 26. ABA, BT-11, and AR-42 enhanced the expression of genes involved in mitochondrial function in H9c2 cardiomyocytes overexpressing LANCL2. Gene expression analysis by qPCR focused on the AMPK/PGC1α/Sirt1 signaling pathway, eNOS, SOD2 and GPX4. Cells overexpressing LANCL2 (OVL2) or silenced for LANCL2 expression (SHL2) were treated with 10 µM of ABA, BT-11, or AR-42 for 4 hours. Following treatment, total RNA was extracted, and cDNA was synthesized from 1 µg of RNA for subsequent qPCR analysis. Gene expression levels are presented relative to untreated LANCL2-silenced cardiomyocytes (SHL2). Statistical significance: *$p < 0.01$ compared to respective SHL2 controls (unpaired t-test).

3.12. Preliminary investigation of the interaction between recombinant hLANCL2 and the AR-42 LANCL2 agonist by Surface Plasmon Resonance (SPR) and Thermal Shift Assay (TSA) analyses

Recombinant human LANCL2 (hLANCL2) was expressed as an N-terminal fusion protein with the enzyme glutathione S-transferase (GST) and purified by affinity chromatography on glutathione (GSH)–Sepharose 4B resin. hLANCL2-GST fusion protein was eluted from GSH-Sepharose-4B by incubating half part of resin with 10 mM GSH in 50 mM Tris–HCl, pH 8.0. In parallel hLANCL2 was released from GST fusion protein immobilized on the rest of GSH-Sepharose-4B by incubation with PreScission Protease. The purity of both proteins hLANCL2-GST and hLANCL2 purity was checked by SDS-PAGE, revealing a single band of approximately 75 and 50 kDa, respectively, as expected (**Figure 27**).

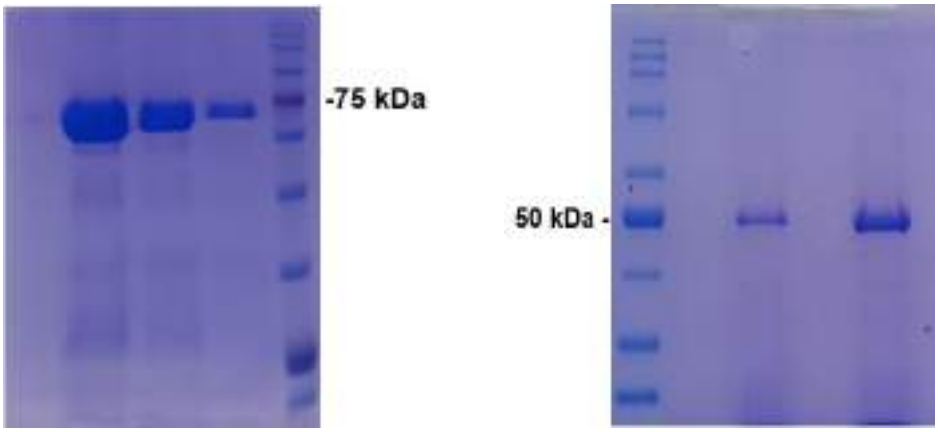

Figure 27. Determination of recombinant hLANCL2-GST and hLANCL2 protein purity; left panel, representative SDS-PAGE of three different amounts (20, 10, 5 µg) purified hLANCL2-GST used in the SPR experiments; right panel, representative SDS-PAGE of two different amounts (5 and 10 µg) purified hLANCL2 used in the TSA experiments. The gels were stained with QC Colloidal Coomassie Staining solution; hLANCL2-GST and hLANCL2 migrated as a single band with an apparent molecular mass of 75 kDa and 50 kDa, respectively.

Surface Plasmon Resonance (SPR) experiments to verify the binding of AR42 to recombinant proteins was performed using the fusion protein hLANCL2-GST. The fusion protein was chosen because protein immobilization on the chip surface requires low-pH conditions, which are known to destabilize native hLANCL2 [53]. Prior to immobilisation, a pH scouting experiment was performed, whereby the ligand was diluted in Na Acetate at different pHs (4, 4.5, 5 and 5.5) and concentrated onto the chip surface by a process of electrostatic attraction. This allows the determination of the optimal net charge of the protein for pre-concentration on the chip. The results suggested performing

the covalent amine coupling of hLANCL2-GST to the carboxymethyl groups of the sensor chip in 10 mM Na acetate pH 4 (**Figure 28,** upper panel, red line). The total amount of hLANCL2-GST immobilized was 29000 resonance units (RUs) (**Figure 28**, lower panel).

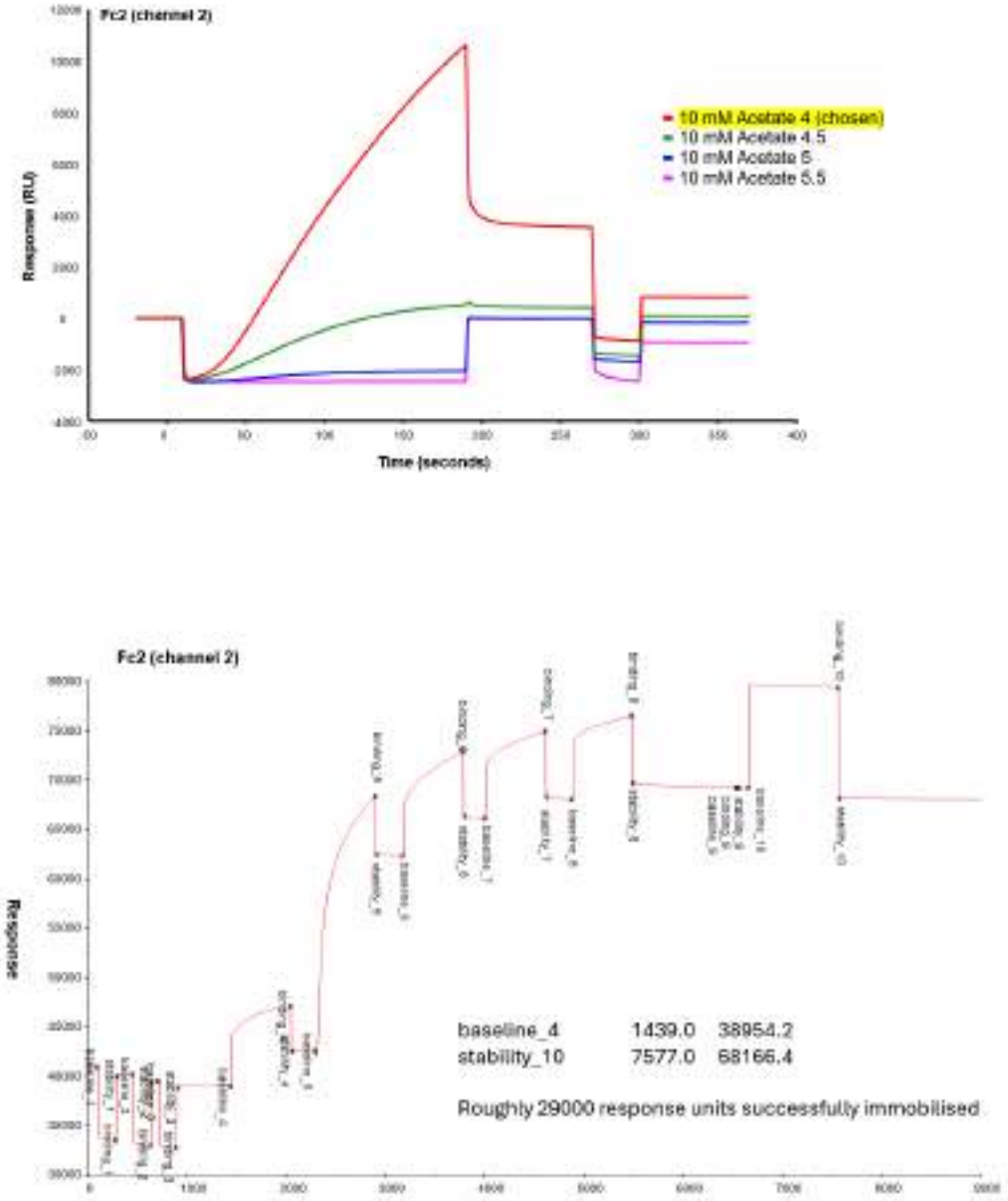

Figure 28. SPR analysis: upper panel, the pre-concentration ability of hLANCL2-GST on the chip used for SPR analysis was evaluated in a range of pH values compatible with protein stability (10 mM Na acetate, pH 4, 4.5, 5 and 5.5), at a protein concentration of 30 µg/ml. Traces from a representative experiment are shown; lower panel, hLANCL2-GST was immobilized by amine coupling on a CM7 chip in 10 mM Na acetate pH 4, yielding a total immobilization level of 29,000 resonance units (RUs).

The binding of AR42 to hLANCL2-GST was evaluated by injecting AR42 dissolved in DMSO at nanomolar concentrations. Additional analyses were also carried out at micromolar concentrations; however, data acquisition was completely compromised due to DMSO mismatch and its resulting interference. SPR analysis at nanomolar concentrations revealed the presence of a weak binding site for AR42, characterized by a very low affinity constant in the millimolar range and no saturation was achieved within this concentration range (**Figure 29**). The experiments need to be repeated using AR42 resuspended in ethanol, as the presence of DMSO in SPR assays causes significant interference with data acquisition. When DMSO is used, it is necessary to perform a calibration curve with the same DMSO concentration as that of the compound and subsequently subtract the baseline noise due to DMSO. The weak binding signal previously observed is likely attributable to this interference. Under identical conditions, ABA binding was also assessed as previously reported [53]; in this case, the determined Kd value was higher than the one previously published [53], thereby confirming that measurements performed in the presence of DMSO are not quantitatively reliable.

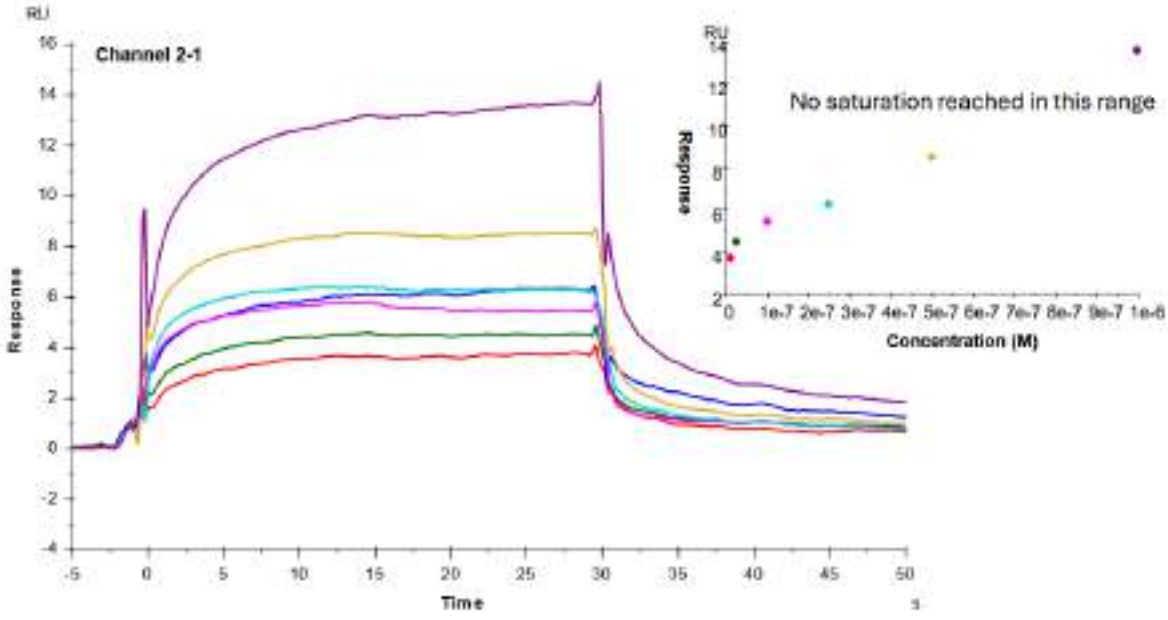

Figure 29. The steady-state Kd value was estimated using the Biacore T200 Evaluation Software. The experiments, conducted with nanomolar concentrations of AR42, revealed the presence of a weak binding site for AR42 characterized by a very low affinity constant; moreover, no saturation was observed within this concentration range.

Preliminary Thermal Shift Assay (TSA) experiments were performed to assess AR-42 binding to recombinant human LANCL2 (h-LANCL2). LANCL2 (5 μM) was incubated for 30 minutes with AR-42 (5–250 μM) in Tris–HCl pH 7.5, 150 mM NaCl, 1 mM DTT, and Protein Thermal Shift™ dye. Negative controls included buffer plus dye and dye with AR-42 without protein. After incubation, the samples were subjected to a temperature increase from 65°C to 99°C in accordance with the specified thermal protocol described, and melt curve analysis was performed using Protein Thermal Shift™ Software v1.4. **Figure 30** shows the fluorescence and derivative melt curves (upper and lower panel), and the histogram shows changes of melting temperature (T_m) values calculated from these melt curves obtained with different AR42 concentrations. The presence of 5 μM AR42 did not affect the curves and T_m values. The thermal stability of LANCL2 decreased in a concentration-dependent manner in the presence of AR42, with T_m values approximately 1.5°C lower at 125 and 250 μM AR42 compared to the control LANCL2 NT sample.

These results indicate that AR42 interacts with LANCL2, although this binding appears to induce destabilization of the protein. Normally, an agonist molecule stabilizes the protein, leading to an increase in melting temperature, since a more stable protein denatures at higher temperatures. In this case, however, the opposite result was observed, suggesting that AR42 binding induces protein destabilization. This may occur because the binding of the agonist can induce conformational changes that make the protein thermally less stable, disrupt internal interactions such as hydrogen bonds or hydrophobic contacts that normally stabilize the structure, or favor a functional state of the protein that is intrinsically less stable than the inactive or unbound state. In some cases, the agonist may also act as an allosteric effector, altering the protein's dynamics and reducing its thermal resistance. In summary, although agonist binding is often associated with protein stabilization, it can also result in a shift toward lower melting temperatures if it induces a more flexible or thermally unstable conformation. This shift thus represents an indicator of structural and functional changes in the protein upon agonist binding. Further experiments under modified experimental conditions will help to clarify the interaction between AR42 and LANCL2.

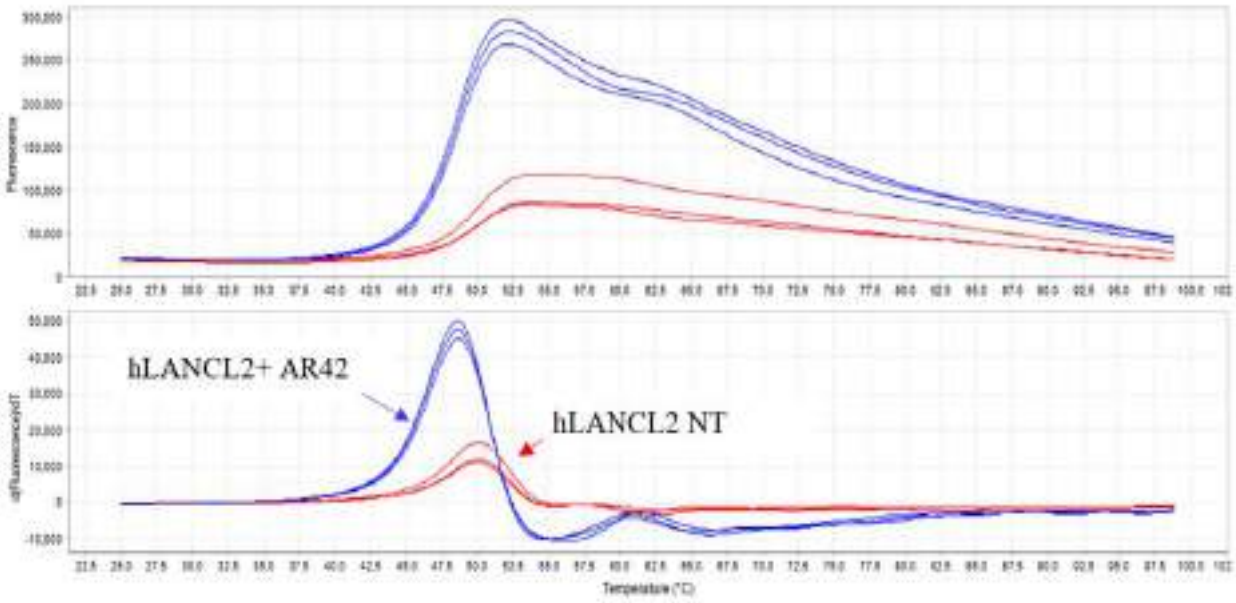

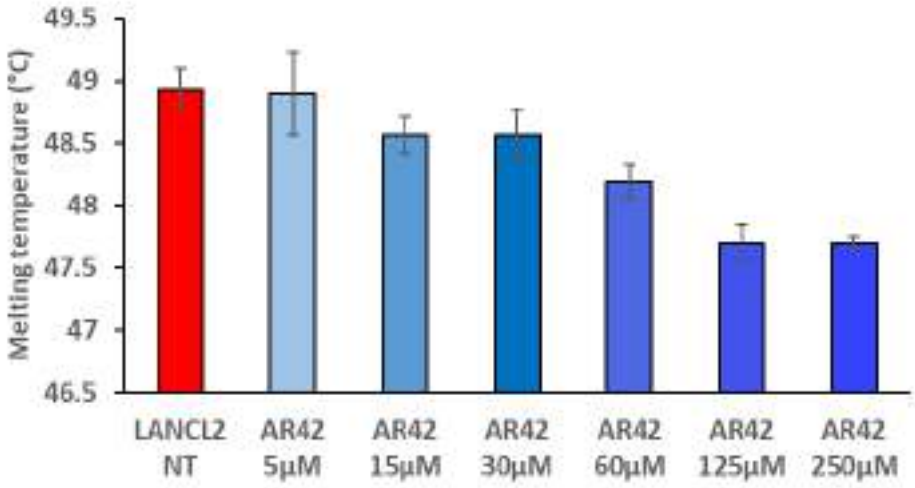

Figure 30. Thermal shift assay for LANCL2 and AR42. Fluorescence intensity versus temperature curves and derivative melt curve (-dF/dT versus temperature where the peak corresponds to the T_m) are shown in upper and lower panels. Histogram illustrating the change in protein melting temperature (°C) observed with increasing concentrations of AR42.

Part 3: Role of the ABA/LANCL1-2 system in regulating the expression of genes involved in skeletal muscle differentiation, mitochondrial functions and thermogenesis

3.13. LANCL1-2 Overexpression and silencing in C2C12 cells

The C2C12 cells derived from murine skeletal muscle cells is a well-established model to study muscle regeneration and differentiation [137]. To investigate the role of the ABA/LANCL1-2 system in skeletal muscle metabolism, differentiation, and thermogenesis, we generated C2C12 myoblast cell lines with either simultaneous overexpression or silencing of both LANCL1 and LANCL2 receptors. Overexpression (OVL1+2) was achieved through retroviral transduction, while silencing (SHL1+2) was obtained via lentiviral-mediated delivery of specific shRNAs targeting both genes followed by puromycin selection to ensure stable integration, as described for H9c2 cardiomyocytes. The efficiency of overexpression and knockdown was confirmed by Western blot analysis. Overexpressing cells displayed a fold-increase of approximately 8 for LANCL1 and 20 for LANCL2 compared to cells infected with the empty control vector (PLV) (**Figure 31)**

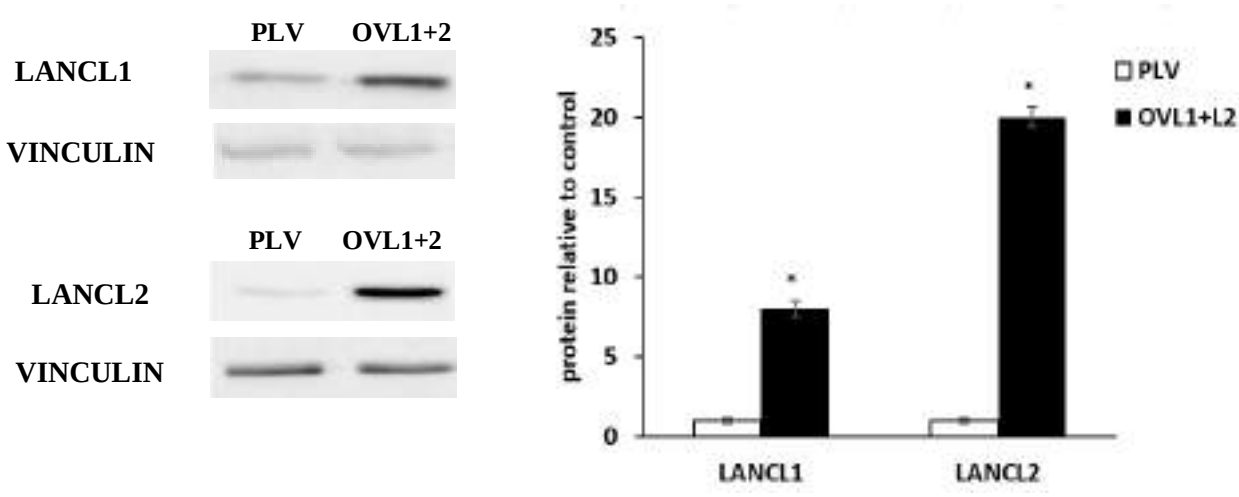

Figure 31: Western blots (left) and densitometric quantification analysis (right) of LANCL1 and LANCL2 expression normalized to vinculin in double-overexpression LANCL1+2 (OVL1+2) and control C2C12 cells (PLV). *p < 0.01 vs. control PLV, unpaired Student's t-test.

Stable knockdown of LANCL1 and LANCL2 was validated by both quantitative Western blotting (**Figure 32,** upper panel) and real-time PCR (qRT-PCR) analyses (**Figure 32,** lower panel) demonstrating a reduction in mRNA and protein expression levels of approximately 70% for LANCL1 and 90% for LANCL2, relative to control cells (SCR). These modified C2C12 cell lines provided a reliable model to study the downstream effects of the ABA/LANCL1-2 axis on key molecular pathways involved in skeletal muscle physiology.

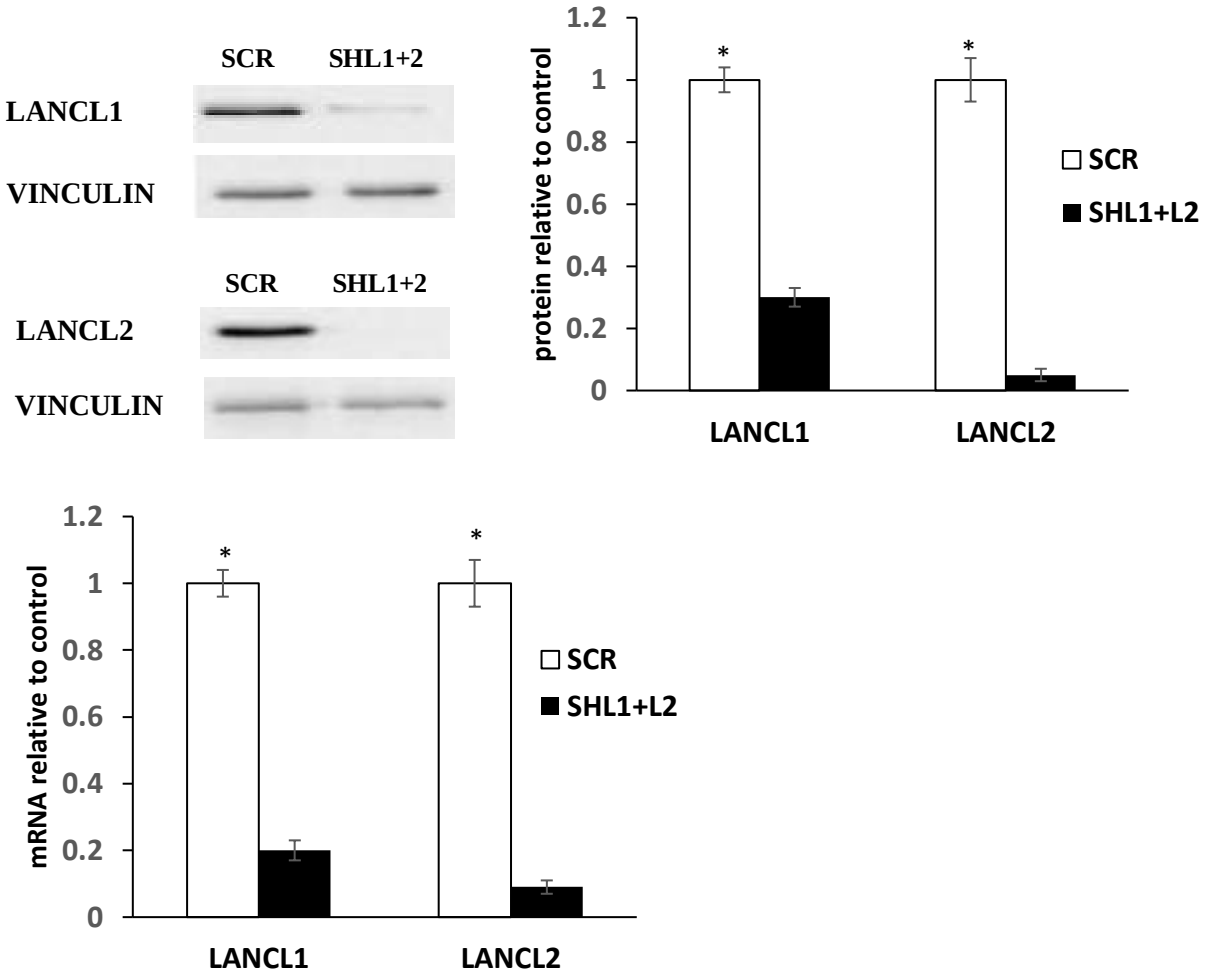

Figure 32: Western blots (upper, left) and densitometric quantification analysis normalized to vinculin (upper, rightl) of LANCL1 and LANCL2 in double-silenced (SHL1+2) and scrambled control (SCR) C2C12 cells. LANCL1/2 mRNA levels in silenced cells relative to control (lower panel). *$p < 0.01$ vs. control SCR for silencing), unpaired Student's t-test.

3.14. Overexpression of LANCL1-2 receptors in differentiated C2C12 cells promotes the expression of markers involved in myogenic differentiation and mitochondrial function

C2C12 cells overexpressing (OVL1+2) or silenced (SHL1+2) for LANCL1 and LANCL2 were differentiated following the protocol described in Materials and Method. Briefly, cells were cultured under parallel experimental conditions to induce or not differentiation. For the maintenance of undifferentiated myoblasts, cells were incubated in DMEM without any supplements. In contrast, myogenic differentiation was promoted by culturing the cells in DMEM supplemented with either B27, a defined serum-free supplement containing hormones, vitamins, antioxidants, and other essential growth factors, or with horse serum (HS), a well-established inducer of myotube formation. This experimental setup enabled the evaluation of the role of LANCL1/2 expression levels under different differentiation conditions.

The B27 supplement was found to enhance myogenic differentiation more efficiently than horse serum (HS), promoting the development of a slow-twitch, oxidative metabolic muscle phenotype [125, 138]. In contrast, differentiation in the presence of HS resulted in the formation of a more heterogeneous population of myotubes, typically associated with a faster, glycolytic phenotype [125]. After 7 days of culture in three different media, unsupplemented DMEM, DMEM supplemented with B27, and DMEM supplemented with HS, cell morphology was monitored to evaluate both cell proliferation and differentiation status (**Figure 33**). Under differentiating conditions, C2C12 myoblasts fused to form elongated, multinucleated myotubes, leading to the appearance of organized myofiber-like structures.

Figure 33. Representative phase-contrast images of C2C12 undifferentiated (DMEM, left panel), and differentiated with B27 supplement (central panel) and Horse serum (right panel).

After differentiation, cells were harvested for RNA extraction and subsequent quantitative real-time PCR (qPCR) analyses to evaluate the expression of key myogenic and thermogenic markers.

During differentiation of C2C12 cells, myoblasts undergo remodeling to form mature myotubes in parallel with the increased expression of muscle specific genes. This process requires activation of myogenic regulatory factors (MRF), including myogen termination gene (Myod), miogenin (Myog) and myogenic factor 5 (Myf5) [139-143]. During myogenesis, MRFs are actived and regulate the transcription of genes, such as MyHC [140]. In adult skeletal muscle, MyHC mRNA isoforms are expressed in a distinct pattern, including MyHC-I and MyHC-II. It has been confirmed that MyHC is expressed in late and terminal differentiation, and that it is the most suitable marker of muscle fibers [140, 144].

To study the role of LANCL receptor modulation on differentiation process and in order to quantify the levels of muscle differentiation in overexpressing LANCL1-2 C2C12 cells compared to silenced cells for both receptors, we investigate the expression of different markers. At the end of differentiation, total RNA was extracted from cells and qPCR analyses was performed as described

before. We analyzed miogenin, a key myogenic, regulatory factor involved in the differentiation of C2C12 myoblasts into mature muscle cells that promotes the progression of myoblasts to form multinucleated myotubes [145], MyHC-I, MyHC-IIb and MYH7 [144]. During myogenic differentiation, myosin heavy chain (MyHC) isoforms are differentially expressed, reflecting the specialization of muscle fibers. MyHC-I, which characterizes slow-twitch oxidative fibers, and MyHC-II, associated with fast-twitch glycolytic fibers, are both upregulated as myoblasts mature into myotubes. In particular, the MyHC-IIb isoform represents the most glycolytic form, predominantly expressed in fast-twitch fibers specialized for rapid, high-force contractions and low fatigue resistance [146]. In addition, the MYH7 gene encoding the beta (β)-myosin heavy chain, also known as myosin-7, which is a major protein in cardiac muscle and type I (slow-twitch) skeletal muscle fibers [147,148] was analyzed. **Figure 34** shows that all the myogenic markers anlyzed increased in LANCL1-2 overexpressing C2C12 differentiated cells respect to LANCL1-2 silenced both differentiated and undifferentiated C2C12 cells. To further investigate the role of LANCL1-2 in myogenesis, C2C12 cells either overexpressing or silenced for both LANCL1-2 genes were induced to differentiate using two distinct protocols: treatment with B27 supplement or Horse Serum. Under both differentiation conditions, a pronounced increase in the expression of myogenic markers, myogenin, MyHC-I, MyHC-IIb, and MYH7, was observed (2.46, 140, 44 and 18.5 fold respectively in LANCL1-2 overexpressing C2C12 differentiated with B27 versus undifferentiated LANCL1-2 silenced cells; 7, 31, 105 and 20.5 fold respectively in LANCL1-2 overexpressing C2C12 differentiated with HS versus undifferentiated LANCL1-2 silenced cells).

As expected, differentiation in the presence of B27 supplement led to the highest expression of MyHC-I, a marker of slow-twitch fibers, in LANCL1-2 overexpressing cells. Conversely, differentiation with Horse Serum induced the highest expression of MyHC-II, a marker of fast-twitch fibers, in the same overexpressing cells. In addition, the expression of the MT-ND1 gene, which encodes a key subunit of mitochondrial NADH dehydrogenase (complex I of the mitochondrial electron transport chain), was found to increase during differentiation, particularly in LANCL1-2 overexpressing C2C12 cells differentiated with both B27 supplement and horse serum (22 fold and 13 fold respectively compared to LANCL1-2 undifferentiated cells). These results underscore the essential role of ABA/LANCL1-2 in regulating mitochondrial function, as previously reported in cardiomyocytes [19].

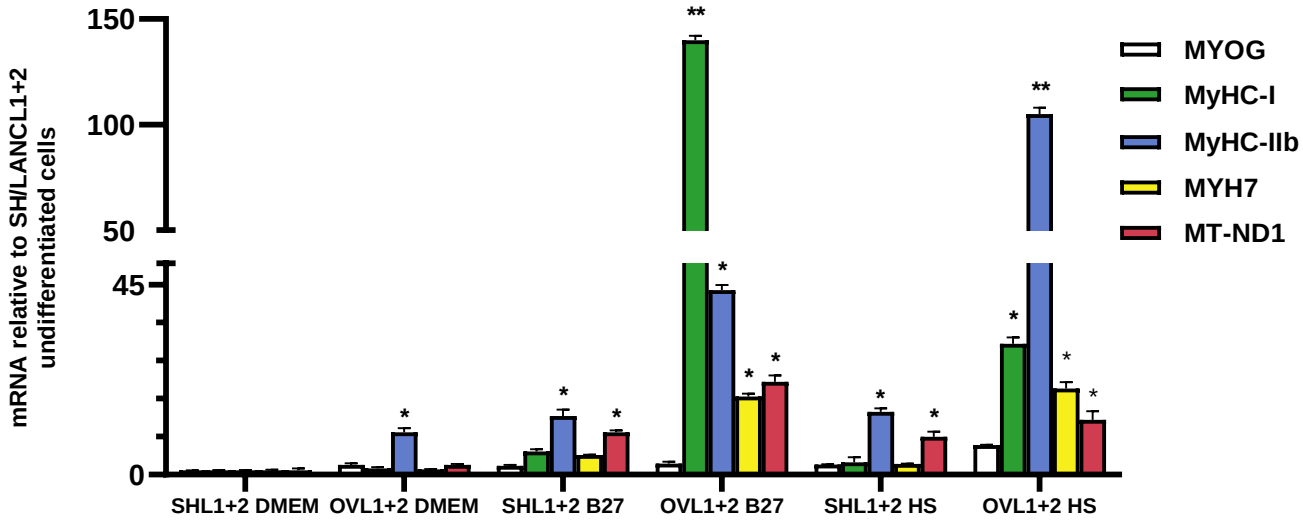

Figure 34. Overexpression of LANCL1 and LANCL2 enhanced the expression of genes involved in myogenic differentiation and mitochondrial functions in C2C12 cells. C2C12 myoblasts overexpressing LANCL1/2 (OVL1+2) or silenced for both genes (SHL1+2) were subjected or not (DMEM) to differentiation using two distinct protocols, one supplemented with B27 and the other with horse serum (HS). Following differentiation, total RNA was extracted, and complementary DNA (cDNA) was synthesized from 1 µg of RNA for subsequent qPCR analysis. Gene expression levels were calculated relative to SHL1+2 undifferentiated C2C12 cells. Statistical significance: **p< 0.001, *p < 0.01 compared to respective SHL1+2 undifferentiated C2C12 (unpaired t-test).

3.15 ABA receptors regulate the expression of key genes involved in and thermogenesis in differentiated C2C12 myoblasts

Recent studies on human brown adipocytes and rat cardiomyocytes have revealed the role of the ABA/LANCL1-2 hormone–receptor system in cellular thermogenesis [16,19]. In both cell types, overexpression of LANCL1-2 enhances, whereas simultaneous silencing of both genes reduces, the transcription and expression of mitochondrial OXPHOS uncoupling proteins, specifically UCP1–3 in brown adipocytes and in cardiomyocytes. The logarithmic increase in uncoupling protein expression observed in LANCL1/2-overexpressing cells, compared with double-silenced cells, is accompanied by elevated levels of mitochondrial DNA, respiration, and ATP production in the overexpressing cells [16,19]. In muscle rat L6 cells, the action of ABA is dependent on AMPK/PGC1α activation, which subsequently enhances GLUT4 and GLUT1 expression, mitochondrial respiration, and the production of uncoupling proteins such as sarcolipin and UCP3 [17,109, 110]. The observed increase in uncoupling protein expression aligns with recent findings in rat H9c2 cardiomyocytes, where the ABA/LANCL receptor system was shown to regulate cellular

thermogenesis, as evidenced by higher heat production in LANCL1/2-overexpressing cells compared with double-silenced cells [111]. These previous results suggest investigating the role of the ABA/LANCL1-2 system in regulating the expression of genes involved in skeletal muscle thermogenesis in LANCL1-2 overexpressing and silenced C2C12 cells. The expression of genes involved in both shivering and nonshivering thermogenesis in skeletal muscle was analyzed, including the mitochondrial uncoupling protein UCP3 and sarcolipin (SLN), SERCA pump and creatine kinase (CK), both involved in ATP-consuming futile cycles useful as energy dissipating mechanisms [149, 150]. The expression of all analyzed genes was markedly upregulated in LANCL1-2 overexpressing C2C12 undifferentiated cells compared to LANCL1-2 silenced undifferentiated cells. Interestingly, under both differentiation conditions B27 and horse serum, cells overexpressing LANCL1/2 exhibited a strong induction of SLN and CK expression relative to undifferentiated LANCL1-2 overexpressing cells. Specifically, SLN and CK transcript levels increased by approximately 105-fold and 9-fold, respectively, in cells differentiated with B27 supplement, and by 50-fold and 18-fold, respectively, in cells differentiated with horse serum (**Figure 35**).

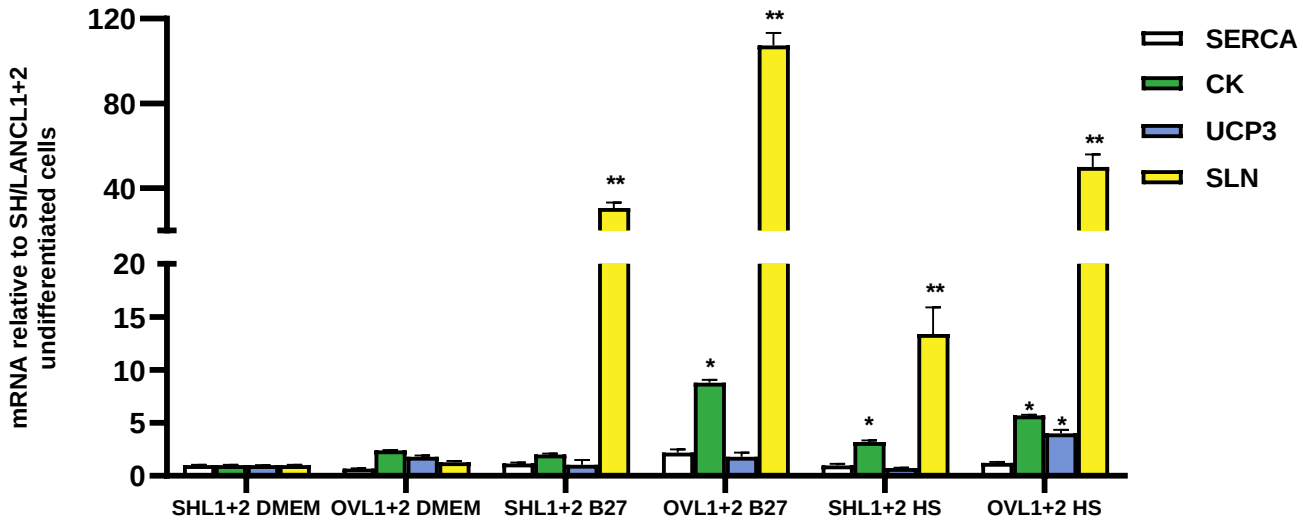

Figure 35. LANCL1-2 overexpression enhanced the expression of genes involved in thermogenesis in C2C12 cells. qRT-PCR analysis of SERCA pump, creatine kinase CK, UCP3 and sarcolipin SLN in overexpressing (OVL1+2) or silenced (SHL1+2) differentiated with B27 and Horse Serum HS supplement or not differentiated (DMEM). Gene expression levels were calculated relative to SHL1+2 undifferentiated C2C12 cells. Statistical significance: **p< 0.001, *p < 0.01 compared to respective SHL1+2 undifferentiated C2C12 (unpaired t-test).

4. DISCUSSION

The ABA/LANCL1-2 System Controls ROS metabolism in cardiomyocytes.

The study presented in this thesis uncovers a previously unrecognized role of the ABA/LANCL1-2 hormone–receptor system in cardiomyocyte protection against ROS-dependent oxidative stress, acting through the transcription factor ERRα. These data demonstrate that LANCL1/2 expression directly influences the transcriptional balance between ROS-generating and ROS-detoxifying enzymes, thereby modulating the redox homeostasis of cardiac cells.

Despite their higher mitochondrial respiratory activity and steeper proton gradient [19], LANCL1/2-overexpressing H9c2 cells exhibited markedly lower levels of mitochondrial ROS (Figure 16 and 17) and lipid hydroperoxides (Figure 12) compared with double-silenced cells, resulting in enhanced survival under oxidative stress. This apparent paradox highlights the efficiency of the ABA/LANCL1-2/ERRα axis in coordinating mitochondrial function with antioxidant defense mechanisms.

At the molecular level, LANCL1/2 overexpression significantly suppressed key ROS-producing enzymes (Figure 13), including COX2, NOX4, and XO, all major contributors to oxidative injury during inflammation and ischemia/reperfusion. Conversely, the expression of ROS-scavenging enzymes was strongly induced (Figure 14). SOD2, a mitochondrial superoxide dismutase, was upregulated over 40-fold, promoting the conversion of superoxide to hydrogen peroxide, while GPX4 increased over 45-fold, preventing lipid peroxidation and ferroptosis, a form of oxidative cell death implicated in cardiovascular pathologies [151]. These findings position GPX4 and SOD2 as downstream effectors of the protective LANCL1/2–ERRα pathway.

Treatment with ABA further reduced mitochondrial ROS exclusively in LANCL1/2-overexpressing cells (Figure 17), but not in silenced or ERRα-deficient cells, confirming that the beneficial antioxidant effects of ABA require a functional LANCL1/2–ERRα signaling cascade. Thus, the ABA/LANCL1-2 system serves as a molecular link between metabolic activation and redox protection, ensuring that elevated mitochondrial respiration is balanced by enhanced ROS detoxification capacity.

The protective role of ABA and LANCL proteins appears to be cell-type independent, as similar redox-regulatory effects have been reported in prostate carcinoma PC3 cells, in hepatocytes and spermatids [152-155]. In PC3 cells, LanCL1 promotes prostate cancer cell proliferation and helps protect cells from damage caused by oxidative stress [152]; in hepatocellular carcinoma cells, LANCL1 expression inversely correlated with ROS accumulation and ROS-responsive gene expression [153]; in hepatocytes ABA reduces lipid accumulation, inflammation, and oxidative stress via the NRF2 and AMPK pathways allieviating non-alcoholic fatty liver disease in mice [154] while

LANCL2 deletion in testicular cells led to glutathione imbalance, reduced SOD activity, and increased oxidative damage [155]. These consistent observations across tissues highlight the evolutionarily conserved antioxidant function of the ABA/LANCL system.

Taken together with previously published findings [13,18,19], these results highlight a multifaceted role of the ABA/LANCL1-2 hormone–receptor system in regulating cardiomyocyte metabolism and redox balance (**Figure 36**).

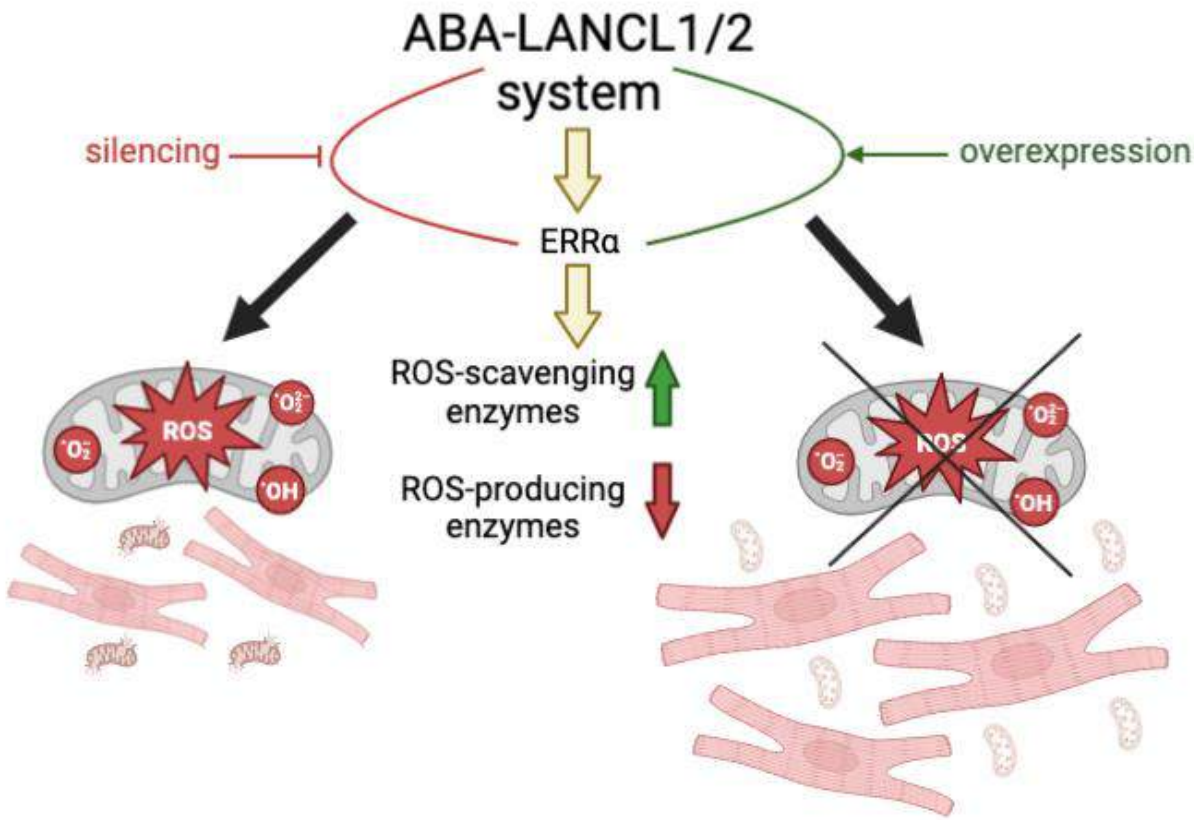

Figure 36. Signaling pathways and functional effects of the ABA/LANCL1-2 system in cardiomyocytes. Activation of the ABA/LANCL1-2 hormone–receptor system stimulates the AMPK/PGC-1α/Sirt1 signaling axis and the orphan nuclear receptor ERRα, enhancing the transcription of ROS-scavenging enzymes while suppressing that of ROS-generating enzymes. This coordinated regulation significantly reduces mitochondrial ROS levels in LANCL-overexpressing H9c2 cells compared to double-silenced counterparts, thereby protecting cardiomyocytes from oxidative stress and improving cellular function.

Activation of the ABA/LANCL1-2 system, achieved either by LANCL1/2 overexpression or by ABA stimulation, whose receptors are highly expressed in cardiac tissue [18], triggers multiple beneficial functional responses in addition to its protective role against oxidative stress. These include: (i) enhanced nitric oxide (NO) production under both normoxic and hypoxic conditions through eNOS

activation via the AMPK/PGC-1α signaling axis; (ii) increased mitochondrial respiration, characterized by higher basal and maximal oxygen consumption rates, greater spare respiratory capacity, and a steeper mitochondrial membrane potential (ΔΨ) during normoxia and after hypoxia/reoxygenation [18,19]; (iii) improved cell viability following oxidative or hypoxic stress; (iv) elevated glucose uptake and oxidation associated with higher NADPH levels; (v) increased fatty acid–driven respiration [19]. These pleiotropic effects rely on a conserved signaling cascade involving AMPK, PGC-1α, and ERRα, key metabolic regulators that promote oxidative metabolism and energy efficiency [156]. Importantly, this pathway not only boosts energy production but also strengthens the cell's capacity to counteract oxidative stress caused by increased electron flux when oxygen becomes limiting. Controlled modulation of electron flow within the respiratory chain, achieved through partial uncoupling of oxidative phosphorylation [19] prevents excessive mitochondrial hyperpolarization and mitigates reverse electron transport, thereby limiting ROS formation [157-160]. Collectively, the ABA/LANCL1-2/AMPK/PGC-1α/ERRα axis emerges as a critical mechanism balancing energy metabolism and redox homeostasis in cardiomyocytes. Consequently, nutraceutical or pharmacological activation of this pathway, either through ABA or its synthetic agonists, or via upregulation of LANCL1/2 expression, may represent a promising therapeutic strategy to enhance cardiomyocyte resilience against oxidative stress and ischemia/reperfusion injury. In light of this evidence, the research group at the University of Genova is currently investigating novel putative LANCL2 agonists, such as AR42 and other derivatives inspired by the chemical structure of previously identified agonists like BT11 [117,123].

Preliminary biochemical assays presented in this thesis, although requiring further and more detailed investigation both *in vitro* and *in vivo*, suggest that LANCL2 agonists could represent a new and promising pharmacological approach to improve mitochondrial efficiency and counteract ROS-mediated inflammation and oxidative damage. Additional and more comprehensive studies will be essential to fully elucidate the efficacy and mechanisms of these molecules in cellular and animal models. In parallel, the research group at the University of Genova is also exploring LANCL1 agonists, as this receptor has been implicated in the regulation of cellular redox balance across multiple pathological contexts, including cancer, amyotrophic lateral sclerosis, and metabolic disorders [161–163]. The combined targeting of LANCL1 and LANCL2 may therefore open new therapeutic avenues aimed at restoring redox homeostasis and mitochondrial function in oxidative stress–related diseases.

ABA/LANCL1-2 System Controls differentiation and thermogenesis in skeletal muscle.

In this thesis, the potential role of the ABA/LANCL1-2 system in regulating skeletal muscle differentiation and thermogenesis was investigated. The preliminary findings presented here provide the first indications that this signaling pathway may be involved in modulating key molecular mechanisms underlying myogenic differentiation and thermogenesis in muscle tissue. Specifically, the analysis of gene expression patterns related to these processes revealed trends suggesting that ABA/LANCL1-2 influence both the acquisition of a specific myogenic phenotype and the regulation of energy expenditure pathways. Although these results are preliminary, they provide an initial basis for a better understanding of the role of the ABA/LANCL1-2 axis in skeletal muscle physiology. Further studies will be needed to clarify the specific molecular mechanisms involved, including the identification of target genes, signaling intermediates, and possible interactions with other regulatory networks that control mitochondrial function, oxidative metabolism, and muscle plasticity as ERRα.

In humans, skeletal muscle accounts for approximately 40% of total body mass [99,100]. It is composed of a heterogeneous population of muscle fibers, each exhibiting distinct mechanical, biochemical, and metabolic properties suited to their specific functional roles. The primary molecular markers used to define muscle fiber types are the myosin heavy chain (MyHC) isoforms. In mammals, skeletal muscle is generally composed of four main MyHC isoforms: MyHC I, IIa, IIx, and IIb [146,147]. Slow oxidative fibers predominantly express MyHC I, whereas fast glycolytic fibers express MyHC IIb. The relative composition of MyHC isoforms can shift in response to physiological stimuli, allowing skeletal muscle to adapt to varying energy and functional demands [164]. Slow oxidative fibers are characterized by a high mitochondrial content and enhanced endogenous ROS scavenging capacity, supporting sustained oxidative metabolism. In contrast, fast glycolytic fibers rely primarily on anaerobic glycolysis to rapidly generate adenosine triphosphate (ATP) for short bursts of high-intensity activity. Fast-twitch fibers are essential for short, high-intensity bursts of activity, whereas slow-twitch fibers are specialized for prolonged, endurance-type exercise. Slow-twitch fibers rely primarily on mitochondrial respiration and therefore contain a high density of mitochondria. Exercise has been shown to influence muscle fiber-type switching through Ca^{2+}-dependent signaling [165], and multiple molecular pathways have been implicated in this adaptive process [166–168]. The composition of muscle fiber types is also closely linked to various muscle-related and metabolic diseases. Slow-twitch fibers exhibit higher antioxidant capacity, contributing not only to improved exercise performance but also to protection against hyperglycemia and insulin resistance [165,169]; in addition, the rate of slow-twitch muscle fibers negatively correlates with muscle atrophy [170]. In contrast, fast-twitch fibers are more prone to exercise-induced damage and

appear to be more vulnerable to metabolic disturbances, such as diabetes, than slow-twitch fibers [171]. Consequently, strategies aimed at promoting the transition from fast-twitch to slow-twitch fibers may represent a promising approach to prevent or ameliorate certain muscle- and metabolism-related disorders.

In our preliminary studies, we observed that C2C12 cells overexpressing LANCL1/2 and differentiated in the presence of B27 supplement exhibited the highest expression of all myogenic markers tested, promoting the development of a slow-twitch, oxidative muscle phenotype. Notably, the expression of MyHC-I, MYH7, and MT-ND1, genes associated with slow-twitch fibers and mitochondrial function, was significantly higher in LANCL1/2-overexpressing cells compared to LANCL1/2-silenced cells differentiated under the same conditions (Figure 34). Conversely, the highest expression of MyHC-IIb, characteristic of fast-twitch fibers, was observed in LANCL1/2-overexpressing cells differentiated with horse serum, a condition that promotes the formation of fast-twitch fibers [125]. Nevertheless, the current preliminary data suggest that LANCL1/2 overexpression may induce a fast-to-slow muscle fiber-type transition. It will be important to assess the effects of ABA in both overexpressing and silenced differentiated C2C12 cells, given that chronic ABA treatment has been shown to enhance physical performance in mice, increasing running time, distance, and maximal speed compared to controls [35]. The role of ABA/LANCL1-2 system on skeletal muscle differentation could be mediated by the ERRα/PGC-1α axis as already observed before. It is known that LANCL1/2 overexpression in cardiomyocytes increases ERRα expression, and studies in both adipocytes and cardiomyocytes have demonstrated that ERRα is directly responsible for the transcriptional effects observed in LANCL1/2-overexpressing cells. ERRα is functionally linked to LANCL proteins through a reciprocal feed-forward mechanism that amplifies transcriptional stimulation [16,19,98,156]. In cardiomyocytes, ERRα, in combination with the AMPK/PGC-1α/Sirt1 axis, regulates cardiac energy metabolism, metabolic flexibility, mitochondrial respiration, and biogenesis [19]. Moreover, ERRα and PGC-1α are coordinately upregulated along with metabolic and skeletal muscle-specific genes early in myogenesis [172]. PGC-1α drives the formation of slow-twitch muscle fibers, and its ability to mediate the switch to slow, oxidative fibers *in vitro* depends on hypoxia-inducible factor 2α (HIF2α). The transcriptional regulation of HIF2α is fully dependent on the PGC-1α/ERRα complex and is further modulated by SIRT1 activity [173]. In addition, activation of ERRα with 17β-estradiol (E2) increases the expression of MYH7, while pretreatment with the ERRα antagonist XCT790 reverses this E2-induced slow fiber-type switch [174]. MYH7 expression in the gastrocnemius muscle is also upregulated through increased PPARδ and ERRα gene expression [175]. Taken together, these findings underscore the need for a more

detailed investigation into the role of the ABA/LANCL1-2 system in skeletal muscle differentiation and its associated signaling pathways.

Another important aspect of skeletal muscle physiology investigated in this thesis is the role of the ABA/LANCL1–2 system in thermogenesis. Thermogenesis is essential for various physiological functions and plays a critical role in energy expenditure and weight management [150]. Thermogenesis in mammals depends on both shivering and non-shivering thermogenesis (NST). Shivering thermogenesis is an ATP-dependent mechanism that occurs through the contraction of skeletal muscles, which generates heat as a byproduct. Non-shivering thermogenesis is defined as an increase in metabolic heat production that is not associated with muscle cantraction activity and occurs in response to environmental temperature in several systems, including skeletal muscle and most notably in brown adipose tissue [150].

Recent studies have highlighted muscle nonshivering thermogenesis (NST) as an important mechanism of heat production ans as an attractive strategy to combat obesity [176]. Unlike shivering, NST generates heat independently of muscle contractions and relies on the activity of the sarco/endoplasmic reticulum Ca^{2+}-ATPase (SERCA1a) pump, which is finely regulated by sarcolipin (SLN). In skeletal muscle, SERCA1a normally transports Ca^{2+} ions from the cytoplasm back into the sarcoplasmic reticulum during muscle relaxation, using energy derived from ATP hydrolysis. When sarcolipin binds to SERCA1a, however, it partially uncouples ATP hydrolysis from Ca^{2+} transport, leading to a phenomenon known as “slippage.” Under these conditions, bound Ca^{2+} ions are released back into the cytoplasm rather than being sequestered, resulting in continuous ATP consumption and the dissipation of energy as heat. Through this mechanism, sarcolipin acts as a molecular switch that converts chemical energy into thermal energy, enhancing the thermogenic capacity of skeletal muscle and contributing to systemic energy balance, metabolic homeostasis, and adaptation to cold environments. Interestingly, the results presented in this thesis showed a markedly higher expression of sarcolipin, along with increased expression of the SERCA pump and UCP3, suggesting that the ABA/LANCL1-2 signaling system may influence these thermogenic processes (Figure 35). The higher expression of sarcolipin and UCP3 was already observed in LANCL overexpressing rat L6 myoblast treated with ABA [17]. The high UCP3 expression found in LANCL1-2 overexpressing C2C12 cells indicates that this system not only triggers thermogenesis through a calcium-mediated ATP futile cycle, but may also induce proton leaking by UCP3 in muscles. In parallel, recent preliminary results from the Biochemistry research group at the University of Genova demonstrated that C2C12 myotubes overexpressing LANCL1-2 exhibited enhanced heat production compared to silenced cells (data not shown), in line with the observed upregulation of sarcolipin, SERCA, and

UCP3, as well as previous findings in cardiomyocytes [111], thus confirming an important role of this system in thermogenesis. Interestingly, overexpression of LANCL1/2 resulted in increased Creatine Kinase (CK) expression in differentiated myoblasts, as observed in this thesis. CK plays a pivotal role in skeletal muscle development by supporting the energetic demands of myogenesis, facilitating the rapid buffering and delivery of ATP, which is essential during the highly energy-consuming stages of myoblast differentiation and fusion into multinucleated myotubes. Beyond its metabolic role, CK has been shown to regulate the orderly progression of myoblast fusion, ensuring proper alignment and maturation of myogenic cells. Isoform-specific expression of CK, such as the muscle-type CK (M-CK), serves not only as a marker of differentiation but also contributes mechanistically to the regulation of myogenic progression, highlighting its dual functional and signaling roles in muscle cell development [137, 143]. In adipose tissue, several studies have described a futile creatine cycle, in which repeated phosphorylation and dephosphorylation of creatine dissipates energy as heat, thereby contributing to adaptive thermogenesis [177-179]. In this cycle, creatine kinase utilizes mitochondrial ATP to generate phosphocreatine (PCr), maintaining elevated local ATP/ADP ratios at sites of high energetic demand [178]. The continuous turnover of creatine and phosphocreatine results in energy dissipation, acting in concert with UCP1-mediated mitochondrial uncoupling in beige and brown adipocytes [180]. Wallimann et al. [181] proposed that this cycle may additionally support Ca^{2+} handling by sustaining high ATP/ADP ratios at the sarco/endoplasmic reticulum Ca^{2+}-ATPase (SERCA) pump, linking creatine metabolism to thermogenic capacity in muscle. Collectively, these findings indicate a broader role for creatine metabolism in the regulation of energy expenditure and mammalian thermogenesis. Recent studies suggest that exercise can upregulate creatine kinase mitochondrial isoform (CKMT2) expression in skeletal muscle, implying a role for creatine metabolism in muscle energy regulation and possibly thermogenesis [182]. However, the classical skeletal muscle-type creatine kinase (CKM) primarily functions as an energy buffer and shuttle, and while it participates in rapid ATP regeneration, a canonical "futile creatine cycle" similar to that formally described in adipose tissue thermogenesis has not been conclusively demonstrated in skeletal muscle. Two recent reviews clarify the role of creatine as a major coordinator of energy exchange between organs and introduce an innovative BLSA “Brain-Liver-Skeletal muscle–Adipose” creatine metabolic axis model (**Figure 37**) [183,184]. According to this model, creatine synthesized by the liver is distributed to various tissues and organs through the bloodstream, where it enters the intracellular creatine cycle. In skeletal muscle, creatine serves as a crucial link between mitochondrial oxidative phosphorylation and glycolysis, facilitating targeted energy transfer via mitochondrial supercomplexes. Exercise has been shown to enhance creatine transporter expression in skeletal muscle via the AMPK/PGC-1α signaling pathway, thereby

improving phosphocreatine shuttle efficiency and overall energy metabolism. In parallel, exercise-induced exosomes and microRNAs may modulate the futile creatine cycle in adipose tissue, stimulating UCP1-independent thermogenesis, enhancing energy dissipation and metabolic flexibility and alleviating obesity. In the brain, the creatine cycle appears to function as a metabolic sensor, capable of detecting systemic energy status and coordinating inter-organ energy expenditure through neural and endocrine pathways. Notably, the hypothalamus plays a central role in this regulatory network, maintaining energy balance and systemic homeostasis [185]. This model defines creatine as the core regulator of systemic energy distribution, enabling diverse energy allocation through creatine cycles in different tissues. Future research should aim to elucidate the potential crosstalk between ABA/LANCL1-2 signaling and creatine metabolism in skeletal muscle, adipose tissue, and the brain, as well as their cooperative role in thermogenic regulation. Such investigations could open new therapeutic therapeutic strategies aimed at treating metabolic disorders and obesity.

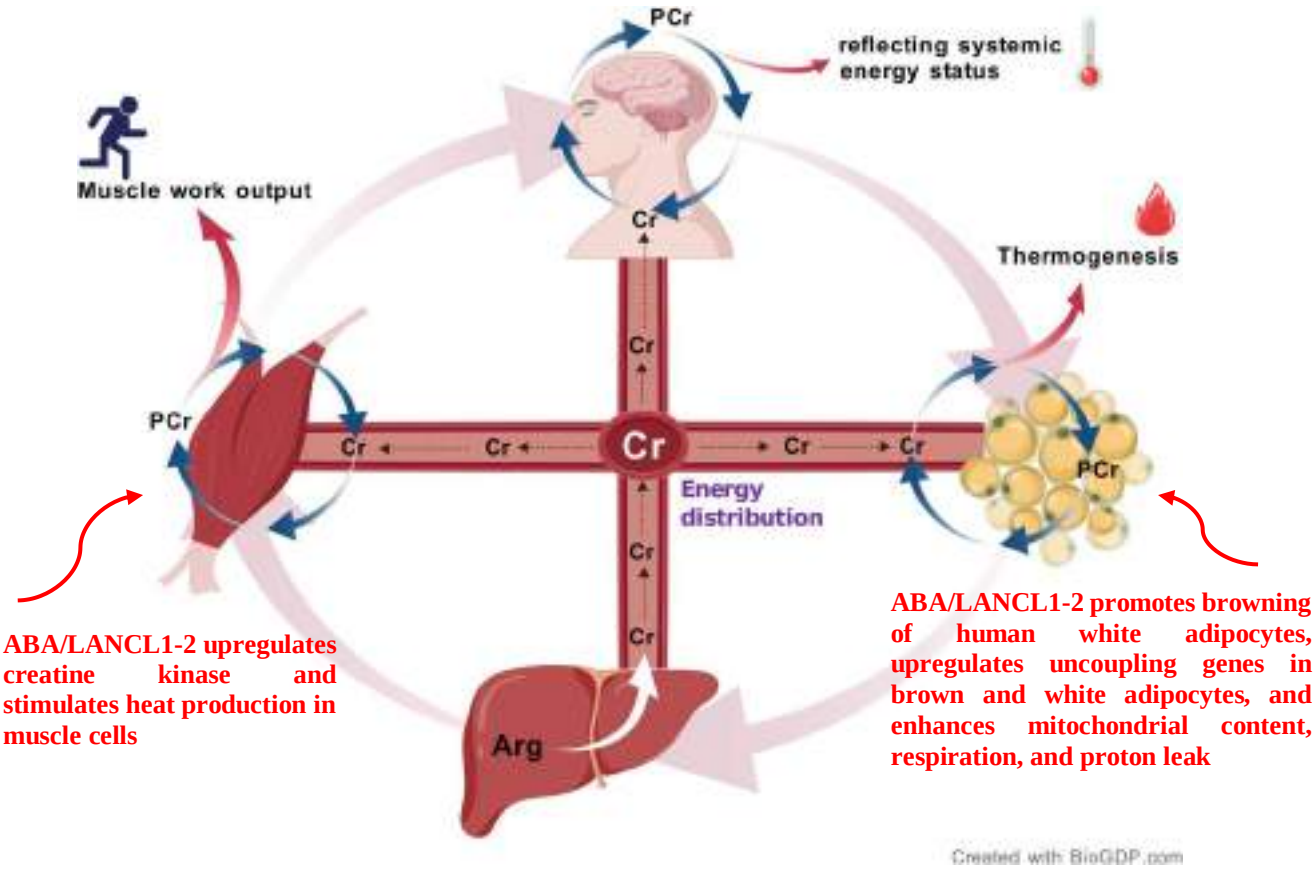

Figure 37. The BLSA Metabolic Axis Model of Creatine mofified from [183]. Creatine synthesized in the liver circulates to various organs, entering tissue-specific creatine cycles. In skeletal muscle, it supports ATP production; in adipose tissue, it drives thermogenesis; and in the brain, it senses systemic energy status and coordinates inter-organ energy balance. Modulating the creatine cycle may restore energy balance and counteract obesity, diabetes, and other metabolic disorders. Future studies will investigate the role of the ABA/LANCL1-2 system and its interaction with creatine metabolism and thermogenesis.

5. BIBLIOGRAPHY

1. Hey, S.J.; Byrne, E.; Halford, N.G. The interface between metabolic and stress signalling. Ann. Bot. 2010, 105, 197–203.
2. Lin, B.L.; Wang, H.J.; Wang, J.S.; Zaharia, L.I.; Abrams, S.R. Abscisic acid regulation of heterophylly in Marsilea quadrifolia L.: effects of R-(–) and S-(+) isomers. J. Exp. Bot. 2005, 56(421), 2935–2948.
3. Cutler, S.R.; Rodriguez, P.L.; Finkelstein, R.R.; Abrams, S.R. Abscisic acid: Emergence of a core signaling network. Annu. Rev. Plant Biol. 2010, 61, 651–679.
4. Zocchi, E.; Carpaneto, A.; Cerrano, C.; Bavestrello, G.; Giovine, M.; Bruzzone, S.; Guida, L.; Usai, C. The temperature-signaling cascade in sponges involves a heat-gated cation channel, abscisic acid and cyclic ADP-ribose. Proc. Natl. Acad. Sci. USA 2001, 98, 14859–14864.
5. Puce, S.; Basile, G.; Bavestrello, G.; Bruzzone, S.; Cerrano, C.; Giovine, M.; Arillo, A.; Zocchi, E. Abscisic acid signaling through cyclic ADP-ribose in hydroid regeneration. J. Biol. Chem. 2004, 279, 39783–39788.
6. Bruzzone, S.; Ameri, P.; Briatore, L.; Mannino, E.; Basile, G.; Andraghetti, G.; Grozio, A.; Magnone, M.; Guida, L.; Scarfì, S.; Salis, A.; Damonte, G.; Sturla, L.; Nencioni, A.; Fenoglio, D.; Fiory, F.; Miele, C.; Beguinot, F.; Ruvolo, V.; Bormioli, M.; Colombo, G.; Maggi, D.; Murialdo, G.; Cordera, R.; De Flora, A.; Zocchi, E. The plant hormone abscisic acid increases in human plasma after hyperglycemia and stimulates glucose consumption by adipocytes and myoblasts. FASEB J. 2012, 26, 1251–1260.
7. Bruzzone, S.; Bodrato, N.; Usai, C.; Guida, L.; Moreschi, I.; Nano, R.; Antonioli, B.; Fruscione, F.; Magnone, M.; Scarfì, S.; Zocchi, E. Abscisic acid is an endogenous cytokine in human granulocytes with cyclic ADP-ribose as second messenger. Proc. Natl. Acad. Sci. USA 2007, 104, 5759–5764.
8. Magnone, M.; Ameri, P.; Salis, A.; Andraghetti, G.; Emionite, L.; Murialdo, G.; De Flora, A.; Zocchi, E. Autocrine abscisic acid plays a key role in quartz-induced macrophage activation. FASEB J. 2012, 26, 1261–1271.
9. Scarfì, S.; Bruzzone, S.; Magnone, M.; Zocchi, E.; Usai, C.; Guida, L. The plant hormone abscisic acid stimulates the proliferation of human hemopoietic progenitors through the second messenger cyclic ADP-ribose. Stem Cells 2009, 27, 2469–2477.
10. Magnone, M.; Ameri, P.; Salis, A.; Andraghetti, G.; Emionite, L.; Murialdo, G.; De Flora, A.; Zocchi, E. Microgram amounts of abscisic acid in fruit extracts improve glucose tolerance and reduce insulinemia in rats and in humans. FASEB J. 2015, 29,4783–4793.

11. Zocchi, E.; Hontecillas, R.; Leber, A.; Einerhand, A.; Carbo, A.; Bruzzone, S.; Tubau-Juni, N.; Philipson, N.; Zoccoli-Rodriguez, V.; Sturla, L.; et al. Abscisic Acid: A Novel Nutraceutical for Glycemic Control. Front. Nutr. 2017, 4, 24.
12. Magnone, M.; Sturla, L.; Guida, L.; Spinelli, S.; Begani, G.; Bruzzone, S.; Fresia, C.; Zocchi, E. Abscisic Acid: A Conserved Hormone in Plants and Humans and a Promising Aid to Combat Prediabetes and the Metabolic Syndrome. Nutrients 2020, 12,1724
13. Spinelli, S.; Magnone, M.; Guida, L.; Sturla, L.; Zocchi, E. The ABA/LANCL Hormone/Receptor System in the Control of Glycemia, of Cardiomyocyte Energy Metabolism, and in Neuroprotection: A New Ally in the Treatment of Diabetes Mellitus? In. Sci. 2023, 24, 1199.
14. Spinelli S, Humma Z, Magnone M, Zocchi E, Sturla L. Role of Abscisic Acid in the Whole Body Regulation of Glucose Uptake and Metabolism. Nutrients 2024,17, 132025.
15. Sturla, L.; Mannino, E.; Scarfì, S.; Bruzzone, S.; Magnone, M.; Sociali, G.; Booz, V.; Guida, L.; Vigliarolo, T.; Fresia, C.; et al. Abscisic acid enhances glucose disposal and induces brown fat activity in adipocytes in vitro and in vivo. Biochim. Biophys. Acta 2017,1862, 131–144
16. Spinelli, S.; Cossu, V.; Passalacqua, M.; Hansen, J.B.; Guida, L.; Magnone, M.; Sambuceti, G.; Marini, C.; Sturla, L.; Zocchi, E. TheABA/LANCL1/2 Hormone/Receptor System Controls Adipocyte Browning and Energy Expenditure. Int. J. Mol. Sci. 2023, 24,3489
17. Spinelli, S.; Begani, G.; Guida, L.; Magnone, M.; Galante, D.; D'Arrigo, C.; Scotti, C.; Iamele, L.; de Jonge, H.; Zocchi, E.; et al. LANCL1 binds abscisic acid and stimulates glucose transport and mitochondrial respiration in muscle cells via the AMPK/PGC-1α/Sirt1 pathway. Mol. Metab. 2021, 53, 101263
18. Spinelli, S.; Guida, L.; Vigliarolo, T.; Passalacqua, M.; Begani, G.; Magnone, M.; Sturla, L.; Benzi, A.; Ameri, P.; Lazzarini, E.; et al. The ABA-LANCL1/2 Hormone-Receptors System Protects H9c2 Cardiomyocytes from Hypoxia Induced Mitochondrial Injury via an AMPK- and NO-Mediated Mechanism. Cells 2022, 11, 2888.
19. Spinelli, S.; Guida, L.; Passalacqua, M.; Magnone, M.; Cossu, V.; Sambuceti, G.; Marini, C.; Sturla, L.; Zocchi, E. Abscisic Acid and Its Receptors LANCL1 and LANCL2 Control Cardiomyocyte Mitochondrial Function, Expression of Contractile, Cytoskeletal and Ion Channel Proteins and Cell Proliferation via ERRα. Antioxidants 2023, 12, 1692.
20. Ohkuma, K.; Lyon, J.L.; Addicott, F.T.; Smith, O.E. Abscisin II, an abscission-accelerating substance from young cotton fruit. Science 1963, 142, 1592–1593.
21. Addicott, F.T.; Lyon, J.L.; Ohkuma, K.; Thiessen, W.E.; Carns, H.R.; Smith, O.E.; Cornforth, J.W.; Milborrow, B.V.; Ryback, G.; Wareing, P.F. Abscisic Acid: A New Name for Abscisin II (Dormin). Science 1968, 159, 1493.

22. Davis, L.A.; Addicott, F.T. Abscisic Acid: Correlations with abscission and with development in the cotton fruit. Plant Physiol.1972, 49, 644–648.
23. Ali, F.; Qanmber, G.; Li, F.; Wang, Z. Updated role of ABA in seed maturation, dormancy, and germination. J. Adv. Res. 2021, 35, 199–214.
24. Singh, A.; Roychoudhury, A. Abscisic acid in plants under abiotic stress: Crosstalk with major phytohormones. Plant Cell Rep.2023, 42, 961–974.
25. Le Page-Degivry, M.T.; Bidard, J.N.; Rouvier, E.; Bulard, C.; Lazdunski, M. Presence of abscisic acid, a phytohormone, in the mammalian brain. Proc. Natl. Acad. Sci. USA 1986, 83, 1155–1158.
26. Togashi, K.; Hara, Y.; Tominaga, T.; Higashi, T.; Konishi, Y.; Mori, Y.; Tominaga, M. TRPM2 activation by cyclic ADP-ribose at body temperature is involved in insulin secretion. EMBO J. 2006, 25, 1804–1815.
27. Zocchi, E.; Basile, G.; Cerrano, C.; Bavestrello, G.; Giovine, M.; Bruzzone, S.; Guida, L.; Carpaneto, A.; Magrassi, R.; Usai, C. ABA and cADPR-mediated effects on respiration and filtration downstream of the temperature-signaling cascade in sponges. J. Cell Sci. 2003, 116, 629–636.
28. Sturla, L.; Fresia, C.; Guida, L.; Bruzzone, S.; Scarfì, S.; Usai, C.; Fruscione, F.; Magnone, M.; Millo, E.; Basile, G.; et al. LANCL2 is necessary for abscisic acid binding and signaling in human granulocytes and in rat insulinoma cells. J. Biol. Chem. 2009, 284,28045–28057.
29. Sturla, L.; Fresia, C.M.; Guida, L.; Grozio, A.; Vigliarolo, T.; Mannino, E.; Millo, E.; Bagnasco, L.; Bruzzone, S.; De Flora, A.; Zocchi, E. Binding of abscisic acid to human LANCL2. Biochem. Biophys. Res. Commun. 2011, 415, 390–395.
30. Lu, P.; Bevan, D.R.; Lewis, S.N.; Hontecillas, R.; Bassaganya-Riera, J. Molecular modeling of lanthionine synthetase component C-like protein 2: A potential target for the discovery of novel type 2 diabetes prophylactics and therapeutics. J. Mol. Model. 2011, 17, 543–553.
31. Lu, P.; Hontecillas, R.; Philipson, C.W.; Bassaganya-Riera, J. Lanthionine synthetase component C-like protein 2: A new drug target for inflammatory diseases and diabetes. Curr. Drug Targets 2014, 15, 565–572.
32. Spinelli, S.; Begani, G.; Guida, L.; Magnone, M.; Galante, D.; D'Arrigo, C.; Scotti, C.; Iamele, L.; De Jonge, H.; Zocchi, E.; Sturla, L. LANCL1 binds abscisic acid and stimulates glucose transport and mitochondrial respiration in muscle cells via the AMPK/PGC-1α/Sirt1 pathway. Mol. Metab. 2021, 53, 101263.
33. Magnone, M.; Leoncini, G.; Vigliarolo, T.; Emionite, L.; Sturla, L.; Zocchi, E.; Murialdo, G. Chronic Intake of Micrograms of Abscisic Acid Improves Glycemia and Lipidemia in a Human Study and in High-Glucose Fed Mice. Nutrients 2018, 10, 1454–1458.

34. Atkinson, F.S.; Villar, A.; Mulà, A.; Zangara, A.; Risco, E.; Smidt, C.R.; Hontecillas, R.; Leber, A.; Bassaganya-Riera, J. Abscisic Acid Standardized Fig (Ficus carica) Extracts Ameliorate Postprandial Glycemic and Insulinemic Responses in Healthy Adults. Nutrients 2019, 11, 1757.
35. Magnone, M.; Emionite, L.; Guida, L.; Vigliarolo, T.; Sturla, L.; Spinelli, S.; Buschiazzo, A.; Marini, C.; Sambuceti, G.; De Flora, A.; Orengo, A.M.; Cossu, V.; Ferrando, S.; Barbieri, O.; Zocchi, E. Insulin-independent stimulation of skeletal muscle glucose uptake by low-dose abscisic acid via AMPK activation. Sci. Rep. 2020, 10, 1454.
36. Leber, A.; Hontecillas, R.; Tubau-Juni, N.; Zoccoli-Rodriguez, V.; Goodpaster, B.; Bassaganya-Riera, J. Abscisic acid enriched fig extract promotes insulin sensitivity by decreasing systemic inflammation and activating LANCL2 in skeletal muscle. Sci. Rep. 2020, 10, 10463.
37. Tenore, G.C.; Caruso, D.; D'Avino, M.; Buonomo, G.; Caruso, G.; Ciampaglia, R.; Schiano, E.; Maisto, M.; Annunziata, G.; Novellino, E. A Pilot screening of agro-food waste products as source nutraceutical formulations to improve simulated postprandial glycaemia and insulinaemia in healthy subjects. Nutrients 2020, 12, 1292.
38. Fidler, J.; Graska, J.; Gietler, M.; Nykiel, M.; Prabucka, B.; Rybarczyk-Pło´nska, A.; Muszy´nska, E.; Morkunas, I.; Labudda, M. PYR/PYL/RCAR Receptors Play a Vital Role in the Abscisic-Acid-Dependent Responses of Plants to External or Internal Stimuli. Cells 2022, 11, 1352.
39. Wang, Z.Z.; Cao, M.J.; Yan, J.; Dong, J.; Chen, M.X.; Yang, J.F.; Li, J.H.; Ying, R.N.; Gao, Y.Y.; Li, L.; et al. Stabilization of dimeric PYR/PYL/RCAR family members relieves abscisic acid-induced inhibition of seed germination. Nat. Commun. 2024, 15, 8077.
40. Klingler, J.P.; Batelli, G.; Zhu, J.K. ABA receptors: The START of a new paradigm in phytohormone signalling. J. Exp. Bot. 2010,61, 3199–3210.
41. Chen, J.G.; Ellis, B.E. GCR2 is a new member of the eukaryotic lanthionine synthetase component C-like protein family. Plant Signal Behav. 2008, 3, 307–310.
42. Johnston, C.A.; Temple, B.R.; Chen, J.G.; Gao, Y.; Moriyama, E.N.; Jones, A.M.; Siderovski, D.P.; Willard, F.S. Comment on "A G protein coupled receptor is a plasma membrane receptor for the plant hormone abscisic acid". Science 2007, 318, 914.
43. Shin, J.M.; Gwak, J.W.; Kamarajan, P.; Fenno, J.C.; Rickard, A.H.; Kapila, Y.L. Biomedical applications of nisin. J. Appl. Microbiol. 2016, 120, 1449–1465.
44. Bauer, H.; Mayer, H.; Marchler-Bauer, A.; Salzer, U.; Prohaska, R. Characterization of p40/GPR69A as a peripheral membrane protein related to the lantibiotic synthetase component C. Biochem. Biophys. Res. Commun. 2000, 275, 69–74.
45. He, C.; Zeng, M.; Dutta, D.; Koh, T.H.; Chen, J.; van der Donk, W.A. LanCL proteins are not Involved in Lanthionine Synthesis in Mammals. Sci. Rep. 2017, 20, 40980.

46. Mayer, H; Bauer, H.; Breuss, J.; Ziegler, S.; Prohaska, R. Characterization of rat LANCL1, a novel member of the lanthionine synthetase C-like protein family, highly expressed in testis and brain. Gene 2001, 269, 73-80.
47. Landlinger, C.; Salzer, U.; Prohaska, R. Myristoylation of human LanC-like protein 2 (LANCL2) is essential for the interaction with the plasma membrane and the increase in cellular sensitivity to adriamycin. Biochim. Biophys. Acta 2006.
48. Mayer, H.; Bauer, H.; Prohaska, R. Organization and chromosomal localization of the human and mouse genes coding for LanC-like protein 1 (LANCL1). Cytogenet. Cell Genet. 2001, 93, 100–104.
49. Eley, G.D.; Reiter, J.L.; Pandita, A.; Park, S.; Jenkins, R.B.; Maihle, N.J.; James, C.D. A chromosomal region 7p11.2 transcript map: Its development and application to the study of EGFR amplicons inglioblastoma. Neuro Oncol. 2002, 4, 86–94.
50. Gassner, C.; Brönnimann, C.; Merki, Y.; Mattle-Greminger, M.P.; Sigurdardottir, S.; Meyer, E.; Engström, C.; O'Sullivan, J.D.; Jung, H.H.; Frey, B.M. Stepwise partitioning of Xp21: A profiling method for XK deletions causative of the McLeod syndrome. Transfusion. 2017, 57, 2125–2135.
51. Mayer, H.; Salzer, U.; Breuss, J.; Ziegler, S.; Marchler-Bauer, A.; Prohaska, R. Isolation, molecular characterization, and tissue specific expression of a novel putative G protein-coupled receptor. Biochim. Biophys. Acta 1998, 1395, 301–308.
52. Park, S.; James, C.D. Lanthionine synthetase component C-like 2 increases cellular sensitivity to adriamycin by decreasing the expression of P-glycoprotein through a transcription-mediated mechanism. Cancer Res. 2003, 63, 723–727.
53. Cichero, E.; Fresia, C.; Guida, L.; Booz, V.; Millo, E.; Scotti, C.; Iamele, L.; de Jonge, H.; Galante, D. ; De Flora, A.; Sturla, L.; Vigliarolo, T.; Zocchi, E.; Fossa, P. Identification of a high-affinity binding site for abscisic acid on human lanthionine synthetase component C-like protein 2 (LANCL2). Int. J. Biochem. Cell Biol. 2018, 97, 52–61.
54. Fresia, C.; Vigliarolo, T.; Guida, L.; Booz, V.; Bruzzone, S.; Sturla, L.; Di Bona, M.; Pesce, M.; Usai, C.; De Flora, A.; Zocchi, E. G-protein coupling and nuclear translocation of the human abscisic acid receptor LANCL2. Sci. Rep. 2016, 6, 26658.
55. Vigliarolo, T.; Zocchi, E.; Fresia, C.; Booz, V.; Guida, L. Abscisic acid influx into human nucleated cells occurs through the anion exchanger AE2. Int. J. Biochem. Cell Biol. 2016, 75, 99–103.
56. Boursiac, Y.; Léran, S.; Corratgé-Faillie, C.; Gojon, A.; Krouk, G.; Lacombe, B. ABA transport and transporters. Trends Plant Sci. 2013, 18, 325–333.
57. Bassaganya-Riera, J.; Guri, A.J.; Lu, P.; Climent, M.; Carbo, A.; Sobral, B.W.; Horne, W.T.; Lewis, S.N.; Bevan, D.R.; Hontecillas, R. Abscisic acid regulates inflammation via ligand-binding domain-

independent activation of peroxisome proliferator-activated receptor γ. J. Biol. Chem. 2011, 286, 2504–2516.

58. Leber, A.; Hontecillas, R.; Tubau-Juni, N.; Zoccoli-Rodriguez, V.; Hulver, M.; McMillan, R.; Bassaganya-Riera, J. Modeling the role of Lanthionine synthetase C-like 2 (LANCL2) in the modulation of immune responses to Helicobacter pylori infection. PLoS One 2016, 11, e0167440.
59. Ameri, P.; Bruzzone, S.; Mannino, E.; Sociali, G.; Andraghetti, G.; Salis, A.; Ponta, M.L.; Briatore, L.; Adami, G.F.; Ferraiolo, A.; Venturini, P.L.; Maggi, D.; Cordera, R.; Murialdo, G.; Zocchi, E. Impaired increase of plasma abscisic acid in response to oral glucose load in type 2 diabetes and in gestational diabetes. PLoS ONE 2015, 10, e0115992.
60. Magnone, M.; Spinelli, S.; Begani, G.; Guida, L.; Sturla, L.; Emionite, L.; Zocchi, E. Abscisic acid improves insulin action on glycemia in insulin-deficient mouse models of Type 1 Diabetes. Metabolites 2022, 12, 523.
61. Derosa, G.; Maffioli, P.; D'Angelo, A.; Preti, P.S.; Tenore, G.; Novellino, E. Abscisic Acid Treatment in Patients with Prediabetes.Nutrients 2020, 12, 2931
62. Gharib, A.; Marquez, C.; Meseguer-Beltran, M.; Sanchez-Sarasua, S.; Sanchez-Perez, A.M. Abscisic acid, an evolutionary conserved hormone: Biosynthesis, therapeutic and diagnostic applications in mammals. Biochem. Pharmacol. 2024, 229, 116521.
63. Guri, A.J.; Misyak, S.A.; Hontecillas, R.; Hasty, A.; Liu, D.; Si, H.; Bassaganya-Riera, J. Abscisic acid ameliorates atherosclerosis by suppressing macrophage and CD4+ T cell recruitment into the aortic wall. J. Nutr. Biochem. 2010, 21, 1178–1185.
64. Bassaganya-Riera, J.; Guri, A.J.; Lu, P.; Climent, M.; Carbo, A.; Sobral, B.W.; Horne, W.T.; Lewis, S.N.; Bevan, D.R.; Hontecillas, R. Abscisic acid regulates inflammation via ligand-binding domain-independent activation of peroxisome proliferator-activated receptor gamma. J. Biol. Chem. 2011, 286, 2504–2516.
65. Guri, A.J.; Hontecillas, R.; Bassaganya-Riera, J. Abscisic acid ameliorates experimental IBD by downregulating cellular adhesion molecule expression and suppressing immune cell infiltration. Clin. Nutr. 2010, 29, 824–831.
66. Hontecillas, R.; Roberts, P.C.; Carbo, A.; Vives, C.; Horne, W.T.; Genis, S.; Velayudhan, B.; Bassaganya-Riera, J. Dietary abscisic acid ameliorates influenza-virus-associated disease and pulmonary immunopathology through a PPARgamma-dependent mechanism. J. Nutr. Biochem. 2013, 24, 1019–1027.
67. Sanchez-Sarasúa, S.; Moustafa, S.; García-Aviles, A.; Lopez-Climent, M.F.; Gomez-Cadenas, A.; Olucha-Bordonau, F.E.; SanchezPerez, A.M. The effect of abscisic acid chronic treatment on

neuroinflammatory markers and memory in a rat model of high-fat diet induced neuroinflammation. Nutr. Metab. 2016, 13, 73.

68. Ribes-Navarro, A.; Atef, M.; Sanchez-Sarasúa, S.; Beltran-Bretones, M.T.; Olucha-Bordonau, F.; Sanchez-Perez, A.M. Abscisic Acid Supplementation Rescues High Fat Diet-Induced Alterations in Hippocampal Inflammation and IRSs Expression. Mol.Neurobiol. 2018, 56, 454–464.
69. Bodrato, N.; Franco, L.; Fresia, C.; Guida, L.; Usai, C.; Salis, A.; Moreschi, I.; Ferraris, C.; Verderio, C.; Basile, G.; Bruzzone, S.; Scarfì, S.; De Flora, A.; Zocchi, E. Abscisic acid activates the murine microglial cell line N9 through the second messenger cyclic ADP-ribose. J. Biol. Chem. 2009, 284, 14777–14787.
70. Magnone, M.; Bruzzone, S.; Guida, L.; Damonte, G.; Millo, E.; Scarfì, S.; Usai, C.; Palombo, D.; Sturla, L.; De Flora, A.; Zocchi, E. Abscisic acid released by human monocytes activates monocytes and vascular smooth muscle cell responses involved in atherogenesis. J. Biol. Chem. 2009, 284, 17808–17818.
71. Magnone, M.; Sturla, L.; Jacchetti, E.; Scarfì, S.; Bruzzone, S.; Usai, C.; Guida, L.; Salis, A.; Damonte, G.; De Flora, A.; Zocchi, E. Autocrine abscisic acid plays a key role in quartz-induced macrophage activation. FASEB J. 2012, 26, 1261–1271.
72. Scarfì, S.; Ferraris, C.; Fruscione, F.; Fresia, C.; Guida, L.; Bruzzone, S.; Usai, C.; Parodi, A.; Millo, E.; Salis, A.; Burastero, G.; De Flora, A.; Zocchi, E. Cyclic ADP-ribose-mediated expansion and stimulation of human mesenchymal stem cells by the plant hormone abscisic acid. Stem Cells 2008, 26, 2855–2864.
73. Khorasani, A.; Abbasnejad, M.; Esmaeili-Mahani, S. Phytohormone abscisic acid ameliorates cognitive impairments in streptozotocin-induced rat model of Alzheimer's disease through PPARbeta/delta and PKA signaling. Int. J. Neurosci. 2019, 129, 1053–1065.
74. Espinosa-Fernández, V.; Mañas-Ojeda, A.; Pacheco-Herrero, M.; Castro-Salazar, E.; Ros-Bernal, F.; Sánchez-Pérez, A. M. Early intervention with ABA prevents neuroinflammation and memory impairment in a triple transgenic mice model of Alzheimer's disease. Behav. Brain Res. 2019, 374, 112106.
75. Jeon, S.H.; Kim, N.; Ju, Y.J.; Gee, M.S.; Lee, D.; Lee, J.K. Phytohormone Abscisic Acid Improves Memory Impairment and Reduces Neuroinflammation in 5xFAD Mice by Upregulation of LanC-Like Protein 2. Int. J. Mol. Sci. 2020, 21, 8425.
76. Shabani, M.; Soti, M.; Ranjbar, H.; Naderi, R. Abscisic acid ameliorates motor disabilities in 6-OHDA-induced mice model of Parkinson's disease. Heliyon 2023, 9, e18473.

77. Meseguer-Beltrán, M.; Sánchez-Sarasúa, S.; Landry, M.; Kerekes, N.; Sánchez-Pérez, A.M. Targeting Neuroinflammation with Abscisic Acid Reduces Pain Sensitivity in Females and Hyperactivity in Males of an ADHD Mice Model. Cells 2023, 12, 465.
78. Han, T.; Xu, Y.; Liu, H.; Sun, L.; Cheng, X.; Shen, Y.; Wei, J. Function and Mechanism of Abscisic Acid on Microglia-Induced Neuroinflammation in Parkinson's Disease. Int. J. Mol. Sci. 2024, 25, 4920.
79. Guri, A.J.; Hontecillas, R.; Si, H.; Liu, D.; Bassaganya-Riera, J. Dietary abscisic acid ameliorates glucose tolerance and obesityrelated inflammation in db/db mice fed high-fat diets. Clin. Nutr. 2007, 26, 107–116.
80. Guri, A.J.; Hontecillas, R.; Bassaganya-Riera, J. Abscisic acid synergizes with rosiglitazone to improve glucose tolerance and down-modulate macrophage accumulation in adipose tissue: Possible action of the cAMP/PKA/PPAR γ axis. Clin. Nutr. 2010,29, 646–653.
81. Miragoli, M.; Cabassi, A. Mitochondrial Mechanosensor Microdomains in Cardiovascular Disorders. Adv. Exp. Med. Biol. 2017, 982, 247–264.
82. Morciano, G.; Boncompagni, C.; Ramaccini, D.; Pedriali, G.; Bouhamida, E.; Tremoli, E.; Giorgi, C.; Pinton, P. Comprehensive Analysis of Mitochondrial Dynamics Alterations in Heart Diseases. Int. J. Mol. Sci. 2023, 24, 3414.
83. Huss, J.M.; Garbacz, W.G.; Xie, W. Constitutive activities of estrogen-related receptors: Transcriptional regulation of metabolism by the ERR pathways in health and disease. Biochim. Biophys. Acta 2015, 9, 1912–1927.
84. Villena, J.A.; Hock, M.B.; Chang, V.Y.; Barcas, J.E.; Gigue, V.; Kralli, A. Orphan nuclear receptor estrogen-related receptor is essential for adaptive thermogenesis. Proc. Natl. Acad. Sci. USA 2007, 104, 1418–1423.
85. Sakamoto, T.; Matsuura, T.R.; Wan, S.; Ryba, D.M.; Kim, J.U.; Won, K.J.; Lai, L.; Petucci, C.; Petrenko, N.; Musunuru, K.; Vega, R.B.; Kelly, D.P. A critical role for estrogen-related receptor signaling in cardiac maturation. Circ. Res. 2020, 126, 1685–1702.
86. Ramjiawan, A.; Bagchi, R.A.; Blant, A.; Albak, L.; Cavasin, M.A.; Horn, T.R.; McKinsey, T.A.; Czubryt, M.P. Roles of histone deacetylation and AMP kinase in regulation of cardiomyocyte PGC-1α gene expression in hypoxia. Am. J. Physiol. Cell Physiol. 2013, 304, C1064–C1072.
87. Huss, J.M.; Imahashi, K.; Dufour, C.R.; Weinheimer, C.J.; Courtois, M.; Kovacs, A.; Giguère, V.; Murphy, E.; Kelly, D.P. The nuclear receptor ERRalpha is required for the bioenergetic and functional adaptation to cardiac pressure overload. Cell Metab. 2007, 6, 25–37.
88. Hu, X.; Xu, X.; Lu, Z.; Zhang, P.; Fassett, J.; Zhang, Y.; Xin, Y.; Hall, J.L.; Viollet, B.; Bache, R.J.; Huang, Y.; Chen, Y. AMP activated protein kinase-α2 regulates expression of estrogen-related

receptor-α, a metabolic transcription factor related to heart failure development. Hypertension 2011, 58, 696–703.

89. Lu, Y.; Lu, X.; Wang, L.; Yang, W. Resveratrol attenuates high fat diet-induced mouse cardiomyopathy through upregulation of estrogen related receptor-α. Eur. J. Pharmacol. 2019, 843, 88–95.
90. Sies, H.; Jones, D.P. Reactive oxygen species (ROS) as pleiotropic physiological signaling agents. Nat. Rev. Mol. Cell Biol. 2020, 21, 363–383.
91. Cadenasa, S. ROS and redox signaling in myocardial ischemia-reperfusion injury and cardioprotection. Free Radic. Biol. Med. 2018, 117, 76–89.
92. Shenshu Yang, S.; Lian, G. ROS and diseases: Role in metabolism and energy supply. Mol. Cell. Biochem. 2020, 467, 1–12.
93. Valko, M.; Leibfritz, D.; Moncol, J.; Cronin, M.T.K.; Mazur, M.; Telser, J. Free radicals and antioxidants in normal physiological functions and human disease. Int. J. Biochem. Cell Biol. 2007, 39, 44–84.
94. He, L.; He, T.; Farrar, S.; Jia, L.; Liu, T.; Ma, X. Antioxidants maintain cellular redox homeostasis by elimination of reactive oxygen species. Cell. Physiol. Biochem. 2017, 44, 532–553.
95. Vernier, M.; Dufour, C.R.; McGuirk, S.; Scholtes, C.; Li, X.; Bourmeau, G.; Kuasne, H.; Park, M.; St-Pierre, J.; Audet-Walsh, E.; Giguère, V. Estrogen-related Receptors are Targetable ROS sensors. Genes Dev. 2020, 34, 544–559.
96. Scholtes, C.; Giguère, V. Transcriptional Regulation of ROS Homeostasis by the ERR Subfamily of Nuclear Receptors. Antioxidants 2021, 10, 437.
97. Kong, X.; Wang, R.; Xue, Y.; Liu, X.; Zhang, H.; Chen, Y.; Fang, F.; Chang, Y. Sirtuin 3, a new target of PGC-1alpha, plays an important role in the suppression of ROS and mitochondrial biogenesis. PLoS ONE 2010, 22, e11707.
98. Spinelli, S.; Guida, L.; Passalacqua, M.; Magnone, M.; Caushi, B.; Zocchi, E.; Sturla, L. The ABA/LANCL1-2 Hormone/Receptors System Controls ROS Production in Cardiomyocytes through ERRα. Biomedicines 2024, 12, 2071.
99. Frontera, W.R.; Ochala, J. Skeletal muscle: A brief review of structure and function. Calcif. Tissue Int. 2015, 96, 183–195.
100. Vainshtein, A.; Sandri, M. Signaling Pathways That Control Muscle Mass. Int. J. Mol. Sci. 2020, 21, 4759.
101. Sartori, R.; Romanello, V.; Sandri, M. Mechanisms of muscle atrophy and hypertrophy: Implications in health and disease. Nat. Commun. 2021, 12, 330.

102. Merz, K.E.; Thurmond, D.C. Role of Skeletal Muscle in Insulin Resistance and Glucose Uptake. Compr. Physiol. 2020, 10, 785–809.
103. Li, H.; Wang, C.; Li, L.; Li, L. Skeletal muscle non-shivering thermogenesis as an attractive strategy to combat obesity. Life Sci. 2021, 269, 119024.
104. Dlamini, M.; Khathi, A. Prediabetes-Associated Changes in Skeletal Muscle Function and Their Possible Links with Diabetes: A Literature Review. Int. J. Mol. Sci. 2023, 29, 469.
105. Jager, S.; Handschin, C.; St-Pierre, J.; Spiegelman, B.M. AMP-activated protein kinase (AMPK) action in skeletal muscle via direct phosphorylation of PGC-1α. Proc. Natl. Acad. Sci. USA 2007, 104, 12017–12022.
106. Herman, R.; Kravos, N.A.; Jensterle, M.; Janež, A.; Dolžan, V. Metformin and Insulin Resistance: A Review of the Underlying Mechanisms behind Changes in GLUT4-Mediated Glucose Transport. Int. J. Mol. Sci. 2022, 23, 1264.
107. Peifer-Weiß, L.; Al-Hasani, H.; Chadt, A. AMPK and Beyond: The Signaling Network Controlling RabGAPs and ContractionMediated Glucose Uptake in Skeletal Muscle. Int. J. Mol. Sci. 2024, 25, 1910.
108. Wang, Y.; An, H.; Liu, T.; Qin, C.; Sesaki, H.; Guo, S.; Radovick, S.; Hussain, M.; Maheshwari, A.; Wondisford, F. E.; O'Rourke, B.; He, L. Metformin Improves Mitochondrial Respiratory Activity through Activation of AMPK. Cell Rep. 2019, 29, 1511–1523.e5.
109. Pant, M.; Bal, N.C.; Periasamy, M. Sarcolipin: A Key Thermogenic and Metabolic Regulator in Skeletal Muscle. Trends Endocrinol. Metab. 2016, 27, 881–892.
110. Della Guardia, L.; Luzi, L.; Codella, R. Muscle-UCP3 in the regulation of energy metabolism. Mitochondrion 2024, 76, 101872.
111. Zocchi, G.; Fontanelli, F.; Spinelli, S.; Sturla, L.; Passalacqua, M.; González Urra, J.C.; Delsante, S.; Zocchi, E. Thermal measurements support a role of the ABA/LANCL1-2 hormone/receptors system in thermogenesis. Open Biol. 2024, 14, 2401071.
112. Mengeste, A.M.; Rustan, A.C.; Lund, J. Skeletal muscle energy metabolism in obesity. Obesity 2021, 29, 1582–1595.
113. Pileggi, C.A.; Hooks, B.G.; McPherson, R.; Dent, R.R.M.; Harper, M.E. Targeting skeletal muscle mitochondrial health in obesity. Clin. Sci. 2022, 136, 1081–1110.
114. Lu, P.; Hontecillas, R.; Horne, W.T.; Carbo, A.; Viladomiu, M.; Pedragosa, M.; Bevan, D.R.; Lewis, S.N.; Bassaganya-Riera, J. Computational Modeling-Based Discovery of Novel Classes of Anti-Inflammatory Drugs That Target Lanthionine Synthetase C-Like Protein 2. PLoS ONE 2012, 7, e34643.

115. Diddi, N.; Lai, L.; Nguyen, C.H.; Yan, D.; Nambara, E.; Abrams, S. An Efficient and Scalable Synthesis of a Persistent Abscisic Acid Analog (+)-Tetralone ABA. Org. Biomol. Chem. 2023, 21, 3014–3019.
116. Carbo, A.; Gandour, R.D.; Hontecillas, R.; Philipson, N.; Uren, A.; Bassaganya-Riera, J. An N,N-Bis(Benzimidazolylpicolinoyl) Piperazine (BT-11): A Novel Lanthionine Synthetase C-Like 2-Based Therapeutic for Inflammatory Bowel Disease. J. Med. Chem. 2016, 59, 10113–10126.
117. Leber, A.; Hontecillas, R.; Zoccoli-Rodriguez, V.; Bassaganya-Riera, J. Activation of LANCL2 by BT-11 Ameliorates IBD by Supporting Regulatory T Cell Stability Through Immunometabolic Mechanisms. Inflamm. Bowel Dis. 2018, 24, 1978–1991.
118. Bissel, P.; Boes, K.; Hinckley, J.; Jortner, B. S.; Magnin-Bissel, G.; Werre, S. R.; Ehrich, M.; Carbo, A.; Philipson, C.; Hontecillas, R.; Philipson, N.; Gandour, R. D.; Bassaganya-Riera, J. Exploratory Studies With BT-11: A Proposed Orally Active Therapeutic for Crohn's Disease. Int. J. Toxicol. 2016, 35, 521–529.
119. Birnbaum, E.M.; Xie, L.; Serrano, P.; Rockwell, P.; Figueiredo-Pereira, M.E. BT-11 repurposing potential for Alzheimer's disease and insights into its mode of actions. bioRxiv 2024.
120. Leber, A.; Hontecillas, R.; Zoccoli-Rodriguez, V.; Ehrich, M.; Davis, J.; Chauhan, J.; Bassaganya-Riera, J. Nonclinical Toxicology and Toxicokinetic Profile of an Oral Lanthionine Synthetase C-Like 2 (LANCL2) Agonist, BT-11. Int. J. Toxicol. 2019, 38, 96–109.
121. Leber, A.; Hontecillas, R.; Zoccoli-Rodriguez, V.; Colombel, J. F.; Chauhan, J.; Ehrich, M.; Farinola, N.; Bassaganya-Riera, J. The Safety, Tolerability, and Pharmacokinetics Profile of BT-11, an Oral, Gut-Restricted Lanthionine Synthetase C-Like 2 Agonist Investigational New Drug for Inflammatory Bowel Disease: A Randomized, Double-Blind, Placebo-Controlled Phase I Clinical Trial. Inflamm. Bowel Dis. 2020, 26, 643–652.
122. Leber, A.; Hontecillas, R.; Tubau-Juni, N.; Bassaganya-Riera, J. Safety, Tolerability, and Pharmacokinetics of NIM-1324, an Oral LANCL2 Agonist in a Randomized, Double-Blind, Placebo-Controlled Phase I Clinical Trial. Clin. Transl. Sci. 2025, 18(1), e70129.
123. Scarano, N.; Di Palma, F.; Origlia, N.; Musumeci, F.; Schenone, S.; Spinelli, S.; Passalacqua, M.; Zocchi, E.; Sturla, L.; Cichero, E.; Cavalli, A. New Insights into the LANCL2-ABA Binding Mode towards the Evaluation of New LANCL Agonists. Pharmaceutics 2023, 15(12), 2754.
124. Morita, S.; Kojima, T.; Kitamura, T. Plat-E: An Efficient and Stable System for Transient Packaging of Retroviruses. Gene Ther. 2000, 7, 1063–1066.
125. Jang, M.; Scheffold, J.; Marie Røst, L.; Cheon, H.; Bruheim, P. Serum-Free Cultures of C2C12 Cells Show Different Muscle Phenotypes Which Can Be Estimated by Metabolic Profiling. Sci. Rep. 2022, 12, 827.

126. Livak, K. J.; Schmittgen, T. D. Analysis of Relative Gene Expression Data Using Real-Time Quantitative PCR and the 2-ΔΔCt Method. Methods 2001, 25, 402–408.
127. Vigliarolo, T.; Guida, L.; Millo, E.; Fresia, C.; Turco, E.; de Flora, A.; Zocchi, E. Abscisic acid transport in human erythrocytes. J. Biol. Chem. 2015, 290, 13042–13052.
128. O'Brien, J.; Wilson, I.; Orton, T.; Pognan, F. Investigation of the Alamar Blue (Resazurin) Fluorescent Dye for the Assessment of Mammalian Cell Cytotoxicity. Eur. J. Biochem. 2000, 267, 5421–5426.
129. Pap, E. H.; Drummen, G. P.; Post, J. A.; Rijken, P. J.; Wirtz, K. W. Fluorescent Fatty Acid to Monitor Reactive Oxygen in Single Cells. Methods Enzymol. 2000, 319, 603–612.
130. Gomes, A.; Fernandes, E.; Lima, J.L. Fluorescence probes used for detection of reactive oxygen species. J. Biochem. Biophys. Methods 2005, 65, 45–80.
131. Robinson, K.M.; Janes, M.S.; Pehar, M.; Monette, J.S.; Ross, M.F.; Hagen, T.M.; Murphy, M.P.; Beckmanet, J.S. Selective fluorescent imaging of superoxide in vivo using ethidium-based probes. Proc. Natl. Acad. Sci. USA 2006, 103, 15038–15043.
132. Schneider, C.A.; Rasband, W.S.; Eliceiri, K.W. NIH Image to ImageJ: 25 years of image analysis. Nat. Methods 2012, 9, 671–675.
133. Chen, G.; Yang, Y.; Xu, C.; Gao, S. A Flow cytometry-based assay for measuring mitochondrial membrane potential in cardiac myocytes after hypoxia/reoxygenation. J. Vis. Exp. 2018, 137, 57725.
134. Huynh, K.; Partch, C. L. Analysis of Protein Stability and Ligand Interactions by Thermal Shift Assay. Curr. Protoc. Protein Sci. 2015, 79, 28.9.1–28.9.14.
135. Ransy, C.; Vaz, C.; Lombes, A.; Bouillaud, F. Use of H2O2 to Cause Oxidative Stress, the Catalase Issue. Int. J. Mol. Sci. 2020, 21, 9149.
136. Bassaganya-Riera, J.; Skoneczka, J.; Kingston, D.G.J.; Krishnan, A.; Misyak, S.A.; Guri, A.J.; Pereira, A.; Carter, A.B.; Minorsky, P.; Tumarkin, R.; Hontecillas, R. Mechanisms of action and medicinal applications of abscisic acid. Curr. Med. Chem. 2010, **17**, 467–478.
137. Burattini, S.; Ferri, P.; Battistelli, M.; Curci, R.; Luchetti, F.; Falcieri, E. C2C12 Murine Myoblasts as a Model of Skeletal Muscle Development: Morpho-Functional Characterization. Eur. J. Histochem. 2004, 48, 223–233.
138. Das, M.; Rumsey, J.W.; Bhargava, N.; Gregory, C.; Reidel, L.; Kang, J.F.; Hickman, J.J. Developing a novel serum-free cell culture model of skeletal muscle differentiation by systematically studying the role of different growth factors in myotube formation. In Vitro Cell Dev. Biol. Anim. 2009, **45**, 378–387.
139. Tajbakhsh S. Skeletal muscle stem cells in developmental versus regenerative myogenesis. J Intern Med. 2009; 266, 372–389.

140. Brown, D. M.; Parr, T.; Brameld, J. M. Myosin Heavy Chain mRNA Isoforms Are Expressed in Two Distinct Cohorts during C2C12 Myogenesis. J. Muscle Res. Cell Motil. 2012, 32, 383–390.
141. Zammit, P. S. Function of the Myogenic Regulatory Factors Myf5, MyoD, Myogenin and MRF4 in Skeletal Muscle, Satellite Cells and Regenerative Myogenesis. Semin. Cell Dev. Biol. 2017, 72, 19–32.
142. Asfour, H. Z.; Allouh, M.Z.; Said, R.S. Myogenic Regulatory Factors: The Orchestrators of Myogenesis. Exp. Biol. Med. 2018, 243, 118-128.
143. Shirakawa, T.; Toyono, T.; Inoue, A.; Matsubara, T.; Kawamoto, T.; Kokabu, S. Factors Regulating or Regulated by Myogenic Regulatory Factors in Skeletal Muscle Stem Cells. Cells 2022, 11, 1493.
144. Long, K.; Su, D.; Li, X.; Li, H.; Zeng, S.; Zhang, Y.; Zhong, Z.; Lin, Y.; Li, X.; Lu, L.; Jin, L.; Ma, J.; Tang, Q.; Li, M. Identification of Enhancers Responsible for the Coordinated Expression of Myosin Heavy Chain Isoforms in Skeletal Muscle. BMC Genomics 2022, 23, 519.
145. Zhu, L.-N.; Ren, Y.; Chen, J.-Q.; Wang, Y.-Z. Effects of Myogenin on Muscle Fiber Types and Key Metabolic Enzymes in Gene Transfer Mice and C2C12 Myoblasts. Gene 2013, 532(2), 246–252
146. Schiaffino, S.; Reggiani, C. Fiber Types in Mammalian Skeletal Muscles. Physiol. Rev. 2011, 91, 1447–1531.
147. Murgia, M.; Nogara, L.; Baraldo, M.; Reggiani, C.; Mann, M.; Schiaffino, S. Protein Profile of Fiber Types in Human Skeletal Muscle: A Single-Fiber Proteomics Study. Skelet. Muscle 2021, 11, 24.
148. Tao, L.; Huang, W.; Li, Z.; Wang, W.; Lei, X.; Chen, J.; Song, X.; Lu, F.; Fan, S.; Zhang, L. Transcriptome Analysis of Differentially Expressed Genes and Molecular Pathways Involved in C2C12 Cells Myogenic Differentiation. Mol. Biotechnol. 2025, 67(9), 3640–3655.
149. Blondin, D. P.; Haman, F. Shivering and Nonshivering Thermogenesis in Skeletal Muscles. Handb. Clin. Neurol. 2018, 156, 153–173.
150. Brownstein, A. J.; Veliova, M.; Acín-Pérez, R.; Liesa, M.; Shirihai, O. S. ATP-Consuming Futile Cycles as Energy Dissipating Mechanisms to Counteract Obesity. Rev. Endocr. Metab. Disord. 2022, 23, 121–131.
151. Chen, Z.; Yan, Y.; Qi, C.; Liu, J.; Li, L.; Wang, J. The Role of Ferroptosis in Cardiovascular Disease and Its Therapeutic Significance. Front. Cardiovasc. Med. 2021, 8, 733229.
152. Wang, J.; Xiao, Q.; Chen, X.; Tong, S.; Sun, J.; Lv, R.; Wang, S.; Gou, Y.; Tan, L.; Xu, J.; Fan, C.; Ding, G. LanCL1 Protects Prostate Cancer Cells from Oxidative Stress via Suppression of JNK Pathway. Cell Death Dis. 2018, 9, 197.
153. Huang, H.; Tsui, Y.M.; Ho, D.W.; Chung, C.Y.; Sze, K.M.; Lee, E.; Cheung, G.C.; Zhang, V.X.; Wang, X.; Lyu, X.; Ng, I.O. LANCL1, a cell surface protein, promotes liver tumor initiation through the FAM49B-Rac1 axis to suppress oxidative stress. Hepatology 2024, 79, 323–340.

154. Zhang, L.; Du, F. H.; Kun, K. X.; Yan, Y. Abscisic Acid Improves Non-Alcoholic Fatty Liver Disease in Mice through the AMPK/NRF2/KEAP1 Signaling Axis. Biochem. Biophys. Res. Commun. 2025, 747, 151291.
155. Zhao, Y.; Wang, J.; Shi, S.; Lan, X.; Cheng, X.; Li, L.; Zou, Y.; Jia, L.; Liu, W.; Luo, Q.; Zhang, Y.; Li, H. LanCL2 Implicates in Testicular Redox Homeostasis and Acrosomal Maturation. Antioxidants 2024, 13, 534.
156. Spinelli, S.; Bruschi, M.; Passalacqua, M.; Guida, L.; Magnone, M.; Sturla, L.; Zocchi, E. Estrogen-Related Receptor α: A Key Transcription Factor in the Regulation of Energy Metabolism at an Organismic Level and a Target of the ABA/LANCL Hormone Receptor System. Int. J. Mol. Sci. 2024, 25, 4796.
157. Scialò, F.; Fernández-Ayala, D.J.; Sanz, A. Role of Mitochondrial Reverse Electron Transport in ROS Signaling: Potential Roles in Health and Disease. Front. Physiol. 2017, 8, 428.
158. Ramírez-Camacho, I.; Flores-Herrera, O.; Zazueta, C. The relevance of the supramolecular arrangements of the respiratory chain complexes in human diseases and aging. Mitochondrion 2019, 47, 266–272.
159. Mazat, J.P.; Devin, A.; Ransac, S. Modelling mitochondrial ROS production by the respiratory chain. Cell. Mol. Life Sci. 2020, 77, 455–465.
160. Kreiter, J.; Rupprecht, A.; Škulj, S.; Brklǎjca, Z.; Žuna, K.; Knyazev, D.G.; Bardakji, S.; Vazdar, M.; Pohl, E.E. ANT1 Activation and Inhibition Patterns Support the Fatty Acid Cycling Mechanism for Proton Transport. Int. J. Mol. Sci. 2021, 22, 2490.
161. Yuan, Y.; Li, J.; Wang, M.; Yuan, Q.; Liu, Y.; Yang, W.; Chen, M. Redox regulator LanCL1 suppresses glioma progression by coordinately inhibiting cell growth and regulating mitochondrial metabolism. Free Radic. Biol. Med. 2025, 240, 559–565.
162. Tan, H.; Chen, M.; Pang, D.; Xia, X.; Du, C.; Yang, W.; Cui, Y.; Huang, C.; Jiang, W.; Bi, D.; Li, C.; Shang, H.; Worley, P.F.; Xiao, B. LanCL1 promotes motor neuron survival and extends the lifespan of amyotrophic lateral sclerosis mice. Cell Death Differ. 2020, 27, 1369–1382.
163. Shi, S.; Wang, J.; Gong, H.; Huang, X.; Mu, B.; Cheng, X.; Feng, B.; Jia, L.; Luo, Q.; Liu, W.; Chen, Z.; Huang, C. PGC-1α-coordinated hypothalamic antioxidant defense is linked to SP1-LanCL1 axis during high-fat-diet-induced obesity in male mice. Antioxidants 2024, 13, 252.
164. Soukup, T.; Smerdu, V. Effect of altered innervation and thyroid hormones on myosin heavy chain expression and fiber type transitions: a mini-review. Histochem. Cell Biol. 2015, 143, 123–130.
165. Lee, S.-H.; Kim, B.-J.; Park, D.-R.; Kim, U.-H. Exercise Induces Muscle Fiber Type Switching via Transient Receptor Potential Melastatin 2-Dependent Ca^{2+} Signaling. J. Appl. Physiol. 2018, 124, 364–373.

166. Chen, X.; Guo, Y.; Jia, G.; Liu, G.; Zhao, H.; Huang, Z. Arginine Promotes Skeletal Muscle Fiber Type Transformation from Fast-Twitch to Slow-Twitch via Sirt1/AMPK Pathway. J. Nutr. Biochem. 2018, 61, 155–162.
167. Yu, J.-A.; Wang, Z.; Yang, X.; Ma, M.; Li, Z.; Nie, Q. LncRNA-FKBP1C Regulates Muscle Fiber Type Switching by Affecting the Stability of MYH1B. Cell Death Discov. 2021, 7, 73.
168. Chen, X.; Liang, D.; Huang, Z.; Jia, G.; Zhao, H.; Liu, G. Quercetin Regulates Skeletal Muscle Fiber Type Switching via Adiponectin Signaling. Food Funct. 2021, 12, 2693–2702.
169. Stuart, C. A.; McCurry, M. P.; Marino, A.; South, M. A.; Howell, M. E.; Layne, A. S.; Ramsey, M. W.; Stone, M. H. Slow-Twitch Fiber Proportion in Skeletal Muscle Correlates with Insulin Responsiveness. J. Clin. Endocrinol. Metab. 2013, 98, 2027–2036.
170. Wang, J. E.; Pessin, J. Mechanisms for Fiber-Type Specificity of Skeletal Muscle Atrophy. Curr. Opin. Clin. Nutr. Metab. Care 2013, 16, 243–250.
171. Oberbach, A.; Bossenz, Y.; Lehmann, S.; Niebauer, J.; Adams, V.; Paschke, R.; Schön, M. R.; Blüher, M.; Punkt, K. Altered Fiber Distribution and Fiber-Specific Glycolytic and Oxidative Enzyme Activity in Skeletal Muscle of Patients with Type 2 Diabetes. Diabetes Care 2006, 29, 895–900.
172. Murray, J.; Huss, J.M. Estrogen-related receptor α regulates skeletal myocyte differentiation via modulation of the ERK MAP kinase pathway. Am. J. Physiol. Cell Physiol. 2011, 301, C630–C645
173. Rasbach, K.A.; Gupta, R.K.; Ruas, J.L.; Wu, J.; Naseri, E.; Estall, J.L.; Spiegelman, B.M. PGC-1α regulates a HIF2α-dependent switch in skeletal muscle fiber types. Proc. Natl. Acad. Sci. U.S.A. 2010, 107, 21866–21871.
174. Chen, H.H.; Lu, J.; Guan, Y.F.; Li, S.J.; Hu, T.T.; Xie, Z.S.; Wang, F.; Peng, X.H.; Liu, X.; Xu, X.; Zhao, F.P.; Yu, B.L.; Li, X.P. Estrogen/ERR-α signaling axis is associated with fiber-type conversion of upper airway muscles in patients with obstructive sleep apnea hypopnea syndrome. Sci. Rep. 2016, 6, 27088.
175. Ishikawa, K.; Hara, T.; Mizukawa, M.; Fukano, Y.; Shimomura, T. Natriuretic peptide signaling is involved in the expression of oxidative metabolism-related and muscle fiber constitutive genes in the gastrocnemius muscle. Mol. Cell Endocrinol. 2019, 494, 110493.
176. Li, H.; Wang, C.; Li, L.; Li, L. Skeletal muscle non-shivering thermogenesis as an attractive strategy to combat obesity. Life Sci. 2021, 269, 119024.
177. Kazak, L.; Chouchani, E. T.; Jedrychowski, M. P.; Erickson, B. K.; Shinoda, K.; Cohen, P.; Vetrivelan, R.; Lu, G. Z.; Laznik-Bogoslavski, D.; Hasenfuss, S. C.; Kajimura, S.; Gygi, S. P.; Spiegelman, B. M. A Creatine-Driven Substrate Cycle Enhances Energy Expenditure and Thermogenesis in Beige Fat. Cell 2015, 163, 643–655.

178. Kazak, L.; Spiegelman, B. M. Mechanism of Futile Creatine Cycling in Thermogenesis. Am. J. Physiol. Endocrinol. Metab. 2020, 319, E947–E949.
179. Sharma, A. K.; Khandelwal, R.; Wolfrum, C. Futile Cycles: Emerging Utility from Apparent Futility. Cell Metab. 2024, 36, 1184–1203.
180. Bertholet, A. M.; Kazak, L.; Chouchani, E. T.; Bogaczynska, M. G.; Paranjpe, I.; Wainwright, G. L.; Bétourné, A.; Kajimura, S.; Spiegelman, B. M.; Kirichok, Y. Mitochondrial Patch Clamp of Beige Adipocytes Reveals UCP1-Positive and UCP1-Negative Cells Both Exhibiting Futile Creatine Cycling. Cell Metab. 2017, 25, 811–822.e4.
181. Wallimann, T.; Tokarska-Schlattner, M.; Kay, L.; Schlattner, U. Role of Creatine and Creatine Kinase in UCP1-Independent Adipocyte Thermogenesis. Am. J. Physiol. Endocrinol. Metab. 2020, 319, E944–E946.
182. Rizo-Roca, D.; Guimarães, D.S.P.F.; Pendergrast, L.A.; Di Leo, N.; Chibalin, A.V.; Maqdasy, S.; Rydén, M.; Näslund, E.; Zierath, J.R.; Krook, A. Decreased mitochondrial creatine kinase 2 impairs skeletal muscle mitochondrial function independently of insulin in type 2 diabetes. Sci. Transl. Med. 2024, 16, eado3022.
183. Su, Y.; Liu, N.; Liu, Y.; Sun, Y.; Jiao, Y. The skeletal muscle–adipose creatine metabolic axis: A novel paradigm for lipid metabolism reprogramming and obesity management. Exp. Physiol. 2025.
184. Su, Y. Three-Dimensional Network of Creatine Metabolism: From Intracellular Energy Shuttle to Systemic Metabolic Regulatory Switch. Mol. Metab. 2025, 100, 102228
185. Basu, R.; Flak, J. N. Hypothalamic Neural Circuits Regulating Energy Expenditure. Vitam. Horm. 2025, 127, 79–124.